A SPATIAL ANALYSIS OF THE RELATIONSHIP BETWEEN FOREST DEMOGRAPHIC DYNAMICS AND DIVERSITY UNDER CLIMATE CHANGE

by

Yingying Zhu

A Dissertation Submitted in

Partial Fulfillment of the Requirements for the

Degree of Doctor of Philosophy in Forest Sciences

Faculty of Natural Resources Management

Lakehead University

August 2023

ABSTRACT

Forest dynamics arise from three demographic processes simultaneously, namely recruitment, mortality and growth, all of which are expected to accelerate for the boreal forest under future climate change. Tree species diversity, however, is hypothesized to mitigate the impacts of climate change on the rates of these demographic processes. At the same time, understanding the generation and maintenance of tree species diversity is a historical challenge and requires examining multiple demographic dynamics simultaneously. The purpose of this dissertation is to investigate the complex relationship between tree demographics and diversity under the influence of climate change through spatial analysis of 173 permanent sample plots in the boreal forest of Manitoba, Canada, at the individual-tree level. A mapped dataset of individual stems that were repeatedly measured from 1986 to 2010 forms the basis of three studies.

In my first study, I investigated how tree diversity affects recruitment using spatially explicit neighbourhood analysis. I found that sapling recruitment probability, on average, decreases with neighbourhood crowding, but increases with stand age, neighbourhood shade tolerance dissimilarity and phylogenetic dissimilarity. Further, the positive effect of shade tolerance dissimilarity was strongest in young stands, while phylogenetic dissimilarity had a positive effect only in older stands. Moreover, higher shade tolerance and phylogenetic dissimilarities ameliorate the negative effect of neighbourhood crowding. These findings (1) underline that the role of tree species diversity in promoting sapling recruitment is context-dependent, and (2) provide direct evidence that neighbourhood diversity ameliorates the negative neighbourhood crowding effect on sapling recruitment, particularly in older boreal forest stands.

In my second study, I investigated temporal trends and the indirect effect of climate change through neighbourhood interactions on recruitment. Building a structural equation model,

I found that sapling recruitment had a non-significant response to temporal trend variations in the boreal forest, albeit atmospheric CO_2 concentration, air temperature, and precipitation simultaneously increased over the study period. However, increased mortality and growth of established trees over time exerted indirect negative effects on sapling recruitment. In contrast, increased neighbourhood crowding over time had indirect negative effects, while increased shade tolerance and phylogenetic dissimilarities had weak indirect positive effects on sapling recruitment. In total, variations in the trend through time had a negative effect on sapling recruitment. These results suggest that sapling recruitment does not necessarily compensate for increased mortality under climate change, and even so-called favourable climate change can threaten long-term ecosystem functioning.

In my third study, I investigated the effects of conspecific negative density dependence (CNND) on three demographic rates that change with stand development and, how they may contribute to tree species diversity dynamics following stand-replacing disturbance. The results provided direct evidence that the effects of CNDD varied with different demographic rates and changed with stand development. Specifically, the effects of CNDD included stronger negative density dependence among conspecifics than heterospecifics. Three demographics decreased with stand age and were stronger in young stands. Moreover, the reduced effect of CNDD with increasing stand age included a steeper trend on survival, followed by recruitment, with the least impact on growth rates. These results suggest that stronger CNDD in young stands might contribute to an initial increase in tree species richness from young to mature forests. In contrast, the reduced CNDD in older stands might lead to decreased tree species richness in older forests. These findings provide an alternative hypothesis that competition, rather than the well-accepted

effect of natural enemies, could be the dominant mechanism that drives boreal forest diversity dynamics with stand development.

Overall, this dissertation advances knowledge of the relationship between three measures of individual tree demography and local tree diversity in the context of climate change. Given that continual shifts in three demographic processes simultaneously determine ecosystem functioning, spatial analyses on untangling the complex causes and consequences of multiple demographics will provide insights for better knowledge and predicting the variations in the forest carbon cycle and ecosystem functioning in response to ongoing diversity loss and climate change.

Keywords: boreal forest, demography, competition, functional diversity, phylogenetic diversity, neighbourhood dissimilarity, tree diversity, recruitment, mortality, growth, Janzen-Connell hypothesis

CONTENTS

LIST OF TABLES

LIST OF FIGURES

ACKNOWLEDGEMENTS

I express my sincere gratitude to everyone who has helped me in the completion of this Ph.D. thesis. It has been a long and challenging journey, and I could not have made it without the support and encouragement of many individuals. Firstly, I thank my dissertation supervisors, Drs. Han Chen and Brian McLaren, for their guidance, expertise, and patience throughout my research in ecology. Dr. Chen's invaluable feedback, suggestions, and encouragement have been instrumental in shaping this thesis. I extend my gratitude to my committee members, including Drs. Gordon Kayahara and Jian Wang, and my mentors Drs. Ashley Thomson and Qinglai Dang, and my external examiner, Dr. Andrew Park, for their guidance and support. Their insights and feedback have been critical in developing my research and improving the quality of this thesis. I am also thankful to my colleagues and friends, including Drs. Eric Searle and Chen Chen, who provided me with an inspiring and stimulating environment to work in. Your support and encouragement have helped me to remain motivated and focused. Much appreciated, and best wishes for your future career.

Finally, I express my deepest gratitude to my husband, Nan Zhang, and loved daughters, Brooke and Ayla. You make me independent and responsible. Also, I would not be able to finish this dissertation without the support of my parents, Keyang Zhu, Min Liu and mother-in-law, Yun Liu. Your unconditional love and support for my decisions have inspired and motivated me.

NOTE

This dissertation is a manuscript-based thesis. The chapters were written to suit the publication requirements of the targeted journals. Formatting and reference styles may differ. Since individual chapters reflect the joint contributions of myself and my academic supervisors, I use "we" instead of "I" for individual manuscripts.

Chapters:

2. Zhu, Y., E.R. Searle, & Chen, H.Y.H. (2022). Functionally and phylogenetically diverse boreal forest promote sapling recruitment. *Forest Ecology and Management*, 524, 120522.

3. Zhu, Y. Chen, C, & Chen, H.Y.H. (2023). Sapling recruitment does not compensate for increased tree mortality under climate change. Submitted to *Agricultural and Forest Meteorology*.

4. Zhu, Y., Chen, C., & Chen, H.Y.H. (2023). Conspecific negative density dependence drives tree species diversity through stand development. Submitted to *Ecology Letters*.

CHAPTER 1: GENERAL INTRODUCTION

Three demographics, recruitment, mortality, and growth, drive forest dynamics in terms of composition, productivity, and functioning, and determine carbon sequestration and storage (Astigarraga et al., 2020, Zhang et al., 2015). Anthropogenic global environmental change in terms of biodiversity loss and climate change, driven by a complex interplay of emissions of greenhouse gasses, episodic disturbances, and chronic climate drivers, is accelerating three demographic processes (McDowell et al., 2020). Conservation of biodiversity has been proposed as a solution to mitigate climate change impacts on the functioning of forest ecosystems by alleviating their negative effects and promoting their positive effects on demographic rates (Mace et al., 2012, Tilman et al., 2014, Hisano et al., 2018). In turn, the demographic processes can interact to promote coexistence and maintain diversity in forest ecosystems, which are expected to shift under future climate change (Germain and Lutz, 2022). A comprehensive understanding of the relationship between tree demographics and local diversity is thus required to elucidate forest dynamics in a changing world.

Among the world's forest ecosystems, the boreal forest accounts for 49% of global carbon storage (Dixon et al., 1994). However, the boreal forest is expected to experience twice the rate of average global warming, with unevenly distributed precipitation (IPCC, 2014, IPCC, 2018). Nevertheless, forest demographic dynamics are thought to be primarily driven by community competition, followed by climate change, in the boreal forest of western Canada (Zhang et al., 2015). Higher species diversity in boreal forest generally could reduce competition and climate of boreal forest on tree demographics and lead to higher productivity (Hisano et al., 2019, Hisano and Chen, 2020). However, these diversity-demographics relationships are poorly understood and seemingly bewildering at both local and larger scales.

One reason is that the assumed aggregated homogeneity in the boreal forest community masks the presence of spatial structure on tree demographic performance (Moeur, 1993). For example, canopy gaps occurring during stand development are determinants of tree demographics, especially understorey recruitment (Kneeshaw and Bergeron, 1998, Messier et al., 1998). Spatial analysis can describe neighbourhood interactions on individual tree demographics and can be insightful but complex due to the interplay between individual demographic dynamics and neighbourhood environmental factors, as well as their responses to broader-scale climate change. In this dissertation, describing the dynamics of the boreal forest in Manitoba, I focus on examining how individual tree demographics respond to neighbourhood conditions under climate change, and in turn, how three demographics simultaneously response to neighbourhood heterogeneity, how the response may or may not be density dependent, and how it may contribute to variation in diversity as stands develop.

Sapling recruitment, the transition from larger seedling pools to sapling or juvenile trees, is a bottleneck for long-term forest dynamics and a key process to species composition and forest resilience (McDowell et al., 2020, Berner and Goetz, 2022). The sapling stage may persist for decades due to slow growth in a shaded understorey and the delay while canopy gaps are formed from tree mortality (Kneeshaw and Bergeron, 1999, Hubbell et al., 1999). Since sapling recruitment might determine forest resilience post-disturbance and carbon storage capacity in old-growth boreal forest (Boisvert-Marsh et al., 2019, Kneeshaw and Bergeron, 1999, Gao et al., 2017), an understanding of the neighbourhood effects on sapling recruitment is required. In boreal forests, individual-level processes of sapling recruitment following stand establishment may be predictable from local neighbourhood competition, neighbourhood dissimilarity, and stand developmental stages.

Pervasive shifts in forest dynamics are ongoing and arise directly from climate change and indirect effects mediated by biotic interactions in the trade-offs among demographic processes (Chen et al., 2019a, Lebrija-Trejos et al., 2023). Sapling recruitment often follows resource release from widespread mortality and decreased growth as a response to spatially and temporally varying drivers, making predictions of the net effects of climate change on ecosystems uncertain (Anderegg et al., 2015, McDowell et al., 2020). However, the divergent response of sapling recruitment may result from different rates of regional climate change and their indirect effects on demographic trade-offs, competition, and diversity in neighbourhoods. There is an increased magnitude and importance of the relationship between sapling recruitment and climate change when considering direct and indirect effects combined (Searle et al., 2022). From a more holistic view, warming and unevenly distributed water availability in the boreal forest may result in decreased sapling recruitment probability when competition is intense from increased mortality and increased growth (Searle and Chen, 2020, Luo and Chen, 2015).

How diversity is generated and maintained in forests is a fundamental question in ecology but answering it remains a crucial challenge (Chesson, 2000, Hülsmann et al., 2021, Detto et al., 2019). Over the past five decades, negative density dependence among conspecifics (CNDD), which limits population growth rates and allows less abundant species to thrive, has been hypothesized as a promising mechanism for maintaining local diversity in mature or steady-state tropical forests. Although a linear relationship between stronger CNDD and higher richness across various environmental gradients has been tested globally (Johnson et al., 2012, LaManna et al., 2017b, LaManna et al., 2022, Lebrija-Trejos et al., 2023, Huang et al., 2020), debates persist on conceptual and methodological questions (Detto et al., 2019,

Hülsmann et al., 2021). The maintenance of local tree diversity is an important conservation priority in cold species-poor boreal forest. Understanding the effect of CNDD on three demographic processes across stand ages and how it may contribute to diversity dynamics is essential to elucidate the one of factors responsible for local tree diversity.

The general objective of this dissertation is to advance understanding of the relationship between three demographic processes and local tree diversity under climate change, through spatial analysis of individual trees in a central region of the Canadian boreal forest. To achieve this goal, I first tested how the crowding and stand age-dependence of neighbourhood diversity affected sapling recruitment (Chapter 2). Second, I examined how sapling recruitment might directly respond to presumed variations in climate and indirectly respond to climate differences through neighbourhood interactions (Chapter 3). Third, I examined whether the effects of CNDD on the three demographics change with stand age and how these changes may contribute to local tree diversity (Chapter 4). To achieve these specific objectives, I conducted spatially explicit analysis on a large-spatial mapped and long-term forest inventory data in the Manitoban boreal forest, where wildfire is the dominant disturbance to drive stand development in regions.

CHAPTER 2: FUNCTIONALLY AND PHYLOGENETICALLY DIVERSE BOREAL FOREST PROMOTE SAPLING RECRUITMENT

2.1 Abstract

Sapling recruitment in established forest stands is critical to long-term ecosystem functioning but can be constrained due to competition from increased neighbourhood crowding. Tree species diversity has the potential to ameliorate negative crowding effects; however, the relationship between diversity and sapling recruitment remains unclear. We used data from spatially mapped individual stems, which were repeatedly measured at five-year intervals between 1986 to 2010 from 173 permanent plots in Canada. We analyzed individual sapling recruitment probabilities over five-year survey intervals as a function of neighbourhood crowding index, stand age, neighbourhood diversity from shade tolerance dissimilarity and phylogenetic dissimilarity, and their interactions. We show that sapling recruitment probability, on average, decreases with neighbourhood crowding but increases with stand age and neighbourhood shade tolerance and phylogenetic dissimilarities. The positive effect of shade tolerance dissimilarity was strongest in young stands, while phylogenetic dissimilarity had a positive effect only in older stands. Moreover, sapling recruitment probability in neighbourhoods with high shade tolerance and phylogenetic dissimilarities was less negatively affected by crowding than in more similar neighbourhoods. Our study highlights the possible mechanisms that promote sapling recruitment in diverse neighbourhoods are context-dependent, with niche complementary being more important in young stands and the feedback from pests and pathogens playing a greater role in old boreal stands. Our results provide direct evidence that neighbourhood diversity helps ameliorate the negative neighbourhood crowding effect on sapling recruitment, particularly in old-growth

boreal forest. The mixtures of broadleaves and conifers increase sapling recruitment and are particularly important in the late-successional stages of boreal forest.

2.2 Introduction

Sapling recruitment in established stands is a bottleneck in forest dynamics (Chang‑Yang et al., 2021, Hubbell et al., 1999, Forrister et al., 2019) and might determine carbon storage capacity in old boreal forest stands (Gao et al., 2017). Previous studies in boreal forest have shown lower sapling recruitment in stands with higher competition (Zhang et al., 2015, Muledi et al., 2020). Mixed species stands may experience competition less intensely than single-species stands because individuals of different species in the mixed stand have different niche spaces, whereas the same species in single-species stands compete for similar resources aboveground and belowground (Williams et al., 2017, Brassard et al., 2013). Mixed species stands may therefore have higher rates of sapling recruitment.

Despite the critical importance of sapling recruitment to the long-term functioning of boreal forest stands (Berner and Goetz, 2022), the impact of diversity on sapling recruitment remains equivocal. For example, the effects of tree species diversity on recruitment in boreal forest stands have been reported to be positive (Young et al., 2011), insignificant (Looney et al., 2021), and even negative (Zhang et al., 2016). Species richness averages or stand aggregations may be insufficient to disentangle the drivers of sapling recruitment (LaManna et al., 2017a) because individual-level processes such as sapling recruitment may be largely determined by neighbourhood interactions (Wiegand et al., 2021). To properly understand the possible mechanisms underlying diversity effects on sapling recruitment, spatially explicit neighbourhood analyses are required.

Neighbourhood crowding-induced competition for resources, such as available space, light, and nutrients, may be a strong determinant of sapling recruitment. In boreal forest, neighbourhood crowding is expected to be the dominant driver because a shorter growing season permits higher recruitment synchrony and lower niche partitioning between species than in tropical forests (Usinowicz et al., 2017). Previous studies have shown that neighbourhood crowding reduces the growth and increases the mortality of canopy trees in boreal forest (Searle and Chen, 2020, Luo and Chen, 2011). Growth and survival of sapling recruitment may be even more strongly affected by neighbourhood crowding since saplings are the smallest in the understorey and therefore experience greater light and soil resource limitations than neighbouring mature trees (Lutz et al., 2014, Hubbell et al., 1999). Accordingly, we hypothesized that the sapling recruitment probability would decrease with greater neighbourhood crowding. Moreover, sapling recruitment may increase with stand age since sapling recruitment in the understory of established stands is a slow process (Chang‐Yang et al., 2021).

Neighbourhood diversity may ameliorate the crowding effect on sapling recruitment, and the effects may change with the amount of crowding and stand age. Functional trait-based diversity or dissimilarity increases ecosystem productivity by reducing competition due to spatial and temporal niche partitioning (Wagg et al., 2017). However, neighbourhood trait-based dissimilarity effects remain debated for demographic rates (Kunstler et al., 2016, Searle and Chen, 2020, Muledi et al., 2020, Forrister et al., 2019). One possible reason for the debate may be due to a lack of context-dependence on trait-based effects (Adler et al., 2013). For example, the positive effect of functional dissimilarity on sapling recruitment may increase with neighbourhood crowding and be stronger in younger stands with higher resource

competition since the strength of diversity effect increases with abiotic stress and competition for resources (Hisano et al., 2018). In addition, neighbourhood phylogenetic dissimilarity, which predicts pest and pathogen-mediated density dependence at a finer scale (Castagneyrol et al., 2014, Forrister et al., 2019), has been reported to have a positive relationship with sapling recruitment in tropical forests (Zhu et al., 2015). In mixed-wood boreal forest, the greater phylogenetic distance between broadleaved and coniferous species is expected to reduce the impacts of specialized insect herbivores through host dilution (Jactel et al., 2021, Castagneyrol et al., 2014). Moreover, in fire-driven boreal forests, tree species- or genus-specialized herbivores and diseases tend to accumulate during stand development (Ruess et al., 2021). We hypothesize that phylogenetic dissimilarity-induced reduction in specialized insect herbivores and pathogen damage would become more important with stand development.

In this study, we aimed to gain a better understanding of neighbourhood interactions on sapling recruitment in natural boreal forest stands. Specifically, we tested whether that sapling recruitment probability would: (i) decrease with neighbourhood crowding; (ii) increase from young to mature stands; (iii) increase with neighbourhood functional and phylogenetic dissimilarities. Moreover, we expected that the positive effect of neighbourhood functional dissimilarity would be stronger at the earlier stages of stand development, whereas the positive effect of phylogenetic dissimilarity would increase with stand age.

2.3 Materials and Methods

2.3.1 Study area and forest inventory data

The study area is in the Central Canadian boreal region between 49°04 and 56°99 N in latitude and 95°30 to 101°68 W in longitude (Fig. S2-1). The 30-year long-term (1981-2010) mean annual temperatures and precipitation ranged from -3.1°C to 3.0°C and 443 mm to 674

19

mm, respectively. The major natural stand-replacing disturbance in the region is wildfire, with an average fire return internal differing spatially and temporally, from between 25 to 90 years (Weir et al., 2000).

Since the mid-1980s, the Government of Manitoba has established over 400 permanent sample plots in both natural and managed forests to monitor forest growth over time across the study area. The PSPs were allocated in well-stocked, visually homogenous stands of greater than 1 ha in size, with > 100 m from any openings, to minimize the impacts of edge effects. All plots were 100% forested, circular with a 12.62 m radius and 500 m^2 in size. At the time of plot establishment, the locations of all trees ≥ 1.5 m in height in each plot were spatially mapped by their directions (degrees from the north) and distances (to the nearest cm) from the plot centre. Their diameters at breast height (DBH) were measured, and the species were identified. These PSPs were repeatedly measured for growth, mortality, and recruitment every five years until 2010.

For our study, plots from the PSP network were compiled employing the following data selection criteria: (1) PSPs had originated from a known stand-replacing wildfire and were unmanaged natural forests. (2) only measurements prior to 2011 were selected due to a change in sampling protocol. (3) the survey interval was five years and with at least two consecutive surveys. As a result, 173 plots were selected for our analysis (Fig. S2-1). For individual plots, the initial survey year ranged from 1986 to 2005 ($\overline{x}$ = 1992), the final survey year ranged from 1992 to 2010 ($\overline{x}$ = 2007), and plots were surveyed two to five times ($\overline{x}$ = 4.1) (Fig. S2-2). The stand age at the first survey spanned from 5 to 147 years ($\overline{x}$ = 41) (Fig. S2-2). The number of trees per plot (500 m^2) ranged from 58 to 2955 stems ($\overline{x}$ = 400), the average tree height in a plot ranged from 2.1 to 16.5 m ($\overline{x}$ = 7.8 m), and the average DBH in a plot from 1.24 to 18.87

cm ($\bar{x}$ = 7.03) (Fig. S2-2). In our dataset, all individual trees were tracked with their positions within the plot through repeated surveys.

A total of 21,754 trees died, and there were 10,893 recruits. There were 203,471 observations of 65,542 live trees repeatedly measured over the course of the study period. The abundant tree species included *Picea mariana* (35.2% of living stems), *Pinus banksiana* (27.0%), *Populus tremuloides* (22.1%), and minor tree species included *Abies balsamea* (5.2%), *Betula papyrifera* (3.2%), *Fraxinus nigra* (2.8%), *Picea glauca* (1.9%), *Larix laricina* (1.5%), and *Thuja occidentalis* (1.0%). Other species included *Acer negundo*, *Fraxinus pennsylvanica*, *Pinus resinosa*, *Quercus macrocarpa*, and *Ulmus americana*, which totalled approximately 0.1% of all stems.

We used individual sapling recruitment analyses to accommodate the individual tree neighbourhoods. Sapling recruitment was defined as the occurrence of a new tree sapling with a height ≥ 1.5 m between two consecutive surveys. Sapling recruitment probability per five-year survey interval was derived from tree status, 1 for a recruit and 0 for an established living tree. For each focal stem, including recruits and established trees, we quantified its neighbourhood crowding, shade tolerance dissimilarity and phylogenetic dissimilarity based on the sizes and distances of its neighbouring trees at each survey in each plot.

2.3.2 Explanatory variables

We calculated a neighbourhood crowding index (NCI) of all living trees to quantify the intensity of neighbourhood crowding using previously described methods (Chen et al., 2016b), reflecting the sizes of neighbouring trees and their proximity to the focal stem:

$$NCI_{ijk} = \sum_{n \neq i} \left(\frac{B_{njk}}{(D_{in})_{jk}} \right) \tag{1}$$

where i, j, and k are the ith focal stem, jth survey, and kth plot, respectively, n are the nth neighbour trees. B and D_{in} are the basal area and the distance between the focal stem ith and the nth neighbour trees. Instead of DBH, we used the basal area to reflect the important effect of neighbouring larger trees on sapling recruitment as the neighourhood crowding effect can scale to the basal area of the neighbours (Chen et al., 2016b). We did not include the size of the newly recruited stem between two consecutive surveys because all recruits were below the measurement threshold prior to recruiting. For each period of two consecutive surveys, the NCI of a recruit was calculated based on the survey when it was observed. We also calculated its NCI based on the previous survey by assuming no change in its spatial location. We used the average of the two NCI values to represent the competitive environments of individual stems during a five-year survey interval.

Similar to a previous study for tree mortality (Luo and Chen, 2015), since all plots were circular with a radius of 12.6 m, we included all neighbours within a 12.6 m radius plot to calculate the NCI for each focal stem at each survey. Because focal stems were not at the centre of the plot, we corrected the NCI for edge effects using an area-weighted correction based on the assumption of homogeneous sample stands, which was previously verified for the plot network used in our study (Luo and Chen, 2015). For instance, if 30% of the neighbourhood of the focal stem fell outside of the plot, the estimates of the NCI were divided by 0.7. To confirm that our results were not sensitive to methods from radii selection (Zambrano et al., 2020), we also introduced radii of 10.0-m, 7.5-m, and 5.0-m. The NCI estimates were highly correlated. For instance, NCI estimates using a 12.6-m and 10.0-m radii had an $r = 0.99$. We report the results based on the 12.6 m radius plot in the main text.

We derived neighbourhood diversity, including functional and phylogenetic dissimilarities following a previous study (Searle and Chen, 2020). We focussed on shade tolerance to derive functional dissimilarity. At the community level, tree species with different shade tolerances lead to more efficient light exploitation and utilization (Morin et al., 2011) and shade tolerance heterogeneity is important in driving diversity–productivity relationships in forest communities (Zhang et al., 2012). At the individual tree level, trees with neighbours that have dissimilar shade tolerances grow more quickly than those with neighbours that have similar shade tolerance (Searle and Chen, 2020). We adopted species values of shade tolerance from Niinemets and Valladares (2006), which assigned values from 1 to 5, from highly shade-intolerant to shade-tolerant species that corresponded to the minimum light availability required for an individual species to grow. For boreal forest species, the shade tolerance of small individuals is consistent with their adult shade tolerance ranking (Kneeshaw et al., 2006). For i^{th} focal stem, j^{th} survey, and k^{th} plot, we calculated the neighbourhood shade tolerance dissimilarity (STD) using:

$$STD_{ijk} = \frac{\sum_{n \neq i} abs(ST_i - ST_{nj}) \times \frac{B_{njk}}{(D_{in})_{jk}}}{\sum_1^{n \neq i} \frac{B_{njk}}{(D_{in})_{jk}}} \tag{2}$$

where $abs\,(ST_i - ST_n)$ is the absolute value of shade tolerance difference between focal stem i and the nth neighbour tree; B, Din, i, j, k, n were the same as Eqn. 1.

We obtained a phylogeny for study species using the Phylomatic V3 software web client (http://phylodiversity.net/phylomatic/). We used the *cophenetic* function in R statistical software, 4.1.0 (R Development Core Team, 2021) to form a pairwise phylogenetic distance matrix for the study species, which was then normalized with the maximum dissimilarity set to 1 and maximum similarity (i.e. neighbour of the same species as the focal tree) to 0 by dividing

each value in the matrix by the maximum paired distance (Fig. S2-4). For the ith focal stem, j^{th} survey, and k^{th} plot, we derived its neighbourhood phylogenetic dissimilarity (PD) by substituting normalized phylogenetic distance for shade tolerance distance in Eqn. 2.

Stand age (SA) represents the time since the last stand-replacing fire for each plot. Stand ages in the PSP data were available and were provided by the Manitoba provincial government. These ages were either based on known fire history or coring dominant trees in the plot or outside plots (Senici et al., 2010). When coring was used, the average age of the oldest species was assigned as stand age.

Similar to NCI, the average values of STD, PD and SA between the two consecutive surveys were calculated to model sapling recruitment probability. We removed the first survey of each plot after obtaining the above-mentioned explanatory variables since recruits could only be recognized in the second or in a later survey.

2.3.3 Statistical analyses

We employed a generalized linear mixed model with binomial error distribution with a *logit* link to test the effects of neighbourhood crowding index, stand age, shade tolerance dissimilarity, phylogenetic dissimilarity, and their interactions on sapling recruitment probability over five-year intervals. To determine a proper function for sapling recruitment probability and individual predictors, we first graphically plotted the stem status (1 as a recruit and 0 as a live tree) versus individual predictors using Loess smoothing to explore possible patterns. The graphical assessment indicated that the responses were monotonic for all predictors. We then fitted linear and logarithmic functions with each predictor as the fixed effect and "plot" as the random effect in logarithmic functions and compared the values of the Akaike information criterion (AIC). We found that the logarithmic NCI, logarithmic SA, linear

STD, and linear PD yielded lower AIC values. Accordingly, the corresponding functions were

chosen to relate sapling recruitment probability to respective predictors.

To test our hypotheses, we used the following model:

$$logit(p_{ijkl}) = \beta 0 + \beta 1 \cdot In(NCI)_{ijk} + \beta 2 \cdot In(SA)_{ijk} + \beta 3 \cdot STD_{ijk} + \beta 4 \cdot In(PD)_{ijk}$$

$$+ \beta 5 \ In(SA)_{ijk} \times STD_{ijk} + \beta 6 \ In(SA)_{ijk} \times PD_{ijk}$$

$$+ \beta 7 \cdot In(NCI)_{ijk} \times STD_{ijk} + \beta 8 \cdot In(NCI)_{ijk} \times PD_{ijk}$$

$$+ \beta 9 \ In(NCI)_{ijk} \times In(SA)_{ijk}$$

$$+ \beta 10 \ In(NCI)_{ijk} \times In(SA)_{ijk} \times STD_{ijk}$$

$$+ \beta 11 \ In(NCI)_{ijk} \times In(SA)_{ijk} \times In(PD)_{ijk}$$

$$+ \alpha k + \varepsilon ijkl \tag{3}$$

where p is sapling recruitment probability per five-year interval, NCI, SA, STD, PD are the

middle values of neighbourhood crowding index, stand age, and shade tolerance dissimilarity,

phylogenetic dissimilarity between two consecutive surveys. βs are coefficients to be

estimated, i, j, k are the same as for Eqn. 1. α_k is a random intercept term representing plot k to

account for spatial autocorrelation among trees within each plot, and ε_{ijkl} is a random error.

The models were built and analyzed using the *lme4* package, with restricted maximum

likelihood estimation (Bates et al., 2019).

To facilitate the interpretation of coefficients, we standardized all explanatory

variables, which involved subtracting their mean and then dividing by their standard deviation

prior to analysis. We tested the overdispersion of the full model using the *blmeco* package,

which indicated that there was no overdispersion (Korner-Nievergelt et al., 2019). Next, we

used the VIF (variance inflation factor) in the *car* package to examine the collinearity of

predictors in our model (Fox et al., 2020). Although STD and PD were significantly correlated

(r = 0.67, P <0.001), all predictors in our model had a VIF of < 3.8, indicating that

multicollinearity is not a serious issue in our model (Zuur et al., 2010). Moreover, to avoid

overfitting, we used the *dredge* function of the *MuMIn* package (Barton, 2020) to rank all

alternative models based on their AIC. We found that the full model had the lowest AIC value,

and this model was chosen as the final model for interpretation. We assessed the model

performance by calculating the AUC (Area Under the Curve) and ROC (Receiver Operating

Characteristics) curves using the *pROC* package (Robin et al., 2020), wherein an AUC of > 0.7

was considered acceptable. We bootstrapped the fitted coefficients for 1,000 iterations to

produce 95% confidence intervals (Table 2-1). We determined the relative importance of each

predictor based on the proportion of summed absolute values of their standardized coefficients

(Grömping, 2015).

We tested spatial autocorrelations by using the Mantel test (Borcard and Legendre,

2012). The results indicated no evidence of spatial autocorrelation among the plots for the

mean five-year sapling recruitment rate (Mantel test, r = -0.026, P = 0.821) or the residuals of

plot identity random effect on a five-year sapling recruitment probability (Mantel test, r =

-0.002, P = 0.533). We also tested temporal autocorrelations in model residuals using the

Durbin-Watson test applied to scaled residuals and implemented in the *DHARMa* package

(Hartig, 2022). We found no evidence of temporal autocorrelation (DW = 1.882, P = 0.197).

To illustrate the responses of sapling recruitment probability to predictors, we used

partial dependent plots from the fitted model of Eqn. 2. Specifically, we used the *effect_plot*

function for main effects and *interact_plot function* for interaction effects of the package *jtools*

to plot the figures (Long, 2021). All statistical analyses were performed in R 4.1.3 (R

Development Core Team, 2021).

2.4 Results

The AUC-ROC curve for our model was 0.888, which indicates its excellent discriminatory power. The main effect of neighbourhood crowding on five-year sapling recruitment probability was the most important of the eleven elements, accounting for 27.0% of relative importance (total in 100%), based on the absolute values of their standardized coefficients (Table 2-1, Fig. S2-5). As neighbourhood crowding increased, sapling recruitment probability decreased from a maximum 1 with the lowest crowding to close to 0 at the highest level of crowding (Fig. 2-1a). Stand age was the third most important predictor, accounting for 15.0% of the model explained variation (Table 2-1, Fig. S2-5). Sapling recruitment probability increased significantly as stands aged, from 0.002 at seven years old stands to 0.10 at 164 years old stands (Fig. 2-1b). As the second important predictor (accounting for 22.5%, Table 2-1, Fig. S2-5), neighbourhood shade tolerance dissimilarity increased sapling recruitment probability significantly from 0.01 with a neighbourhood of similar shade tolerance to 0.28 in neighbourhoods with the most diverse shade tolerance (Fig. 2-1c). On average, phylogenetic dissimilarity was a relatively weak predictor (accounting for 4.3% of the variation in sapling recruitment probability, Table 2-1, Fig. S2-5), causing an increase in sapling recruitment probability from 0.01 with conspecific neighbours to 0.04 in phylogenetically diverse neighbourhoods (Fig. 2-1d).

Table 2-1. The five-year sapling recruitment probability associated with neighbourhood crowding index (NCI), stand age (SA), shade tolerance dissimilarity (STD), and phylogenetic dissimilarity (PD) in boreal forest plots (Government of Manitoba). All predictors were scaled, which involved subtracting their mean and then dividing by their standard deviation. The NCI, and SA were natural log-transformed. Coefficient values are the mean estimate with bootstrapped 95% confidence intervals (CI).

Source	Estimate	Confidence intervals	z value	P value
Intercept	-4.152	-4.303 ~ -3.800	-31.043	<0.001
ln(NCI)	-1.166	-1.218 ~ -1.105	-44.455	<0.001
ln(SA)	0.646	0.532 ~ 0.749	12.501	<0.001
STD	0.968	0.922 ~ 1.005	47.937	<0.001
PD	0.185	0.140 ~ 0.225	8.730	<0.001
ln(SA) × STD	-0.637	-0.687 ~ -0.582	-24.766	<0.001
ln(SA) × PD	0.320	0.266 ~ 0.377	10.917	<0.001
ln(NCI) × STD	0.077	0.041 ~ 0.113	4.392	<0.001
ln(NCI)× PD	0.090	0.050 ~ 0.130	4.680	<0.001
ln(NCI) × ln(SA)	0.036	-0.007 ~ 0.078	1.889	0.059
ln(NCI) × ln(SA) × STD	-0.124	-0.164 ~ -0.079	-6.548	<0.001
ln(NCI) × ln(SA) × PD	0.070	0.025 ~ 0.111	3.453	<0.001
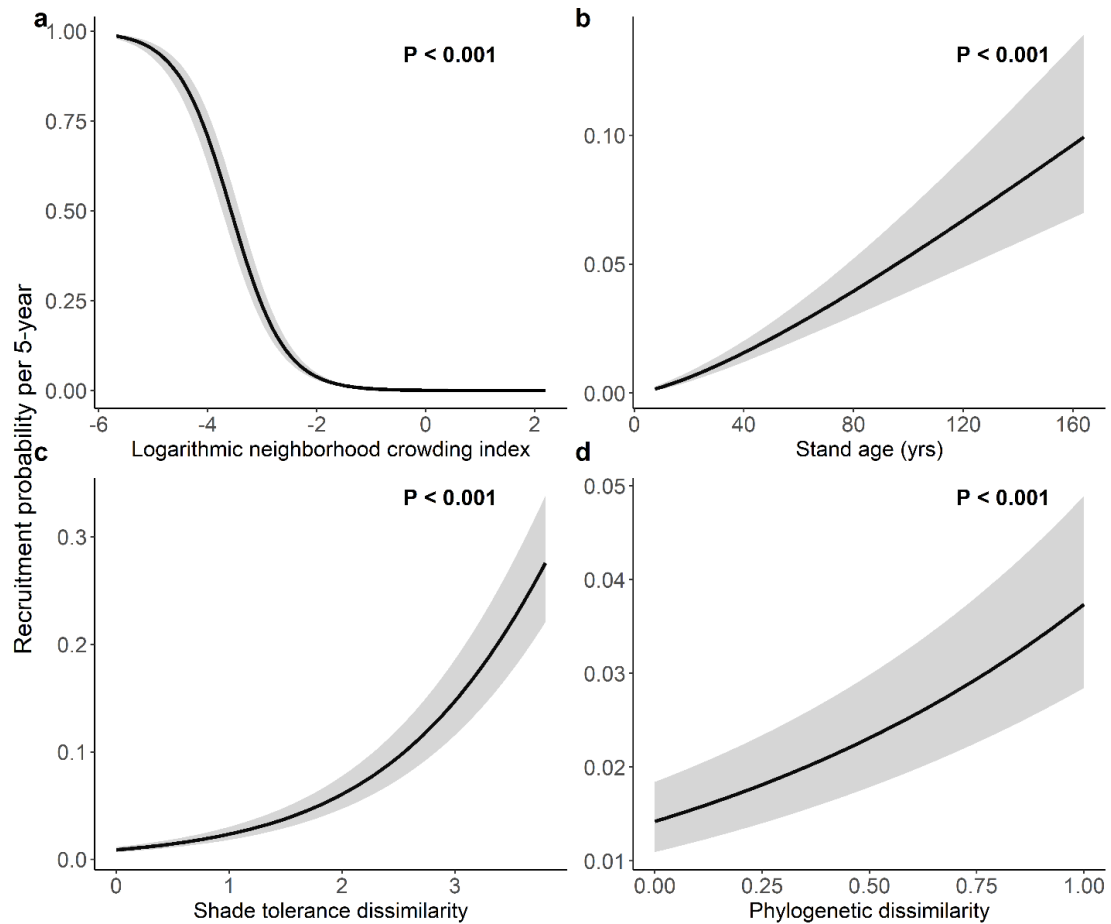
Figure 2-1: The response of five-year sapling recruitment probability to neighbourhood crowding, stand age, and diversity in the boreal forest. a Neighbourhood crowding. b Stand age. c Shade tolerance dissimilarity. d Phylogenetic dissimilarity. Solid lines show average effects, with 95% confidence bands.

The interaction between stand age and shade tolerance dissimilarity was the fourth most important predictor, and the interaction between stand age and phylogenetic dissimilarity was the fifth (Table 2-1, Fig. S2-5). The effects of shade tolerance dissimilarity were stronger in younger stands than in old stands (Fig. 2-2a). By contrast, phylogenetic dissimilarity had a positive effect on sapling recruitment probability in older stands but no significant effect in young stands (Fig. 2-2b). The interaction of crowding and stand age on sapling recruitment was not significant (Table 2-1), and the negative effect of crowding was consistent across stand ages. The interaction between the crowding index and shade tolerance dissimilarity was the

eighth important predictor, while the ninth most important was the interaction between the crowding index and phylogenetic dissimilarity (Table 2-1, Fig. S2-5). Sapling recruitment probability in neighbourhoods with high shade tolerance dissimilarity and high phylogenetic dissimilarity was less negatively affected by neighbourhood crowding than in more similar neighbourhoods (Figs. 2-3a and 2-3b).
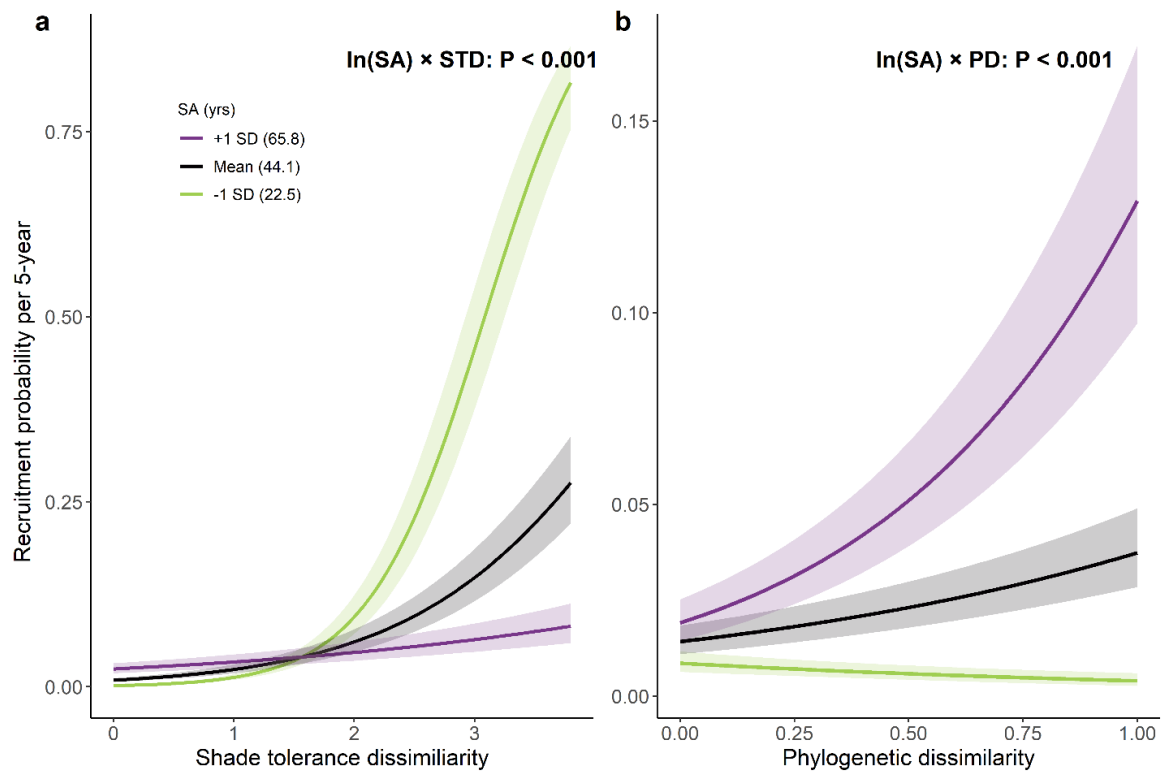
Figure 2-2: The response of five-year sapling recruitment probability to the interaction between stand age and neighbourhood diversity in the boreal forest. a Stand age-dependent effect of shade tolerance dissimilarity. b Stand age-dependent effect of phylogenetic dissimilarity. Solid lines show average effects, with 95% confidence bands.
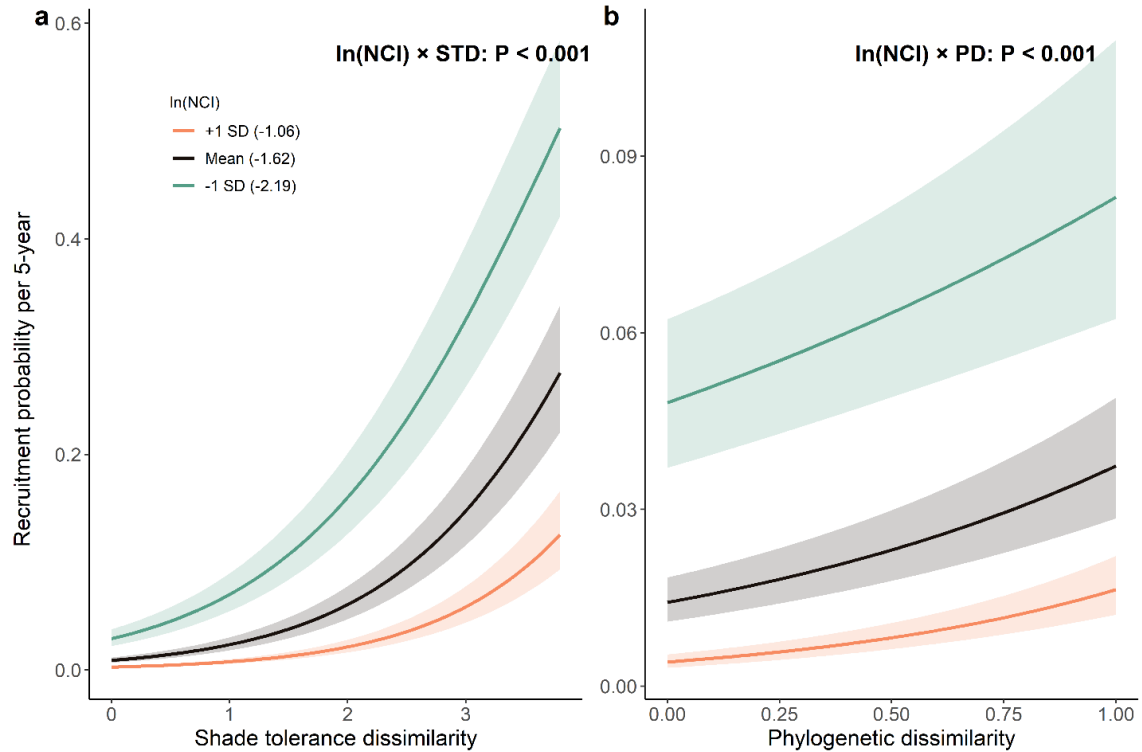
Figure 2-3: The response of five-year sapling recruitment probability to the interaction between neighbourhood crowding and diversity in the boreal forest. a Neighbourhood crowding index-dependent effect of shade tolerance dissimilarity. b Neighbourhood crowding index-dependent effect of phylogenetic dissimilarity. Solid lines show average effects, with 95% confidence bands.

The three-way interactions among shade tolerance dissimilarity (and phylogenetic dissimilarity) and stand age-dependent on crowding had seventh and tenth importance for sapling recruitment probability (Table 2-1, Fig. S2-5). Nevertheless, the positive effect of shade tolerance dissimilarity associated with intense crowding was more pronounced in younger stands (Fig. 2-4a), while the positive effect of phylogenetic dissimilarity associated with crowding was more pronounced in older stands (Fig. 2-4b).
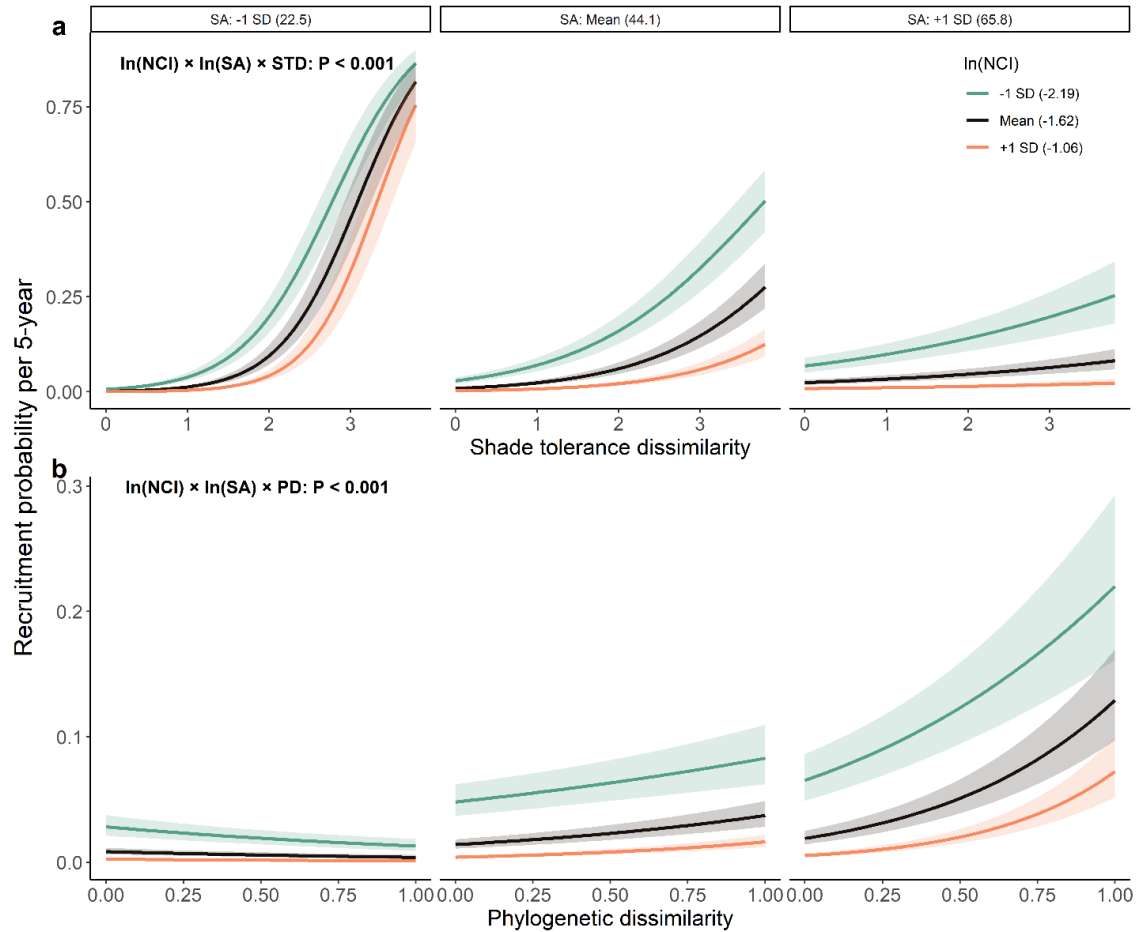
Figure 2-4: The response of five-year sapling recruitment probability to the three-way interactions among neighbourhood crowding, stand age, and neighbourhood diversity in the boreal forest. a neighbourhood crowding, stand age, and shade tolerance dissimilarity. b neighbourhood crowding, stand age and phylogenetic dissimilarity. Solid lines show average effects, with 95% confidence bands.

2.5 Discussion

In this study, we found a positive effect of neighbourhood functional and phylogenetic dissimilarities on sapling recruitment across a wide range of stand crowding and development stages among the Manitoba boreal forest plots. Further, the positive effect of shade tolerance dissimilarity was stronger in young stands, but phylogenetic dissimilarity had a stronger positive effect in older stands. Also, neighbourhoods with higher shade tolerance and phylogenetic dissimilarities had reduced negative impacts of neighbourhood crowding on

sapling recruitment probability, that is, higher shade tolerance and phylogenetic dissimilarities ameliorate the negative effect of neighbourhood crowding. Our results demonstrate strong influences of neighbourhood interactions on sapling recruitment in a wide range of established boreal forest stands, and extend previously observed neighbourhood effects on tree growth and mortality (Luo and Chen, 2015, Searle and Chen, 2020, Chen et al., 2016b). Our results of stand age- and crowding-dependent effects of neighbourhood shade tolerance and phylogenetic dissimilarities suggest that divergent responses from previous studies examining tree species diversity and composition effects on sapling recruitment may be due to differences in stand age- and crowding rather than diversity effects themselves (Young et al., 2011, Looney et al., 2021, Zhang et al., 2016).

As we hypothesized, neighbourhood crowding was a dominant driver for sapling recruitment, as suggested conceptually (Usinowicz et al., 2017) and by the results of stand-level analyses using stand density and stand basal area (Zhang et al., 2015, Muledi et al., 2020). Our results demonstrate a strong decline in sapling recruitment probability as neighbourhood crowding increases, highlighting competition for light and other resources may as the main driver of sapling recruitment in established forests (Hubbell et al., 1999). Moreover, as expected, sapling recruitment probability increased with stand age. This is because in the boreal forest, after rapid post-fire pulse recruitment of pioneer shade-intolerant species in the first several years (Johnstone et al. 2010), the tree canopy closes, and stem exclusion takes place. Under a closed canopy, slow-growing shade-tolerant coniferous species begin to recruit, but the process is slow (Chen and Popadiouk, 2002).

Our finding of positive effects of neighbourhood shade tolerance and phylogenetic dissimilarities on sapling recruitment probability represents the first reported in the boreal

forest, where conspecific replacement is the common successional pathway due to frequent stand-replacing disturbances (Birch et al., 2019, Chen and Popadiouk, 2002). This finding suggests that niche partitioning and facilitation, may as a potential mechanism, influence sapling recruitment, not only in species-rich tropical forests (Hubbell et al., 1999, Wiegand et al., 2021, Zhu et al., 2015), but also in the relatively species-poor boreal forest. We demonstrated that sapling recruitment probability, on average, increased with neighbourhood shade tolerance and phylogenetic dissimilarities. We note that the positive effect of shade tolerance and phylogenetic dissimilarities on sapling recruitment in our study is coupled with the facilitative effects of shade-intolerant, deciduous broadleaved *Populus tremuloides* and *Betula papyrifera* on shade-tolerant, evergreen coniferous *Picea* spp. and *Abies balsamea* (Figs. 2-4) (Chen and Popadiouk, 2002, Looney et al., 2021, Birch et al., 2019). The positive neighbourhood shade tolerance dissimilarity effect indicates that tree crowns of species with different shade tolerance are complementary vertically and horizontally, suggesting that neighbourhood shade tolerance dissimilarity reduces competition for aboveground and belowground growing space and other resources (Williams et al., 2017, Brassard et al., 2013). At the same time, phylogenetic dissimilarity likely reduces pest and pathogen accumulation because species-specific insects and pathogens have evolved with plant species (including tree species) occurred at different times in Earth's history (Parker et al., 2015, Forrister et al., 2019).

We found a strong effect of neighbourhood shade tolerance dissimilarity on sapling recruitment in young stands, but a weak effect in old stands. This finding partially supports those reported in old-growth tropical forests where functional dissimilarity of different life-history traits has no or weak effect on sapling recruitment (Muledi et al., 2020, Forrister et al.,

2019). The strong positive neighbourhood shade tolerance dissimilarity effect in young boreal

forest stands is explained by the fact that shade-intolerant species, such as *Pinus banksiana* and

Populus tremuloides, have difficulty recruiting under their canopy because of insufficient light.

On the other hand, shade-tolerant species, such as *Abies balsamea* and *Picea* spp., freely

recruit under closed canopies of shade-intolerant tree species (Looney et al., 2021). The

reduced effect of shade tolerance dissimilarity on recruitment in older stands at the stages of

canopy transition and gap dynamics is attributable to the fact that both recruits and surrounding

mature trees are most likely shade-tolerant conifers (Chen and Popadiouk, 2002, Birch et al.,

2019). We note that although our shade tolerance trait captures important information about

resource use strategies, it lacks information about defences and belowground traits, which are

difficult to obtain (Forrister et al., 2019).

We demonstrated that phylogenetic dissimilarity had a stronger positive effect on

sapling recruitment in older stands. This finding adds to the evidence that the strength of

phylogenetic dissimilarity does not change only with the life stages of studied individuals (Zhu

et al., 2015), but also for the same life stage, in this case saplings, across stand development

stages. Our finding of the strong positive effect on sapling recruitment in old stands is

consistent with the widely observed positive phylogenetic diversity effect on sapling

recruitment in old-growth tropical forests (Forrister et al., 2019, Zhu et al., 2015). In our study,

high phylogenetic dissimilarity occurs in the mixture of broadleaves and conifers. In these

older boreal forest stands, the mixture of broadleaves and conifers reduces both the impacts on

sapling recruitment from specialized insect herbivores (Jactel et al., 2021), such as

Dendroctonus rufipennis (bark beetle), and its host *Picea glauca, Malacosoma disstria* (forest

tent caterpillar) for *Populus tremuloides* (Birch et al., 2019), and disease, such as aspen canker

(Ruess et al., 2021), and large herbivores, such as beaver (*Castor canadensis*) and moose (*Alces alces*), which typically damage broadleaf saplings but are less damaging to coniferous saplings (Lorentzen Kolstad et al., 2018, Donkor and Fryxell, 2000). The weak or non-existent phylogenetic effects on sapling recruitment in young boreal forest stands are consistent with the fact that insect herbivores and diseases are less detrimental to young boreal forest stands (Ruess et al., 2021), where resource competition is a stronger determinant of sapling recruitment. It is consistent with our finding of a stronger effect of neighbourhood shade tolerance dissimilarity on sapling recruitment.

The finding of less negative effects by crowding in neighbourhoods with high shade tolerance and phylogenetic dissimilarities suggests that crown complementarity and facilitation between live trees and recruits are more important when stand density is high and/or tree crowns are not well differentiated vertically (Jucker et al., 2015). This result improves our understanding that shade tolerance and phylogenetic dissimilarities ameliorate the negative effects of crowding not only on tree growth (Searle and Chen, 2020) but also on sapling recruitment. Importantly, the positive effects of neighbourhood dissimilarities are stronger for the growth of trees with higher neighbourhood crowding (Searle and Chen, 2020) or smaller trees within a stand (Jucker et al., 2014), as well as sapling recruitment probability, as found in this study. These results collectively suggest that individuals with higher resource competition benefit more from neighbourhood diversity, likely due to the increased strength of diversity effect with competition for resources (Hisano et al., 2018).

Our finding provides one of the first pieces of evidence that functional and phylogenetic dissimilarities can reduce the negative effects of crowding on sapling recruitment, a bottleneck in forest dynamics, particularly in old-growth boreal forest. In this study, we have

36

an advanced understanding of how neighbourhood crowding and neighbourhood functional and phylogenetic dissimilarities influence sapling recruitment across a wide range of stand ages and site conditions in the boreal forest. However, more studies are necessary to better understand multiple non-exclusive mechanisms in regulating sapling recruitment in established forest stands. Our results suggest that the role of neighbourhood functional and phylogenetic dissimilarities in promoting sapling recruitment is context-dependent, with niche partitioning and facilitation versus feedback through other trophic levels, i.e., insect herbivores and diseases, operating at different stages of stand development in the boreal forest. Our finding indicates that enhancing tree diversity, particularly intermittent mixtures of broadleaves and conifers, will promote sapling recruitment and the functioning of old-growth boreal forest since stands lacking sufficient tree recruitment can transition into shrublands after pioneer species die off (Chen and Popadiouk, 2002).

CHAPTER 3: SAPLING RECRUITMENT DOES NOT COMPENSATE FOR INCREASED TREE MORTALITY UNDER CLIMATE CHANGE

3.1 Abstract

Sapling recruitment within established stands plays an important role in the long-term functionality of forest ecosystems. However, the direct impacts of climate change on sapling recruitment and its underlying mechanisms remain unclear. We hypothesized that sapling recruitment is directly affected by climate change (herein referring to temporal trends in repeated measurements of permanent forest sample plots [PSPs] and associated changes in atmospheric CO_2, temperature, and water availability) and indirectly affected through the responses of tree mortality and growth, as well as their modification of neighbourhood conditions. We employed a dataset of 173 PSPs with individual stems spatially mapped and monitored at five-year intervals from 1986 to 2010 in the central boreal forest of North America. By constructing structural equation models (SEMs), we examined how sapling recruitment probability may, directly and indirectly, respond to climate change through the mortality and growth of established trees, neighbourhood crowding, as well as functional and phylogenetic dissimilarities. We used the middle calendar year of each five-year survey period to represent recent systematic temporal trends in climate change. Our SEMs revealed that sapling recruitment probability did not respond significantly to temporal variations in the studied forests, where atmospheric CO_2 concentration, air temperature, and climatic water availability simultaneously increased. However, the increased mortality and growth of neighbourhood-established trees (all stems except for recruits) exerted indirect negative effects on sapling recruitment probability. Furthermore, increased neighbourhood crowding had an indirect adverse effect on sapling recruitment probability, while increased neighbourhood

shade tolerance and phylogenetic dissimilarities had weak indirect positive effects on sapling recruitment probability. Collectively, there was a significant total negative effect on sapling recruitment probability over our survey period. Our analysis of different pathways of change demonstrated multiple potential mechanisms that simultaneously regulated the effect of climate change on sapling recruitment. Our results emphasized that sapling recruitment does not necessarily compensate for increased tree mortality. We suggest that even so-called favourable climate change could threaten long-term ecosystem functionality.

3.1 Introduction

Sapling recruitment, along with tree growth and mortality, is one of three demographic processes that are critical to long-term forest ecosystem functionality (McDowell et al., 2020). Conceptually, enhanced resource availability from climate change-induced increases in tree mortality and decreases in tree growth should promote sapling recruitment (McDowell et al., 2020). However, sapling recruitment has been reported both to increase (Chen et al., 2019a) and decrease (Davis et al., 2019) in response to climate change. These divergent responses may result from differences in the direction and magnitudes of regional climate change (Boisvert-Marsh et al., 2019, Boucher et al., 2019) in conjunction with the indirect effects of climate change exerted on established trees (all stems except for recruits; Chen et al., 2019a, 2019n, Yang et al., 2022), whose responses alter neighbourhood conditions for sapling recruitment (McDowell et al., 2020). Given the role of sapling recruitment in maintaining forest functioning and carbon storage under a rapidly changing climate (Hanbury-Brown et al., 2022, Sharma et al., 2022, Berner and Goetz, 2022), we need an elucidation of the direct and indirect effects of climate change on sapling recruitment.

Climate change may directly impact sapling recruitment and indirectly influence the mortality and growth of established trees (Fig. 3-1). Unfavourable climate change, such as heat stress and drought, can directly decrease tree recruitment, increase tree mortality, and decrease tree growth due to resource constraints (van Mantgem et al., 2009, Peng et al., 2011; Fig. 3-1a). Alternatively, sapling recruitment can directly benefit from increasing atmospheric CO_2 concentration, climate warming, and higher water availability, which increase resource availability for tree communities, acting on established trees and recruits (Berner and Goetz, 2022; Fig. 3-1b). Furthermore, climate change may indirectly impact sapling recruitment by altering the mortality and growth of established trees. Sapling recruitment may benefit from the drought-induced acceleration of mortality in larger trees as well as a decrease in their growth due to decreasing asymmetric resource competition of larger or dominant trees (Condit et al., 1995, Lloret et al., 2012; Fig. 3-1c). In contrast, favourable climate change may promote the growth of larger or dominant trees, increasing competition stress on understorey trees, including recruits (Coomes et al., 2011; Fig. 3-1d). Consequently, we hypothesized that sapling recruitment might be affected not only directly by climate change but also indirectly by the effects of climate change on the mortality and growth of established trees, which changes the availability of resources for sapling recruitment (Fig. 3-2).

The effect of climate change on sapling recruitment may also manifest through its influences on neighbourhood interactions (Fig. 3-2). It has long been recognized that warming-induced increases in resource availability can lead to greater stand crowding (Grime, 1979). Sapling recruitment probability decreases with increasing neighbourhood crowding due to higher competition for limited resources and a higher neighbourhood density of hosts for species-specific herbivores and pathogens (Zhu et al., 2022, Parker et al., 2015). Meanwhile,

favourable effects of climate change promote functional and phylogenetic dissimilarities, as longer growing seasons lead to less synchronized recruitment of different species (Usinowicz et al., 2017). In contrast, drought can lead to the loss of functional and phylogenetic dissimilarities (Aguirre-Gutierrez et al., 2020, Harrison et al., 2020). Sapling recruitment benefits from neighbourhood functional and phylogenetic dissimilarities through resource partitioning, abiotic facilitation, and biotic feedback (Barry et al., 2019, Zhu et al., 2022). These changes in neighbourhood interactions may implicitly influence the mortality and growth of established trees (Fig. 3-2). Simultaneously, the impacts of climate change on the mortality and growth of established trees can alter neighbourhood interactions and subsequently influence sapling recruitment (Fig. 3-2).

In this study, our objective was to examine how sapling recruitment probability might directly or indirectly respond to climate change through the mortality and growth of established trees, neighbourhood crowding, and functional and phylogenetic dissimilarities (Fig. 3-2). We employed a dataset of 173 permanent sample plots (PSPs) with individual stems, which were spatially mapped and monitored at five-year intervals from 1986 to 2010 in the central boreal forest of North America (Fig. S3-1), where atmospheric CO_2 concentration, air temperatures, and climate water availability simultaneously increased during the study period (Fig. S3-2).
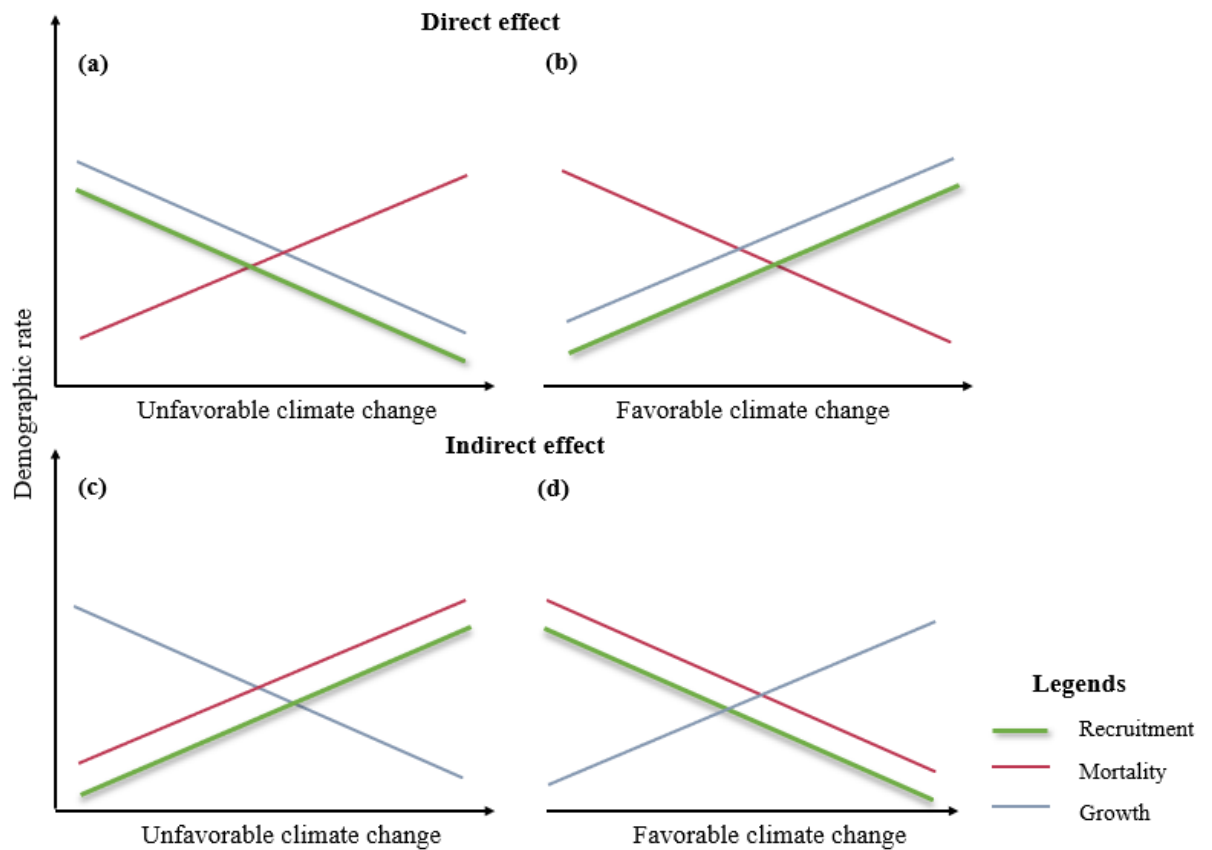
Figure 3-1: Conceptual diagram visualizing how climate change might affect recruitment directly and indirectly through mortality and growth. (a) Unfavourable climate change (e.g. heat stress and drought) decreases recruitment and growth while increasing mortality; (b) Favourable climate change (e.g. rising CO_2, warming in cold climates, and increased water availability) increases recruitment and growth while reducing mortality; (c) Unfavourable climate change increases mortality and decreases growth, which leads to lower neighbourhood competition for recruitment; (d) Favourable climate change increases growth and decreases mortality, and subsequently reduces understory resources for recruitment.
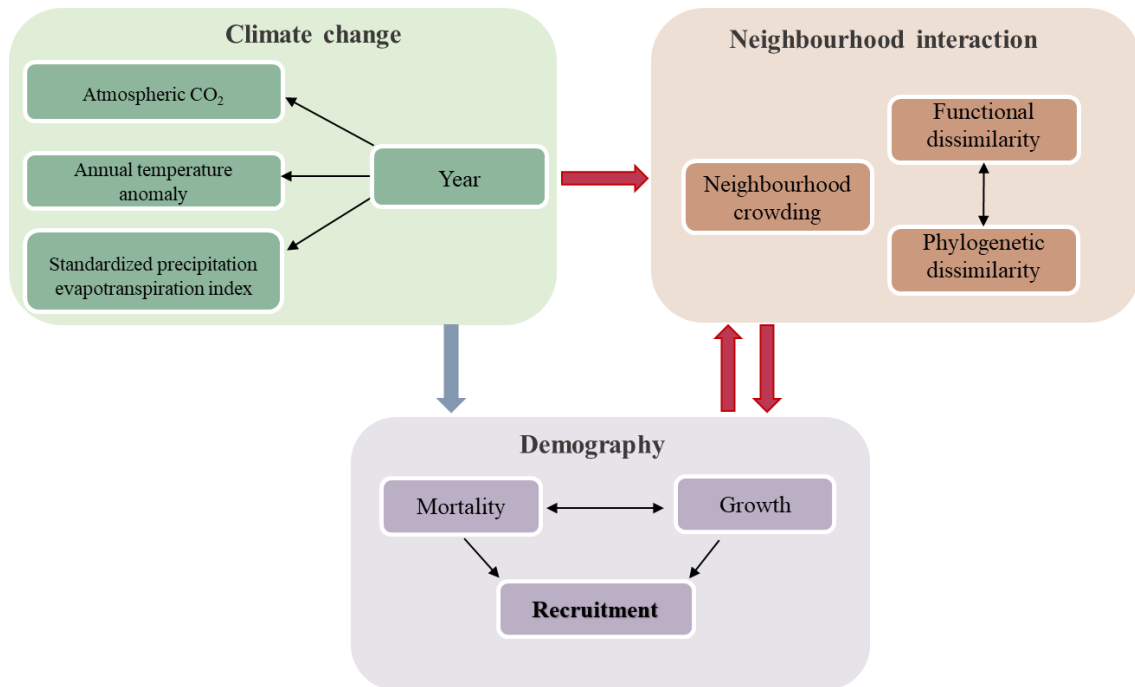
Figure 3-2: Conceptual model showing the relationships between climate change (green box), neighbourhood interactions (brown box), and tree demography (purple box). Blue arrows indicate the direct effects of climate change, and red arrows indicate the indirect effects of climate change through mortality and growth of established trees and neighbourhood interactions on sapling recruitment. Black arrows indicate the effects within each box.

3.2 Materials and Methods

3.3.1 Study area and forest inventory data

The forest stands of this study are in Manitoba, Canada, in a central region of boreal forests in North America. Permanent forest sample plots (PSPs) were created in stands that spanned at least four hectares, which were confirmed by visual assessment to be homogeneous with respect to landform, species composition, age class and growth. The PSPs were located at least 100 m from a stand boundary and 50 m from any trails or other openings to prevent edge effects. Every PSP was 500 m^2, and circular with a radius of 12.6 m.

From the time of plot establishment in the 1980s, all trees above 1.5 m in height were tagged, species were recorded, their diameters at breast height (DBH) were measured, and their

positions were spatially located according to their distances (to the nearest cm) and directions (degrees from north) from the plot centre. The DBHs of surviving trees were remeasured during subsequent visits to the plot, when dead trees were recorded as mortalities, and sapling recruits that had reached 1.5 m in height were also noted, species identified and DBH measured. Sapling recruitment probability was derived from tree status records, in a binary fashion with 1 for a sapling recruit and 0 for an established living tree. The PSPs were measured repeatedly every five years until 2010 when the sampling protocol was modified.

To assess the effects of climate change on sapling recruitment, we compiled plots from the PSP datasets according to the following criteria: (1) they were in stands with a known stand-replacing wildfire and unmanaged, and (2) they were measured over at least two surveys. A total of 173 PSPs met these conditions (Fig. S3-1), with coordinates spanning from 49°04′ to 56°99′ N latitude and 95°30′ to 101°68′ W longitude (Fig. S3-1). The long-term mean annual temperature (MAT) and mean annual precipitation (MAP) over three decades between 1981 and 2010 in this region varied between -3.1 °C (north) and 3.0 °C (south; 1.06 ± 2.53 °C, mean ± std) and 443 to 674 mm (536.9 ± 88.5 mm), respectively. Wildfire is the dominant stand-replacing disturbance for this area, with a return interval of approximately 100 years (Senici et al., 2010).

The initial years of PSP establishment were from 1986 to 2005, and the final survey years were from 1992 to 2010 (Fig. S3-3). PSPs were surveyed two to five times (an average of 4.2 times) and stand age at the initial survey ranged from 5 to 147 years (average of 41 years; Fig. S3-3). During the study period, 175,270 observations were recorded for 65,728 repeatedly measured trees. In the records, 21,754 trees died, and there were 10,893 recruits (Fig. S3-3). Three dominant species accounted for about 85% of all recorded tree stems: black

spruce (*Picea mariana* (Mill.) BSP, 35.2%), jack pine (*Pinus banksiana* Lamb, 27.0%), and trembling aspen (*Populus tremuloides* Michx, 22.2%). Minor tree species (<1% of all tree stems recorded) included *Abies balsamea*, *Betula papyrifera*, *Fraxinus nigra*, *Picea glauca*, *Larix laricina*, and *Thuja occidentalis* (Table S3-1).

3.3.2 Explanatory variables

The middle calendar year (Y) of two consecutive surveys was utilized to represent the overall temporal trends during the survey period (van Mantgem et al., 2009, Peng et al., 2011). Similarly to an earlier investigation (Searle and Chen, 2020), the temporal change associated with atmospheric CO_2, annual temperature anomaly (ATA), and annual standardized precipitation–evapotranspiration index (SPEI) were calculated and averaged over the five-year survey interval. The ambient atmospheric CO_2 concentrations were obtained from the Mauna Loa Baseline Observatory from Global Monitoring Laboratory (https://gml.noaa.gov/obop/mlo/) and averaged for each survey period per plot. Based on plot locations (latitude, longitude, and elevation), we obtained the mean annual temperature (MAT) and annual climate moisture index (CMI) for our study period using BioSIM software from Canadian Forest Service (https://cfs.nrcan.gc.ca/projects/133), which generates historical scale-free climate data interpolated from nearby weather stations. The ATA for each plot was calculated as the difference between the average of observed MAT over the survey period and its long-term mean (1986-2010) during the study period, where higher ATA implied warming. We used the average annual SPEI for each survey period to accurately quantify the availability of water, which reflected drought conditions due to global warming, where lower SPEI values indicated drier conditions (Vicente-Serrano et al., 2010). We calculated the SPEI using the annual CMI and the *SPEI* package in R (Beguería and Vicente-Serrano, 2017).

To assess the influence of mortality and growth of established trees on sapling recruitment, we calculated mortality (basal area loss, M) and growth (net basal area increment, G) of established trees in the neighbourhood of each focal individual (both sapling recruits and living trees) within radii of 12.6 m. Mortality was determined by calculating the total distance-weighted loss of basal area of dead trees per five-year interval in the neighbourhood. G was obtained by summing all distance-weighted net basal area increments of neighbouring living trees. For two consecutive surveys, the average M and G values were calculated to represent the mortality and growth of established trees in the neighbourhood for a given survey interval. For recruits, whose spatial positions only became available after being observed, we calculated their neighbourhood M and G in the previous survey by using their spatial position from the current survey.

We calculated the neighbourhood crowding index (NCI) by summing all distance-weighted basal areas from living neighbouring trees (inclusive of recruits; Canham et al., 2004).

$$NCI_{ijk} = \sum_{n \neq i} \left(\frac{B_{njk}}{(D_{in})_{jk}} \right) \qquad (4)$$

where *i, j,* and *k* are the *i*th focal stem, *j*th survey, and *k*th plot, respectively, *n* are the n*th* neighbour trees, and B and D_{in} are the tree's basal area and the distance between the focal stem *i*th and the *n*th neighbour trees. We used basal area instead of the DBH to emphasize the importance of larger trees on sapling recruitment. Functional and phylogenetic dissimilarities were derived to quantify neighbourhood diversity (Zhu et al., 2022), and shade tolerance was used as our measurement of functional niche, which broadly represented species resource strategies in the forest understory (Chen et al., 1996). We adopted species shade tolerance values from Niinemets and Valladares (2006), who gave values from 1 to 5 to denote highly

shade-intolerant to shade-tolerant species corresponding to the minimum understory light availability required for an individual species to photosynthesize, grow and survive (Chen, 1997, Chen and Klinka, 1997).

The phylogeny of our studied species was obtained using the Phylomatic version 3 website client (http://phylodiversity.net/phylomatic/). The phylogenetic relatedness, i.e., the pairwise phylogenetic distance between all species pairs, was calculated using the cophenetic function. For the studied species, we developed a normalized phylogenetic distance matrix with the maximum dissimilarity set to 1 and maximum similarity (i.e., a neighbour of the same species as the focal tree) to 0 by dividing each value in the matrix by the maximum paired distance.

We calculated the neighbourhood shade tolerance dissimilarity (STD) and phylogenetic dissimilarity (PD) using the following equation:

$$\text{STD or PD}_{ijk} = \frac{\sum_{n \neq i} abs(DIS_{in}) \times \frac{B_{njk}}{(D_{in})_{jk}}}{\sum_1^{n \neq i} \frac{B_{njk}}{(D_{in})_{jk}}} \tag{5}$$

where STD or PD_{ijk} is the weighted mean of neighbourhood shade tolerance dissimilarity or phylogenetic dissimilarity, $abs(DIS_{in})$ is the absolute difference of shade tolerance or phylogenetic relatedness between the focal stem ith and nth neighbour trees, and B and D are basal area and distance. The means of NCI, STD, and PD of two successive surveys were obtained to represent the neighbourhood interactions for a given survey interval. All explanatory variables across the studied plots are presented in Table S3-3. The shade tolerance dissimilarity and phylogenetic dissimilarity of all species compared with the postfire pioneer species *Populus tremuloides* are presented in Fig. S3-5.

47

Because a predefined radius of the local neighbourhood surrounding a focal tree could influence the conclusion about the community pattern (Zambrano et al., 2020), we compared the M, G, NCI, STD, and PD values estimated by different radii from 5.0 m, 7.5 m, 10.0 m to 12.6 m. As focal stems were not at the physical centre of the plot, we corrected for M, G, and NCI for edge effects using an area-weighted correction (Das et al., 2008) based on the analysis that our plots were located in homogeneous forest stands, in terms of tree size and species composition (Luo and Chen, 2015). For instance, if 40% of the focal stem neighbourhood resided beyond the plot's boundaries, M's raw value was divided by 0.6 to obtain the full estimate. We examined the bivariate relationships between sapling recruitment probability and explanatory variables estimated from the different radii. We found that these relationships were consistently similar, and the estimates from the 12.6-m radius yielded the lowest Akaike information criterion (AIC) value. Accordingly, we report results on a radius of 12.6 m.

3.3.3 Statistical analysis

The five-year sapling recruitment probability was analyzed at the individual tree level to evaluate the relationships between sapling recruitment probability (derived from tree status, 1 for a recruit and 0 for an established living tree), Y, M, G, NCI, STD, and PD based on the conceptual model (Fig. 3-2). To assist in the development of structural equation models (SEMs), we assessed the bivariate relationships between each explanatory variable and sapling recruitment probability. We used AIC to compare the alternative functions in a generalized linear mixed model (GLMM, binomial distribution and *logit* link) with the random effects of "plot" and "tree species." Since the bivariate models with linear Y, logarithmic M, logarithmic G, logarithmic NCI, linear STD, and linear PD resulted in lower or similar AIC values, they were used in the SEMs.

Several alternative SEMs were constructed based on our conceptual model (Fig. 3-2, see Supplement Methods in Appendix II and Rcode in Appendix IV). The first alternative SEM assumed that the effects of Y on M and G indirectly impacted NCI, STD, and PD, and simultaneously, the response of NCI, STD, and PD feedback to M and G, and consequently, sapling recruitment (Fig. 3-2). A second SEM assumed that the effects of Y on NCI, STD, and PD influenced M and G, and consequently, sapling recruitment. A third alternative SEM assumed that the effects of Y on M and G influenced NCI, STD, and PD, and consequently, sapling recruitment.

In the PSP database, each plot has a specified known stand establishment year, i.e., the year of the last stand-replacing fire, and stand age (SA) was the difference between the measurement year and the stand establishment year. For longitudinal data, both Y and SA increased with repeated measurements. Although our sample stands had a wide range of initial ages, there was a positive correlation between Y and SA ($r = 0.069$, $P < 0.001$). To account for the potential effects of SA on sapling recruitment, a fourth SEM was developed by integrating SA into the first SEM in parallel with Y, with a correlation between Y and SA. This represented simultaneous changes in climate and stand development since the covariation between Y and SA could not be prioritized (Graham, 2003, Chen et al., 2016a).

The SEMs were implemented using the *piecewiseSEM* package (Lefcheck, 2023), which allowed the use of multiple mixed-effect models to account for the random effects. For both GLMM and LMM submodels in the SEMs, models were performed with "plot nested individual tree" as a random effect to address pseudo-replication resulting from repeated measurements of stems over the study period. In addition, we used "species" as a random effect in the GLMM submodel. However, all SEMs generated a singular (boundary) fit

warning, which could be attributed to overfitting caused by complex random structures, and a variance of the random term close to zero ($<10^{-4}$; Bates et al., 2015). While singular models demonstrate well-defined statistical properties and tend to approach the "best" fitting model, concerns about the reliability of the estimates have been raised. As a result, we followed a method from Barr et al. (2013) and simplified or removed the random effects until convergence was achieved. In sum, the sapling recruitment submodel with GLMM adopted the random effects of "plot" and "species," while submodels with LMM adopted only "plot" as the random effect in all analyses. The Area Under the Curve (AUC) was estimated for the GLMM model performance, using the *pROC* package (Robin et al., 2021), wherein an AUC of > 0.7 was considered acceptable. The model R^2 was estimated for LMM performance using the *rsquared* function in the *piecewiseSEM* package.

Goodness-of-fit statistics (Fisher's C with *P*-values) were employed as criteria to examine the model fit of each SEM (Garrido et al., 2022), while AICs were used to compare alternative SEMs (Table S3-4). A *P*-value greater than 0.05 meant that a model was a good fit for the data when all informative paths were included. We compared the four alternative SEMs (Table S3-4) and focused on presenting the first SEM, which showed a good fit for both our theoretical prediction and the data. The AIC results suggested that the mortality and growth of established trees and neighbourhood interactions could be simplified by their correlations, and stand age could be omitted, as its inclusion led to a larger AIC value (Table S3-4). Finally, Mantel tests were used to examine spatial autocorrelations among the plots for the mean five-year sapling recruitment rate and the plot identity on each relationship within the first SEM using the *ade4* package (Dray et al., 2022), and the results indicated no spatial autocorrelation (Table S3-5). Durbin-Watson tests were used to examine temporal autocorrelations among the

residual of the sapling recruitment in the first SEM using the *DHARMa* package (Hartig, 2022). We found no evidence of temporal autocorrelation (DW = 2.056, P = 0.518).

The direct and indirect effects of climate change on sapling recruitment were quantified as their standardized coefficients (coefficient estimates scaled by one stand deviation of the predictor) (Grömping, 2015, Grace, 2006). This approach was independent of the range of predictor values observed. Indirect effects were calculated by using standardized coefficients along the paths (e.g., the coefficient for Y to M multiplied by the coefficient for M to sapling recruitment). The total effects on sapling recruitment were the sum of the direct and all indirect effects.

To gain mechanistic insights into the effects on sapling recruitment of hypothesized climate change factors, including rising atmospheric CO_2, ATA, and SPEI, we built an SEM with a composite variable of "climate change" to replace Y (Table S3-4, S3-6). The compositive variable was constructed as the first axis value (PC1) of the principal component analysis (PCA) with those three climate change factors that represented 61.5% of the variation (Fig. S3-6). All statistical analyses were performed in the R statistical program, version 4.2.2 (R Development Core Team, 2022).

3.3 Results

The first SEM, with the direct and indirect effects of a temporal trend likely related to climate change, collectively represented by the middle calendar year of a five-year survey, via mortality and growth of established trees and neighbourhood interactions and their correlations, had the lowest AIC among all alternative SEM models (Table S3-4). During the study period, atmospheric CO_2 concentration, temperature, and water availability increased temporally (Fig. S3-2). The SEM with a composite variable of the three climate predictors

(explaining 61.5% of the variation) in place of the calendar year in the first SEM produced a similar AIC (Table S3-4, S3-6). We focused on reporting the first SEM with the calendar year as a temporal trend of climate change (Figs. 3-3, 3-4, Table S3-7).

This SEM revealed that sapling recruitment probability had no direct response to temporal variation (Fig. 3-3, 3-4, Table S3-7). However, mortality and growth of established trees increased over time, in turn causing an indirect negative effect of temporal variation on sapling recruitment via mortality and growth (Figs. 3-3, 3-4, Table S3-7). Neighbourhood crowding, shade tolerance dissimilarity, and phylogenetic dissimilarity also increased over time. Temporal variation had a strong indirect negative effect on sapling recruitment via neighbourhood crowding and weak indirect positive effects via shade tolerance dissimilarity and phylogenetic dissimilarity (Fig. 3-3, 3-4, Table S3-7). The total effect of temporal variation was negative, both direct and indirect effects considered (Fig. 3-4). The same SEM indicated multiple correlated drivers and potential mechanisms that influenced sapling recruitment over time. Mortality and growth of established trees were positively correlated and were positively related to neighbourhood crowding (Fig. 3-3, Table S3-7). Shade tolerance and phylogenetic dissimilarity were positively correlated (Fig. 3-3, Table S3-7). The mortality of established trees was positively correlated with shade tolerance and phylogenetic dissimilarity (Fig. 3-3, Table S3-7). Growth of established trees was negatively correlated with shade tolerance dissimilarity but positively correlated with phylogenetic dissimilarity (Fig. 3-3, Table S3-7).
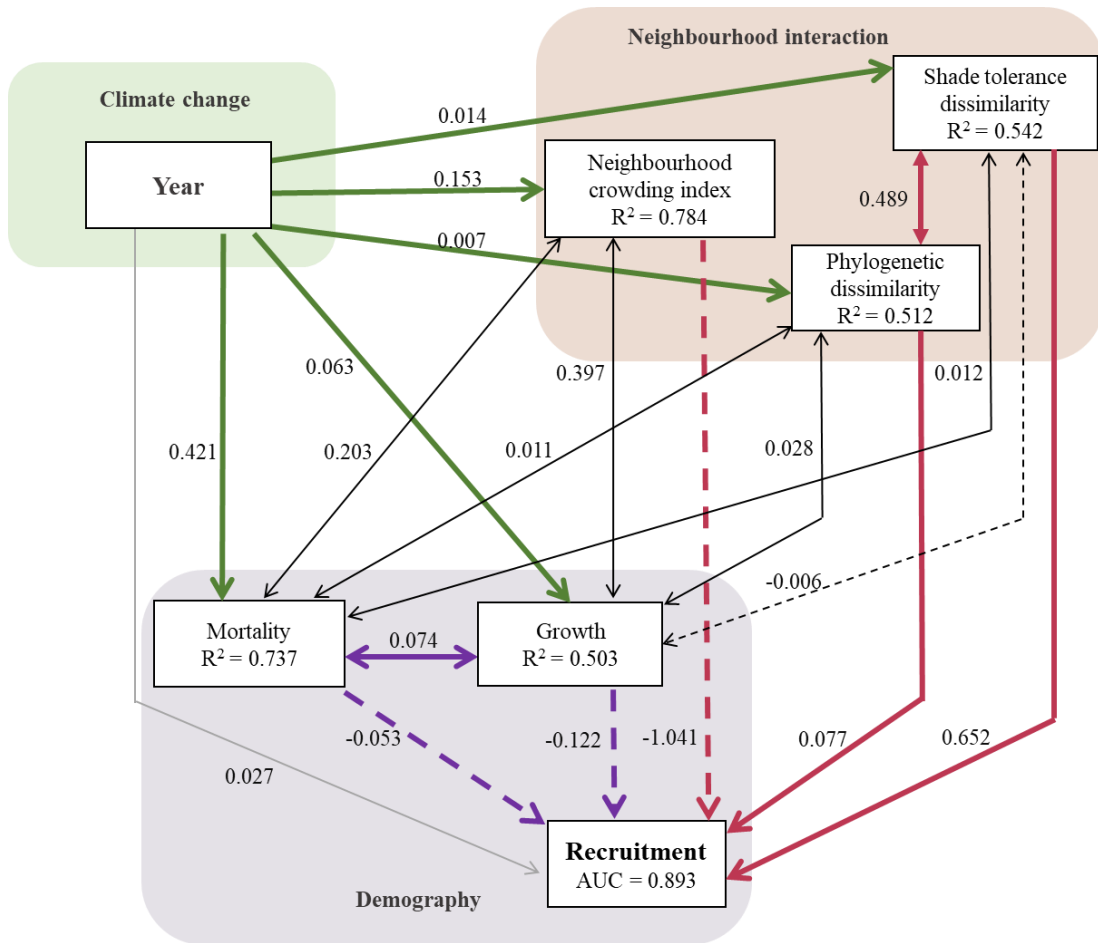
Figure 3-3: Structural equation model links the direct and indirect effects of climate change (calendar year to represent climate change associated temporal trend as a whole) through mortality and growth of established trees, neighbourhood crowding, shade tolerance dissimilarity, and phylogenetic dissimilarity. The values are standardized coefficients for the corresponding path. Colours represent the effect from or correlation within each box in figure 3-2, black represents the correlation between each box, and grey represents nonsignificant pathways. Solid lines represent positive relationships, and dashed lines represent negative relationships. Single-direction arrows represent the effect, while black double-direction arrows represent correlations. The AUC represents the area under the curve, while R^2 is conditional, including fixed and random effects.
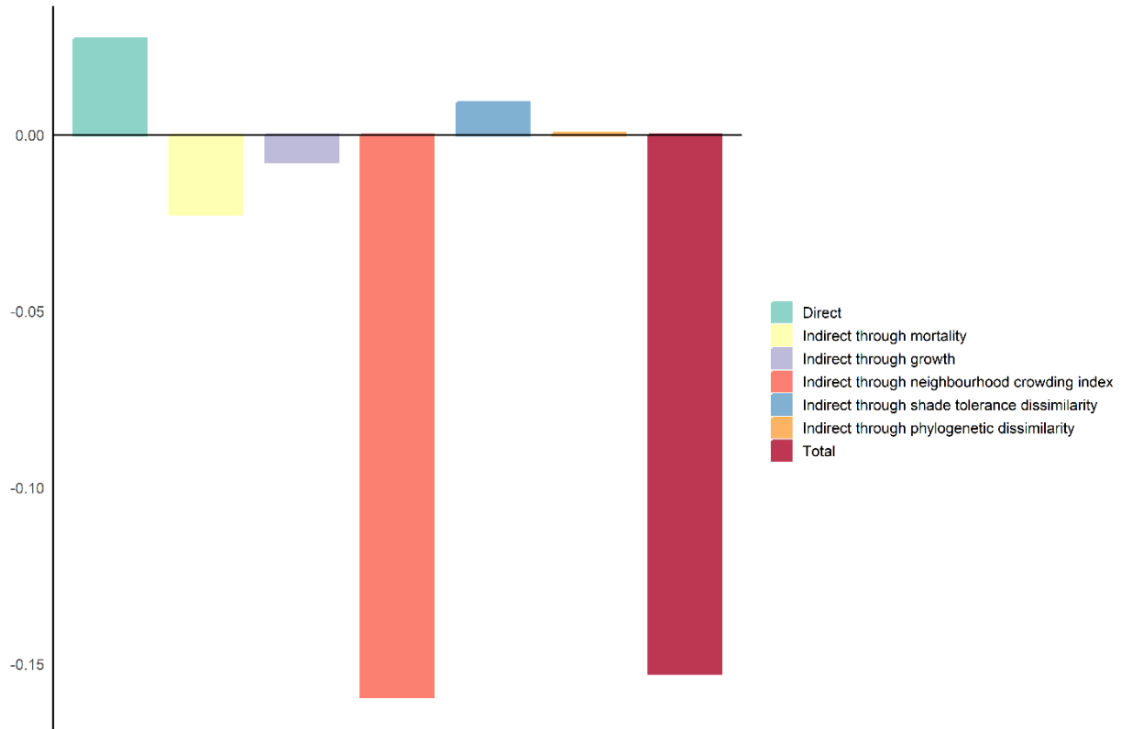
Figure 3-4: Standardized effects of direct, indirect, and total impacts of temporal variations on sapling recruitment. The total effect was summed with both direct and indirect effects.

3.5 Discussion

Direct effect of climate change on sapling recruitment

Our structural equation model revealed that the calendar year to represent temporal variation had no direct effect on sapling recruitment in the central boreal forest of North America. This result is consistent with some previous studies suggesting that climate change has at best a weak effect on sapling recruitment in the forest understorey (Zhang et al., 2015), as a dense or closed forest canopy can buffer against macroclimate temperature extremes experienced by its understorey (De Frenne et al., 2021, Zellweger et al., 2020). Some earlier studies in North America demonstrated that long-term water deficits reduce tree recruitment in established forests (van Mantgem et al., 2009, Peng et al., 2011). During the monitoring period

of our studied plots, water availability increased temporally without apparent climate change-induced drought events (Luo and Chen, 2015). Rising CO_2, warming and longer growing seasons may alleviate resource and metabolic constraints in forests when water is abundant (Berner and Goetz, 2022). Our best-fit structural equation model, using the composite variable of the three major climate change drivers (rising CO_2, warming, and increasing water availability), suggested that sapling recruitment may directly benefit from these three favourable outcomes of climate change (Table S3-6). However, other climate change drivers that were not examined could offset their positive effects. For example, increased evaporation associated with warming may lead to water deficits during the growing season (Reich et al., 2022), and earlier phenology triggered by warmer springs may create a higher risk of frost damage (Marquis et al., 2020).

Indirect effects of climate change via mortality and growth on sapling recruitment

We found that mortality, measured at the neighbourhood scale, and growth of established trees both increased over the study period. As temperatures increased over time, an increase in mortality could be due to a vapour pressure deficit under heat stress experienced by canopy trees during midsummer (Trugman et al., 2018). The increased tree mortality in our study region could also be attributed to intensified intraspecific competition from the warming-induced faster growth of shade-intolerant species, such as *Populus* spp. and early successional conifers, such as *Pinus* spp. (Searle and Chen, 2017, Luo and Chen, 2015). Furthermore, higher mortality may have resulted from faster growth promoted by climate change, which reduces tree longevity as a trade-off (Brienen et al., 2015, Searle and Chen, 2018). Increased neighbourhood growth of established trees in this study suggests that tree growth may benefit more from extended growing seasons and warming springs over the long term (Berner and

Goetz, 2022). The positive relationship between mortality and the growth of established trees indicates that resources released from dead trees may benefit the growth of established trees, which is consistent with observations elsewhere (Chen et al., 2016a, Chen et al., 2019b).

In contrast to our expectations, the mortality of established trees had a negative direct effect on sapling recruitment, which led to temporal variation having an indirect negative effect on sapling recruitment via increased mortality. This result contrasts with the idea that new saplings can occupy canopy gaps formed by tree mortality (Hubbell et al., 1999, Chen and Popadiouk, 2002). This result also appears to contradict evidence showing that the compensating role of recruitment can be promoted by increased tree mortality caused by climate change (Lloret et al., 2012, McDowell et al., 2020, Berner and Goetz, 2022). Our result showing that sapling recruitment probability decreased from increased mortality from neighbouring established trees suggests that sudden exposure of saplings to canopy gaps formed from tree mortality may result in heat stress during the day and frost damage during the night (De Frenne et al., 2021, Zellweger et al., 2020). Moreover, falls of dead trees may have directly destroyed some saplings and increased the probability of physical damage to saplings due to strong winds and heavy snowpacks at high latitudes (Kroiss and Hillerslambers, 2015, Franklin et al., 2002). Our result extends the findings that climate change can increase the mortality of seedlings without compensating it by increases in tree recruitment of old-growth forests >80 years, where water availability has been decreasing (van Mantgem et al., 2009, Peng et al., 2011).

In alignment with our expectations, we found that temporal variation had indirect negative effects on sapling recruitment via increased growth of established trees. Our results contrast with the previous result showing that favourable climate change could accelerate

positive synchronization of tree growth and recruitment (Fajardo and McIntire, 2012, McDowell et al., 2020). The loss of synchrony from decreased sapling recruitment with the increasing growth of established trees may be attributable to the asymmetric competition from larger trees (Coomes et al., 2011), whose increased size and expanded leaves and branches decrease light availability for sapling recruitment (Chen et al., 2019a). Our results highlight the competition effect on sapling recruitment from the growth of established trees, especially that of fast-growing species, on the recruitment of saplings, which are most likely shade-tolerant coniferous species that reside in the understory for decades (Hanbury-Brown et al., 2022). In contrast with previous observations of drought-induced indirect positive effects from increased mortality to canopy loss on sapling recruitment in moist tropical forests (Chen et al., 2019a), here we propose with caution that favourable climate change, such as increased CO_2, temperature and water availability could cause indirect adverse effects from increased the growth of established trees on sapling recruitment in the colder boreal forest.

Indirect effects of climate change via neighbourhood interactions on sapling recruitment

We found that temporal variations had an indirect negative effect on sapling recruitment via increased neighbourhood crowding of established trees. The increase in neighbourhood crowding suggested that increases in growth induced by temporal trend changes overwhelmed mortality in our studied forests. The growth of surrounding fast-growing species, such as *Populus tremuloides*, can offset climate change-induced tree mortality loss that reduces competition (Luo et al., 2019, Chen et al., 2016a). The increase in neighbourhood crowding was expected to exert a negative impact on sapling recruitment because neighbourhood crowding is a dominant driver for tree demographic processes, especially for sapling recruitment in the understorey, where light is one of the most limiting resources

(Hubbell et al., 1999, Yang et al., 2022, Zhu et al., 2022, Chen et al., 2019a). Our results did demonstrate that neighbourhood crowding increased over time and decreased resources available for sapling recruitment. We cautiously weighed the relative importance of competition and climate change, considering the relationship between forest structure, stand age, and demography undergoes spatial and temporal changes (Astigarraga et al., 2020). We did find that the increase in neighbourhood crowding was positively associated with the mortality and growth of established trees. These factors together exerted strong negative effects on sapling recruitment.

Despite the small magnitudes of their effects, we found that temporal variation had indirect positive effects on sapling recruitment via increased neighbourhood dissimilarities in shade tolerance and phylogeny. This result suggests that favourable climate change can amplify the positive effects of neighbourhood interactions to accommodate more species (Usinowicz et al., 2017). Consistent with our expectations and the previous analysis of Zhu et al. (2022), sapling recruitment responded positively to greater shade tolerance dissimilarities, which promotes crown complementarity (Barry et al., 2019). Furthermore, increased neighbourhood phylogenetic dissimilarity induced by temporal variations positively influenced sapling recruitment, likely by reducing the impacts of specialized pathogens and insect herbivores through host dilution. Our results extended the understanding of neighbourhood dissimilarities in mediating changing climate on sapling recruitment in forests with high species diversity (Chen et al., 2019a, 2019b) to species-poor forests, where the difference in mixture of broadleaves and conifers plays an important role in determining stand development stages (Zhu et al., 2022). However, since the positive effects of neighbourhood dissimilarities

only partially ameliorated the negative crowding effect, the overall effect of neighbourhood interactions on sapling recruitment is still negative.

Conclusion

We demonstrate that temporal variation can exert an overall negative effect on sapling recruitment probably due to the stronger negative indirect effect of neighbourhood trees over the direct benefits of climate change on saplings. Although atmospheric CO_2 concentration, temperature, and water availability simultaneously increased during the three decades of the study period, sapling recruitment did not show a significant direct response to temporal variation. By explicitly analyzing the simultaneous responses of all three demographics to temporal variations and their modifications to neighbourhood interactions, our results provide evidence that sapling recruitment is driven largely by the indirect effects of temporal variation through altered neighbourhood conditions. In contrast to the theoretical prediction (McDowell et al., 2020), our findings reveal that sapling recruitment does not necessarily compensate for the increased mortality of established trees. The released resource from increased tree mortality is prioritized by the growth of established trees, which in turn exerts an indirect negative effect on sapling recruitment. This interpretation suggests that faster turnover in the overstorey, with higher mortality and increased growth of established trees under current climate change, could adversely affect sapling recruitment. In this way, decreased sapling recruitment, mainly for shade-tolerant species, can affect forest succession and species composition in the long term. Temporal increase of climate change-associated neighbourhood crowding, shade tolerance and phylogenetic dissimilarities were tracked, with negative and positive effects on recruitment and an overall negative effect of climate change-induced neighbourhood interactions. Our results

suggest that even so-called favourable climate change can pose a threat to long-term ecosystem functionality.

CHAPTER 4: CONSPECIFIC NEGATIVE DENSITY DEPENDENCE DRIVES TREE SPECIES DIVERSITY THROUGH STAND DEVELOPMENT

4.1 Abstract

Conspecific negative density dependence (CNDD) is the process that decreases individual demographic performance (the three demographics of tree recruitment, survival, and growth) at high conspecific densities to facilitate less abundant species. CNDD has been demonstrated to maintain tree species diversity in mature and old-growth forests Although tree species diversity changes with stand development, it remains unclear how CNDD influences the three demographics simultaneously and how their specific strengths shift following stand development in a way that contributes to regulating tree species diversity dynamics. Using a dataset of spatially mapped, repeatedly measured stems with stand ages ranging from 8 to 166 years after fire in the central boreal forest of North America, we provide strong evidence that CNDD effects on the three demographics resulted from stronger negative density dependence of conspecifics than heterospecifics, and they decreased significantly with stand age. The stand age-dependent CNDD effect was more pronounced changes in the CNDD effects on recruitment and survival than on growth. The strong CNDD effects in young stands provide the potential to contribute to initial increases in tree species richness, but the lack of CNDD effects in older stands leads to reduced species richness, resulting in a hump-shaped species richness pattern with stand age. Our findings also suggest that the CNDD effects may be manifested by resource competition rather than natural enemy attacks in shaping tree species diversity along stand development.

4.2 Introduction

Understanding the generation and maintenance of species diversity remains a critical challenge for ecologists. Conspecific negative density dependence (CNDD) is a process that reduces individual demographic performance at a high-conspecific adult density due to increased resource competition (Tilman, 1982, Chesson, 2000) and attacks by natural enemies, such as insects and pathogens (Janzen, 1970, Connell, 1971). As a result, CNDD is hypothesized to be the critical mechanism responsible for maintaining highly diverse tropical forests by facilitating the survival of less abundant species (Comita et al., 2010, Connell et al., 1984). Over the past five decades, many studies have shown evidence of CNDD in promoting localized plant species coexistence in different ecosystems (Adler et al., 2018) and have revealed that greater CNDD maintains higher tree species richness regardless of latitude (LaManna et al., 2022), elevation (Lebrija-Trejos et al., 2023, Huang et al., 2020), and moisture and nutrient gradients (Lebrija-Trejos et al., 2023, Huang et al., 2020). However, more recent studies question the methodology used in studies of CNDD, suggesting that it may overestimate CNDD effects (Connell, 1978). Nevertheless, tree species diversity changes with stand development and is collectively regulated by the three demographic processes of recruitment, survival and growth (Connell et al., 1984). Yet, it remains unclear whether the effects of CNDD on these three demographic rates change during stand development and, in turn, how they may contribute to tree species diversity dynamics following a stand-replacing disturbance.
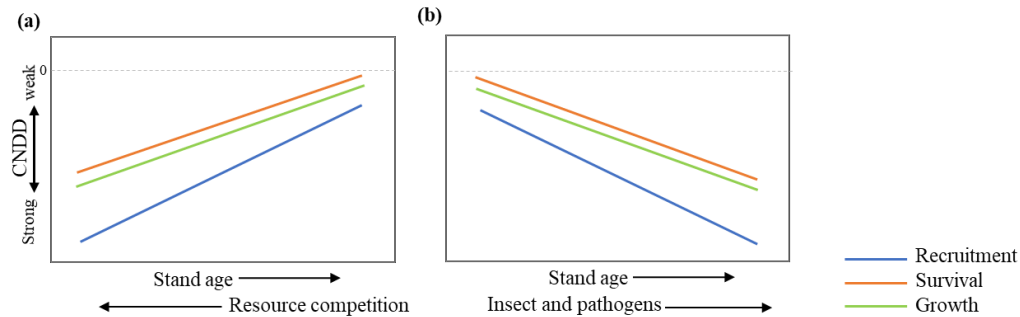
Figure 4-1: The hypotheses in the strength of conspecific negative density dependence (CNDD) on recruitment, survival and growth along stand age. (a) The strength of CNDD is hypothesized to decrease with stand age due to alleviated competition, stronger on recruitment than survival and growth due to asymmetric competition. (b) The strength of CNDD is hypothesized to increase with stand age due to accumulated pests and pathogens, stronger on recruitment which is more vulnerable to recruitment than survival and growth. CNDD is the difference in the effects of conspecific density (same species) and heterospecific density (other species) below 0.

CNDD may simultaneously affect the three demographics but with different strengths. Studies focusing on the response of one particular demographic component to CNDD may not represent the entire life cycle and fitness of the whole community (Hülsmann et al., 2021, Barry and Schnitzer, 2021). Thus, it has been recommended to simultaneously examine different demographic components under CNDD (Detto et al., 2019, LaManna et al., 2021). Sapling recruitment integrates several processes at the early life stage, including seed germination, survival and growth of seedlings, and their transition to saplings, and may be more strongly affected by CNDD than the survival and growth of larger established trees. Compared with established trees, seedlings and saplings have been reported to experience stronger CNDD due to size-asymmetric competition, especially for light, and they are more susceptible to herbivores and pathogens (Zhu et al., 2018, Yao et al., 2020, Zhu et al., 2015). In addition, for long-lived organisms, the effects of CNDD on survival and growth might be

diluted through ontogeny, as larger trees typically have higher shade tolerance and defence against natural enemies (Zhu et al., 2015).

The effects of CNDD may change with stand age (Fig. 4-1). If the effect of CNDD is predominantly manifested as resource-based competition (Chesson, 2000, Tilman, 1982), then the strength of the effects of CNDD may decrease with stand age (Fig. 4-1a). This hypothesis is based on the strong competition that tends to occur in young stands, characterized by the rapid growth of smaller stems after stand establishment and limited resources such as space and light; as the stand develops, resource competition tends to weaken when shade-intolerant pioneer cohorts begin to senesce (Franklin et al., 2002, Chen and Popadiouk, 2002). Moreover, the effects of CNDD might be stronger on recruitment compared with survival and growth in young stands because of the asymmetric competition for resources prioritized for larger trees (Luo and Chen, 2011), but the different effects of CNDD on the three demographics may become minimal with more available resources from canopy gaps in older stands. However, if the effect of CNDD is dominantly manifested by natural enemy attacks (Forrister et al., 2019, Janzen, 1970, Connell, 1971), its impact may increase with stand age due to the accumulation of insects and pathogens following stand-replacing fire (Parker et al., 2006; Fig. 4-1b). Accordingly, the increase in CNDD effect with stand age may be more pronounced for recruitment than for survival and growth.

Tree species diversity generally exhibits a non-linear pattern with stand development and peaks at intermediate stages (Taylor et al., 2020, Connell, 1978). These temporal diversity dynamics may result from the changes in CNDD (Fig. 4-1). Recent studies have suggested that a certain level of CNDD effects is necessary for the maintenance of diversity in mature or steady-state old-growth forests (LaManna et al., 2017b, Johnson et al., 2012, Comita et al.,

2010, Lutz et al., 2014). Conceptually, greater effects of CNDD are required to generate higher diversity than to maintain a similar level of diversity. Specifically, the negative effect of conspecific density (CD) overcomes an intrinsic fitness advantage from heterospecific density (HD) as each species becomes less dominant. Recent studies indicate that a stronger effect of CNDD on mortality at early life stages contributes to increased tree species diversity in later stages (Green et al., 2014, Lebrija-Trejos et al., 2023). Regrettably, no studies have explored the possible connection between CNDD and tree diversity dynamics associated with stand development. The lack of such studies may be attributed to the fact that long-term repeated measurements of multiple demographic rates are necessary to obtain robust estimates of CNDD effects and their contribution to diversity dynamics (Detto et al., 2019, LaManna et al., 2021).

Here, we analyzed individual stem data from 153 permanent sample plots (PSPs) in the central North American boreal forest aged from 8 to 166 years. The plots were repeatedly measured and spatially mapped at five-year intervals for 25 years. We used the plot information to explore the effect of CD and HD on recruitment probability, survival probability, and growth rate. We specifically examined 1) whether the strength of the effect of CNDD differs among recruitment, survival, and growth, 2) how these CNDD effects change with stand age, and 3) how the CNDD effects may influence tree species diversity dynamics at different stand ages.

4.3 Materials and Methods

4.3.1 Study area and plots

This study was conducted from data collected in a permanent sample plot (PSP) network located in Manitoba, Canada, a central region of the boreal forest in North America

that spans from 49°04′ to 56°99′ N latitude and from 95°30′ to 101°68′ W longitude (Fig. S4-1). The plot elevations range from 159 m to 426 m. The region has a subarctic climate characterized by long, cold winters and short, cool summers. During the 30-year climate normal from 1981-2010, the average temperate ranged from -3.1 to 3.0 °C, and average annual precipitation from rainfall and snowfall varied from 443 to 674 mm. The primary natural stand-replacing disturbance has been wildfire, with the return frequency typically less than 100 years (Senici et al. 2010). Following stand-replacing wildfire, stands undergo various stages of development, including stand initiation, stem exclusion, canopy transition, and gap dynamics (Chen & Popadiouk 2002).

The PSPs were established to monitor tree growth and yield in the mid-1980s. Trees were spatially mapped and repeatedly measured as much as every five years. All PSPs were created with a fixed diameter of 12.6 m and an area of 500 m^2 in stands that span at least four hectares to protect edge effects from the boundary. The PSPs were allocated in visually homogenous stands to avoid differences in soil nutrients and elevation. For this study, plots from the PSP network were selected by employing the following criteria: (1) PSPs were established after a stand-replacing fire and contained natural forest without any management; (2) the survey interval was five years with at least two consecutive surveys; (3) PSPs were not a monoculture, with at least two species mixed in plots. As a result, 153 plots were selected for our analysis (Fig. S4-1).

4.3.2 Measurements of recruitment, survival, and growth

During plot establishment, all trees ≥ 1.5 m in height were tagged, identified by species, and assigned diameters at breast height (DBH); they were mapped by their directions (degrees

66

from north) and distances (to the nearest cm) from the plot center. Subsequent measurements were taken every five years until 2010 when the sampling protocol was modified. These measurements included recording the DBHs of surviving trees, noting dead trees without living branches at 1.5 m as mortality, and recording recruits that had grown to 1.5 m height with species identified and DBHs measured. Individual tree growth was estimated as the annual basal area increment (cm^2 $year^{-1}$) of living trees. Annual basal area growth was computed by taking the difference between the basal area measurements at two consecutive survey periods divided by five years.

A total of 10,433 recruits, 19,380 trees of mortality, and 215,612 total observations of 63,548 live trees were repeatedly measured over the course of the study period (Table S4-1, Fig. S4-2). The dominant tree species in the PSPs included *Picea mariana* (36.9%, relative abundance, percentage of total living tree counts), *Pinus banksiana* (25.3%), and *Populus tremuloides* (21.4%). The minor tree species included *Abies balsamea* (5.7%), *Betula papyrifera* (2.8%). *Fraxinus nigra* (3.1%), *Picea glauca* (2.0%), *Larix laricina* (1.6%), and *Thuja occidentalis* (1.1%; Table S4-1). Other species included *Ulmus americana*, *Quercus macrocarpa, Acer negundo, Fraxinus pennsylvanica*, and *Pinus resinosa*. The relative abundance of recruits mirrored the rank of adult trees, including *Picea mariana* (65.7%), *Populus tremuloides* (11.1%), *Pinus banksiana* (9.8%), *Abies balsamea* (3.6%), *Betula papyrifera* (4.3%), *Fraxinus nigra* (2.5%), *Picea glauca* (1.0%), *Larix laricina* (0.3%), and *Thuja occidentalis* (1.2%).

4.3.3 Predictor variables

We derived stand age (SA, years) as the difference between the years of measurement for stands established and the stand initiating fire, as fire records became available for

Canadian forests in the early 20th century. Similar to a previous study (Senici et al., 2010), for the stands without fire records, dendrochronological aging was employed based on coring dominant or co-dominant trees outside the plot and using the average tree ring counts of the oldest species at the time of plot establishment.

Crowding between neighbouring trees is a good proxy for resource competition and the density of potential pests and pathogens. Similar to a previous study of recruitment probability (Zhu et al., 2022), we used the neighbourhood crowding index (NCI) to integrate the summed basal area of living neighbouring trees and their distance from the focal tree (living tree or recruit), defined as:

$$\text{NCI}_{ijk} = \sum_{n \neq i} \left(\text{BA}_{njk} * \frac{1}{(\text{D}_{in})_{jk}} \right) \tag{6}$$

where NCI is the neighbourhood crowding index; i, j, and k are the ith focal stem, jth plot, and kth survey, respectively; n is the nth neighbour tree; BA and D_{in} are the basal area and the distance between the focal stem of the ith and the nth neighbouring tree.

Unlike recruits that had no initial stage information before the survey where they occurred, an established tree had an initial size, so for survival and growth, we used the Hegyi index (H), which quantifies the neighbourhood crowding based on summed neighbouring tree sizes relative to the focal tree size and their distance to the focal tree (living and dead tree, not a recruit; Hegyi, 1974). We modified the H using BA to replace DBH, to upscale the importance of larger trees, as follows:

$$H_{ijk} = \sum_{n \neq i} \left(\frac{\text{BA}_{njk}}{\text{BA}_{ijk}} * \frac{1}{(\text{D}_{in})_{jk}} \right) \tag{7}$$

where H is the Hegyi index; i, n, j, k, BA, and D are the same as in Eqn. 1.

We calculated conspecific density (CD) as conspecific neighbourhood crowding values and heterospecific density (HD) as neighbourhood crowding values based on equations 1 and 2. The CD and HD for individual trees can change between two consecutive surveys due to changes in tree sizes and mortality. Since recruitment was only recorded in the second of two consecutive surveys, we calculated its CD or HD for the first census by assuming no change in a recruit's spatial location. We used the average CD and HD of the two consecutive censuses to represent the neighbourhood crowding of individual stems during a five-year survey interval.

Improving the estimate of CNDD effects requires an appropriate metric of spatial scale (Detto et al., 2019). We employed radii of 5.0 m, 7.5 m, 10.0 m and 12.6 m to quantify CD and HD within each sample plot. Because our plots were located in homogeneous forest stands in terms of tree size and species composition (Luo and Chen, 2015), we corrected plot edge effects using an area-weighted edge correction (Das et al., 2008). For instance, if 30% of the focal stem neighbourhood resided beyond a plot's boundaries, the raw value of CD was divided by 0.7 to obtain the full estimate within a 12.6-m radius. The CD or HD values were highly correlated among the estimates of different radii ($r > 0.79$ in all cases), and the statistical models (see Eqn. 3 below) with the CD and HD from a radius of 12.6 m yielded the lowest AIC. Accordingly, we focus on reporting the results based on the radius of 12.6 m.

4.3.4 Statistical analysis

For recruitment and survival probability over five years, we employed generalized linear mixed models (GLMM) with a binomial distribution and *logit* link. For the annual growth rate, we used a linear mixed model (LMM) with a Gaussian distribution. For each

demographic rate, we used the following model to simultaneously examine the effects of the

CD, HD and SA and their interactions:

$$y_{ijklm} = \beta_0 + \beta_1 \cdot CD_{ijk} + \beta_2 \cdot HD_{ijk} + \beta_3 \cdot SA_{ijk} + \beta_4 \cdot CD_{ijk} \times SA_{ijk} + \beta_5 \cdot$$

$$HD_{ijk} \times SA_{ijk} + \alpha_k + \alpha_l + （\alpha_m + ） \varepsilon_{ijkl}/\varepsilon_{ijklm} \tag{8}$$

where y_{ijklm} is the recruitment probability or survival probability over a five-year interval or

the annual growth rate; CD, HD, and SA are the average values of conspecific density,

heterospecific density, and stand age over the five-year interval (Table S4-2); β is the

coefficient to be estimated; *i, j, k* are the same as for Eqn. 1; α_k, and α_l are random intercept

terms representing the plot, species, and α_m is random intercept terms representing the

individual tree nested in the plot, only for the tree growth model with LMM, not for the

recruitment and survival model with GLMM with discrete event modelling, and $\varepsilon_{ijkl}/\varepsilon_{ijklm}$ is

the random error.

As recommended by Detto et al. (2019), we introduced an exponent parameter c to CD

and HD to regulate nonlinearity from local interactions on demographics and avoid the

spurious trend from an underestimation of CNDD for the more abundant species. We selected

the exponent parameters with the maximum likelihood value, based on allotted difference

values from 0.01 to 1.00 for CD and HD in the main model (Fig. S4-3). Values of c < 1

allowed for diminishing effects of density on demographics at a higher local density and had

no additional effects on demographics. We selected the exponent parameters with the

maximum likelihood value of the main model (Fig. S4-3). The exponent c was assigned as 0.38

for CD and HD in the recruitment model, 0.09 in the survival model, and 0.12 in the growth

model. Logarithmic SA was in all three models, which yielded lower AIC values for the

models than the alternative linear form of SA. All predictors were standardized, i.e., subtracting their mean and then dividing by their standard deviation, to facilitate a direct comparison between the effects of CD and HD.

To assess the potential for overfitting, we used the *dredge* function of the *MuMIn* package (Barton, 2020) to rank all alternative models suggested by *dredge* based on the AIC. We found the full models had the lowest AIC values for all three demographic rates. We also examined the collinearity of predictors in our models using the *VIF* function in the *car* package (Fox et al., 2020). All predictors had a VIF < 3.0, indicating little collinearity among predictors. Furthermore, we tested the overdispersion of the recruitment and survival models using the *blmeco* package, which revealed no overdispersion (Korner-Nievergelt et al., 2019). For the recruitment and survival models with binary classification, we assessed model performance by calculating the Area Under the Curve (AUC) and Receiver Operating Characteristics (ROC) curves using the *pROC* package (Robin et al., 2020), wherein an AUC of > 0.7 was considered acceptable. For the growth model, For the growth model with Gaussian distribution, we used R^2, the output of the *r.squaredGLMM* function in the *MuMIn* package to evaluate the model performance (Barton, 2020).

We also examined spatial autocorrelations based on the geographic locations of study plots using Mantel tests in the *ade4* package (Borcard and Legendre, 2012). The results indicated no evidence of spatial autocorrelation at $P = 0.05$ on residuals of plot identity over the five-year recruitment probability, the five-year survival probability, and the annual growth rate (Table S4-3). We also tested temporal autocorrelations in those model residuals using the Durbin-Watson test in the *DHARMa* package (Hartig, 2022). We found no evidence of temporal autocorrelation (Table S4-3).

71

We quantified CNDD as the difference between the coefficients of CD and HD in Eqn. 8 for each demographic model, like in previous studies (Jevon et al., 2022, Comita et al., 2010). For CD - HD < 0, = 0, and > 0, there is evidence of the existence of CNDD, lack of CNDD, and positive effects of conspecific density, respectively (LaManna et al., 2022).

Since we were interested in how the effects of CD and HD changed with stand age, we calculated CD effects as $\beta_1 + \beta_4 \cdot SA_{ijk}$ and HD effect as $\beta_2 + \beta_5 \cdot SA_{ijk}$ by the 10-year interval from 10 to 100 years on each demographic rate from the fitted model based on Eqn. 8. Fire intervals in the studied boreal forest are typically less than 100 years, resulting in only a few stands aged above 100 years (4 out of 153 plots in our dataset, Fig. S4-2e). To reduce overfitting, we limited our plotting to stands aged under 100 years. The mean of CD - HD was derived from the difference between the mean of the CD effect and the HD effect at the designated stand age. The standard error (SE) of CD - HD was calculated as $\sqrt{SE_{CD}{}^2 + SE_{HD}{}^2}$, where the SE_{CD} and SE_{HD} were the SE of CD and HD effect at designated stand age, respectively.

To determine how tree species diversity dynamics change with stand age, we used species richness (SR) to represent tree diversity, which was the number of unique species present in a plot at a given census. To quantify the relationship between SR and stand age, we compared the linear, 2nd and 3rd polynomial functions of stand age as the fixed effect and "plot" as the random effect and fitted the stand age-dependent SR using a Poisson generalized linear model. Then we presented the 2nd polynomial transformed stand age as it yielded the lowest AIC value for the SR and stand age relationship. We bootstrapped the model 1000 times to produce coefficient estimates and 95% confidence intervals. All analyses were performed

using the *lme4* package (Bates et al., 2015) in the R statistic program, version 4.2.2 (R Development Core Team, 2022).

4.4 Results

The AUC-ROC curve for recruitment and survival models were 0.903 and 0.854, which indicates the models' excellent discriminatory power. The simultaneous growth model accounted for 55.2% of the variation in the data from the fixed effects and 89.6% of the variation in the data from the random effect.

Overall, conspecific density, CD, had stronger negative effects than heterospecific density, HD, on all three demographic rates (Table 4-1). From the lowest to the higher end of CD, recruitment became significantly lower from a probability of 0.54 (maximum 1) to close to 0 (Fig. 4-2a); survival probability decreased from 1.00 (maximum 1) to 0.27 (Fig. 4-2b); annual growth rate decreased from 0.53 to 0.06 cm^2 y^{-1} (Fig. 4-2c). With increasing HD, recruitment decreased significantly from a probability of 0.04 to close to 0 (Fig. 4-2d), survival probability decreased from 0.93 to 0.80 (Fig. 4-2e), and annual growth rate decreased from 0.50 to 0.09 cm^2 y^{-1} (Fig. 4-2f). As stand age increased from 10.5 to 164 years, recruitment increased significantly from a probability of 0 to 0.09, while survival and growth decreased significantly, from a probability of 0.99 to 0.11 and a rate of 0.59 to 0.34 cm^2 y^{-1}, respectively (Figs. 4-2g-i).

The negative effects of CD became weaker with stand age for all three demographics (Table 4-1, Fig. 4-3a-c). They shifted from strongly negative to less negative, to even a positive effect on survival at a stand age of 100 years (Fig. 4-3b). The trend was similar but less pronounced for HD (Fig. 4-3). The negative effect of HD on recruitment strongly decreased with stand age, from strongly negative to less negative to even a positive effect of

HD in older stands. The decreasing trend of HD was weaker for survival and non-significant for growth (Fig. 4-3).

On average, CNDD effects existed for all three demographic rates, as indicated by greater negative coefficients of conspecific than heterotrophic density, and they were highest for recruitment (mean coefficients of CD - HD = -0.87), followed by survival (CD - HD = -0.80) and growth (CD - HD = -0.33; Table 4-1). These CNDD effects were most pronounced in young stands and became weaker with stand age (Fig. 4-3). Furthermore, the stand age-dependent CNDD effects were strongest for survival, followed by recruitment, and relatively weak for growth (Fig. 4-3). In response to stand age, tree species richness increased initially, reaching the highest at the age of approximately 80 years and decreasing in older stands (Fig. 4-4).

Table 4-1. 5-year recruitment probability, 5-year survival probability and annual growth rate associated with conspecific density (CD), heterospecific density (HD), stand age (SA), and their interactions. All predictors were standardized, which involved subtracting their mean and dividing by their standard deviation. The CD and HD had a parameter exponent c of 0.38 for recruitment, 0.09 for survival and 0.12 for the growth model. The SA was natural log-transformed. Estimate values are coefficients with bootstrapped 95% confidence intervals (CI) in brackets. The z value was fitted for the recruitment and survival models, and the t value was fitted for the growth model.

Source	Estimate	Confidence interval	z value/t value	P value
Recruitment probability per 5-year				
Intercept	-4.30	-4.72 to -3.52	-12.96	1.8×10^{-38}
CD	-1.47	-1.48 to -1.37	-55.35	$<1.0 \times 10^{-300}$
HD	-0.60	-0.65 to -0.50	-16.62	4.8×10^{-62}
SA	0.60	0.46 to 0.69	10.79	3.8×10^{-27}
CD × SA	0.44	0.38 to 0.47	18.30	8.7×10^{-75}
HD × SA	0.31	0.24 to 0.35	10.51	7.9×10^{-26}
Survival probability per 5-year				
Intercept	1.97	0.94 to 2.88	3.98	6.9×10^{-5}
CD	-1.05	-1.08 to -1.03	-76.66	$<1.0 \times 10^{-300}$
HD	-0.25	-0.29 to -0.21	-14.73	4.2×10^{-49}
SA	-1.26	-1.32 to -1.19	-40.53	$<1.0 \times 10^{-300}$
CD × SA	0.44	0.41 to 0.46	36.32	7.5×10^{-289}
HD × SA	0.07	0.05 to 0.10	5.47	4.5×10^{-8}
Annual growth rate				
Intercept	-0.78	-1.24 to -0.35	-3.48	0.004
CD	-0.81	-0.82 to -0.80	-191.56	$<1.0 \times 10^{-300}$
HD	-0.48	-0.49 to -0.46	-78.35	$<1.0 \times 10^{-300}$
SA	-0.09	-0.10 to -0.08	-13.14	2.1×10^{-39}
CD × SA	0.09	0.09 to 0.10	26.16	4.1×10^{-150}
HD × SA	0.00	-0.01 to 0.01	-0.07	0.944
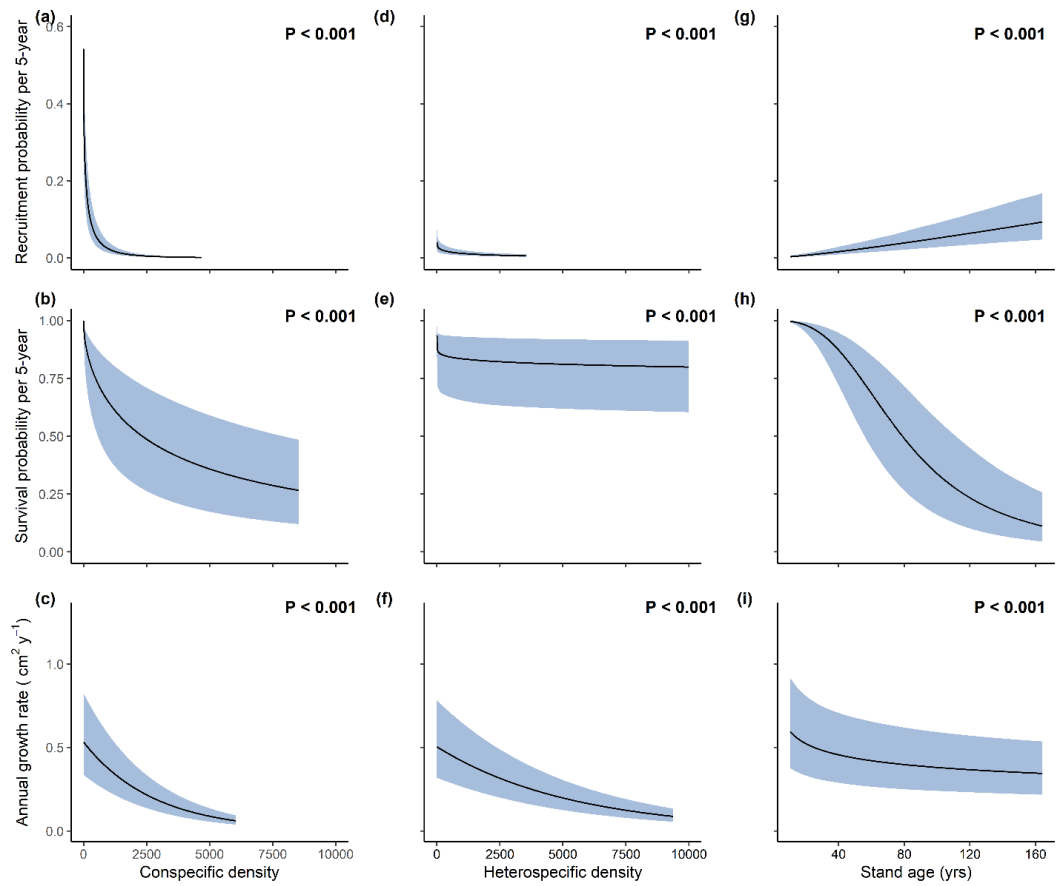
Figure 4-2: Demographic rates in response to conspecific density, heterospecific density, and stand age. Solid black lines show average effects with 95% confidence bands in blue, which are generated by coefficient estimates presented in Table 4-1.
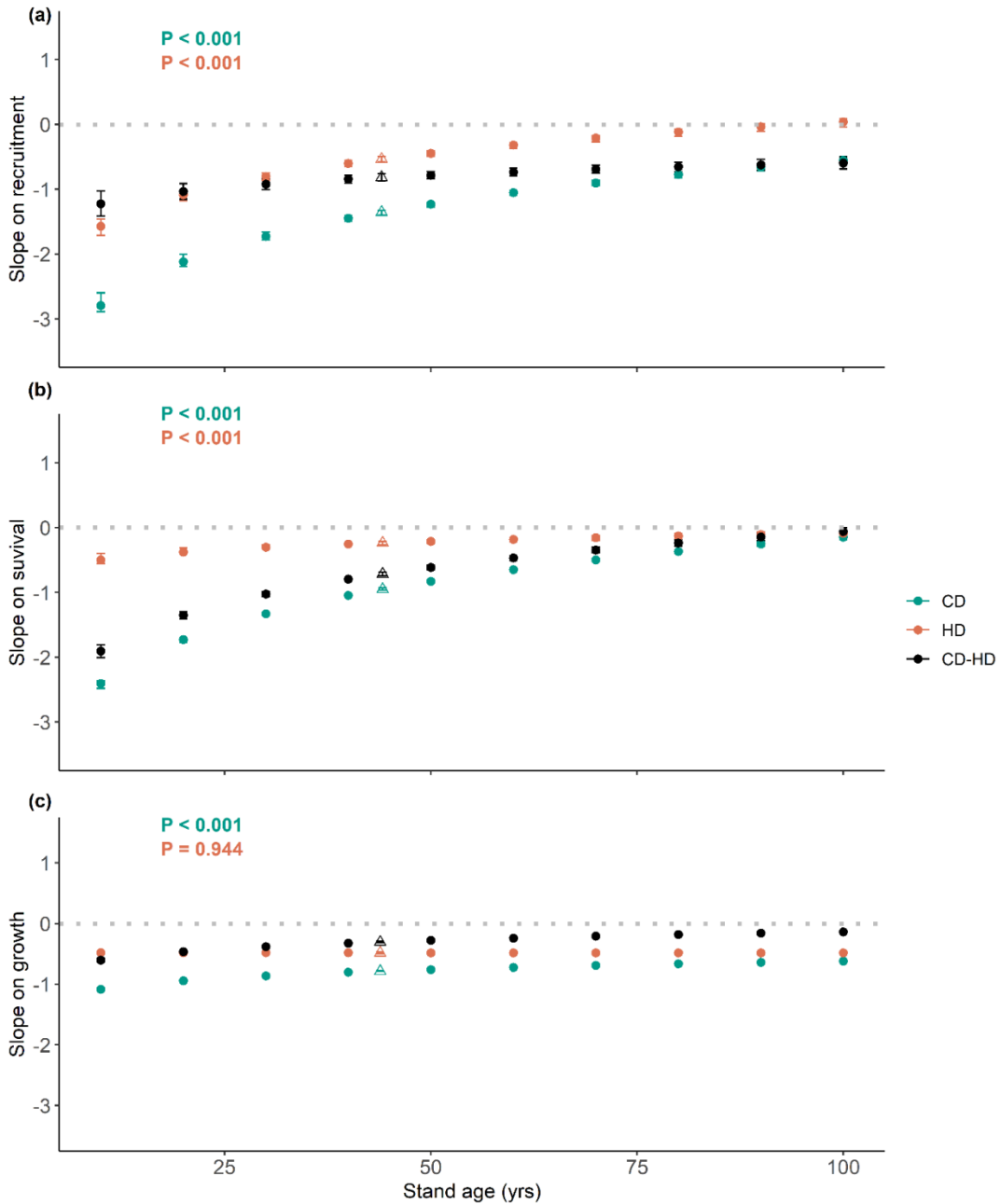
Figure 4-3: Stand age-dependent of conspecific negative density dependence, conspecific density, and heterospecific density effects. Values are mean and bootstrapped 95% confidence interval (CI) generated by coefficient estimates presented in Table 4-1; filled circles indicate the effect of conspecific or heterospecific density dependence at the average stand age experienced by an individual in this study. The CD-HD was derived from the difference between the effect of conspecific density (CD) and the effect of heterospecific density (HD) on each demographic rate.
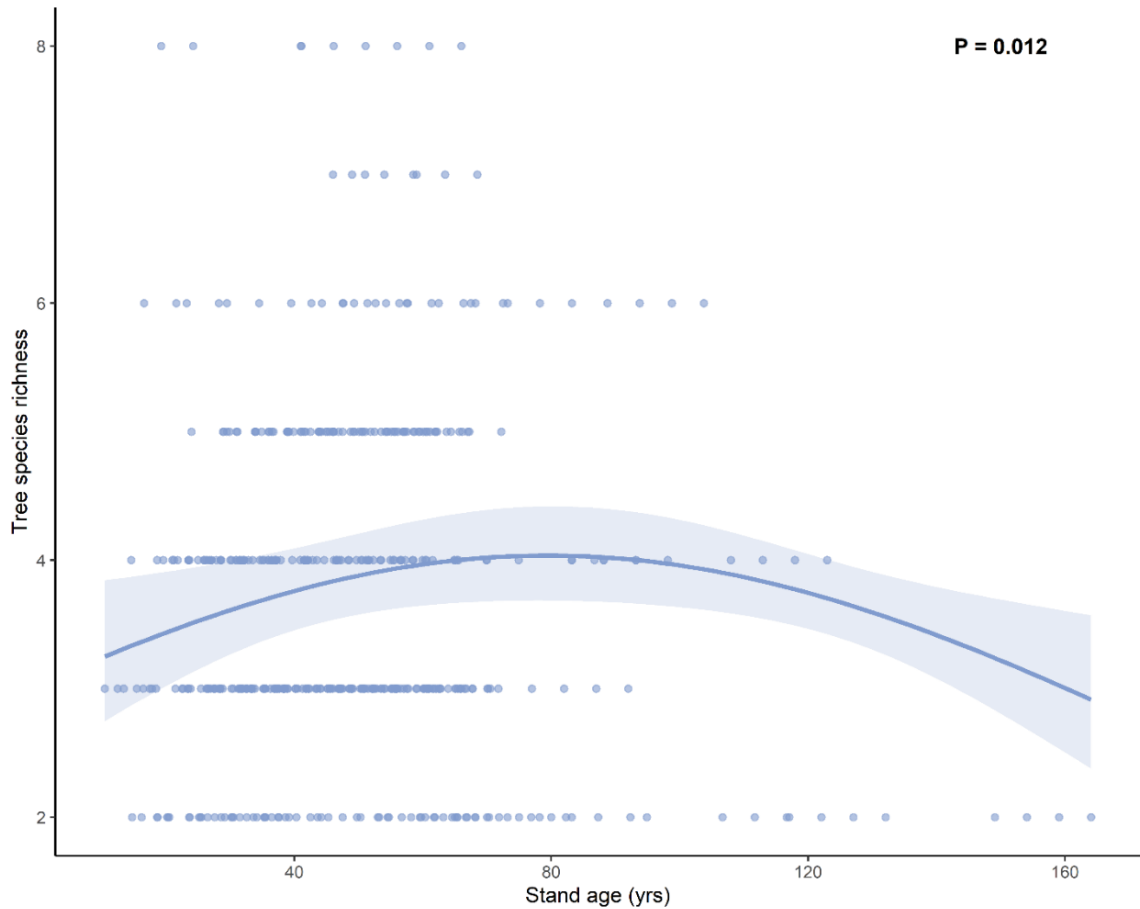
Figure 4-4: Relationship between tree species richness and stand age**.** The solid line shows the fitted relationship with 95% confidence bands in blue. Background points are observed values from each plot at each census.

4.5 Discussion

Our analysis of long-term repeatedly measured demographic data over a wide range of stand ages provides direct evidence that the effects of CNDD vary with different demographic rates and change with stand development. Specifically, we found that the effects of CNDD derived from the divergent response of CD and HD decreased with stand age and were strongest in young stands but weaker in older stands. Moreover, the reduced trend of CNDD with stand age was strongest for survival, shifting toward conspecific positive density dependence in older stands, followed by recruitment, with the least impact on growth. Our

results suggest that stronger CNDD in young stands might contribute to an initial increase in tree species richness from young to mature forests, whereas the reduced CNDD in older stands leads to decreased tree species richness in older forests. CNDD could be one of the potential reasons for an observed hump-shaped pattern of species richness with stand development.

Overall, our results support the hypothesis that CNDD effects occurred during recruitment, survival, and growth simultaneously. Our results provide direct evidence for a multi-dimensional insight that the effects of CNDD regulate the three demographic rates with different strengths, and all three demographic rates regulate whole community responses, as determined from theory (Hülsmann et al., 2021, Detto et al., 2019) and empirical evidence (Germain and Lutz, 2022). The prevalence of CNDD effects on three demographics of species-poor boreal forests confirmed that the widely presumed negative effect of CD was stronger than that of HD at local scales of tropical and temperate forests (Comita et al., 2010, Jevon et al., 2022) and other ecosystems (Adler et al., 2018).

Moreover, we found stronger CNDD effects on recruitment and survival than on growth. The strong CNDD effect on recruitment is expected because of size-asymmetric competition and the higher vulnerability of younger trees to herbivores and pathogens (Zhu et al., 2018, Yao et al., 2020, Zhu et al., 2015). However, contrary to a previous study that found a diluted CNDD effect with ontogeny (Zhu et al., 2015), the survival of established trees experienced a CNDD effect similar to that for recruitment in our study. A possible explanation is that dead trees had a mean DBH of 4.1 cm, while live trees had a mean DBH of 5.9 cm, and the small sizes, especially in young stands, amplified the CNDD effects on survival; that is, trees of different species had reduced competition for crown space, light, and belowground resources. On the other hand, a weaker CNDD effect on the growth of trees, which are larger

and occupy dominant crown positions, might be explained by a lower effect of competition and higher resistance to insects and pathogens with more resources available for defence.

In alignment with our hypothesis, the effects of CNDD decreased with stand age, resulting from a more pronounced reduction of the CD effect than the HD effect. The strongest CNDD in young forests could be attributed to the intensive competition for resources due to the fast growth rates of individual stems, which could also be sensitive to herbivores and pathogens (Fig. 4-2i); in contrast, alleviated CNDD effects in older stands resulted from resource limitations due to the dieback of canopy pioneers (Franklin et al., 2002, Chen and Popadiouk, 2002). Unlike well-accepted specialized natural enemies and pathogens that act as stabilizing factors for CNDD in stable old-growth forests, such as in Barro Colorado Island (Forrister et al., 2019, Lebrija-Trejos et al., 2016), our findings suggest that competition appears to be the primary mechanism driving stronger CNDD in young boreal forest, where natural enemies and pathogens are rare shortly after stand-replacing fire. Although insects and pathogens would accumulate in older growth, the effects of CNDD decreased dramatically and still shifted toward a less negative or even a conspecific positive density dependence effect.

Decreases in the effects of CNDD with increased stand age were stronger on survival, followed by recruitment, and weakest on growth. The strongest effect of stand age-dependent CNDD on survival was observed when the negative effect of CD was drastically reduced, whereas the effect of HD was more stable with stand age. Our results affirmed the occurrence of conspecific density-dependent self-thinning with stand development, which is more pronounced in clusters of smaller trees and decreases as tree size increases (Birch et al., 2019). During this process, the weak and unhealthy trees die, reducing competition, whereas surviving trees will capture released resources to achieve larger sizes. However, stronger CNDD gave

way to particularly weak effects on survival in older stands due to the more uniform large size and dispersed distribution of mature trees from environmental filtering with stand development (Getzin et al., 2008, Zhu et al., 2015). Compared with survival, the CNDD effect on recruitment decreased with stand age to a lesser extent, resulting from simultaneous reductions in CD and HD effects. This may be attributed to a more consistent influence of CNDD on recruitment across all stand ages. In contrast, growth was less affected by the age-dependent CNDD effect, with a steady reduction of CD but a non-significant change in HD. The well-established surviving trees in boreal forest, such as *Abies balsamea* and *Picea mariana,* may adapt their growth strategies, shed lower branches, and redirect more energy to grow taller and stronger (Kneeshaw and Bergeron, 1998).

Our findings indicate that CNDD effects on the three demographic rates may work as a potential mechanism to generate temporal diversity dynamics. Particularly, the strong CNDD effects in younger ages of forest contribute to an initial increase in tree species richness, joined by accumulating evidence of the importance of the early-stage effect of CNDD on seedling survival in determining long-term changes in tree diversity (Green et al., 2014, Lebrija-Trejos et al., 2023). Our findings further indicate that the effects of CNDD not only on survival but also on recruitment and growth in young stands contributed to temporal diversity dynamics. We show that lack of or reduced CNDD effects decrease tree species richness in older stands.

In conclusion, our 25-year observations of multiple demographic data across stand development stages represent an initial step to elucidate whether CNDD differs across all three demographics within the community and how CNDD shifts with stand age in driving temporal changes in tree species diversity. Our results demonstrate that CNDD effects decreased with stand age and were stronger in young stands. Our findings show the importance of early-stage

81

effects of CNDD on recruitment, as well as on survival and growth, which might drive

increased tree species diversity at later stages. Although other possible factors may not be ruled

out, CNDD could be one of the reasons for variation in diversity dynamics across stand

development. In contrast with well-accepted ideas that CNDD is driven by natural enemies,

our findings suggest that the influence of CNDD on competition could be the primary

mechanism driving diversity dynamics with stand development.

CHAPTER 5: GENERAL CONCLUSION

Three tree demographic processes govern forest dynamics, and forest dynamics influence ecosystem carbon, energy and function. Anthropogenic global environmental change in terms of biodiversity loss and climate change poses a significant threat to forest dynamics through changes to demographic processes, which can interrupt the functioning of forests as a massive carbon sink. My dissertation has attempted to address these questions based on a spatially explicit analysis to examine individual tree demographic performance associated with neighbourhood environments (e.g., competition, diversity) under climate change. I showed how neighbourhood diversity affects sapling recruitment in different crowding and stand age contexts. I revealed how climate change may affect indirectly, other than directly, through altered neighbourhood effects on sapling recruitment. I also found that conspecific negative density dependence (CNDD) drives three demographics changes along stand development and may work as a potential mechanism to regulate boreal forest diversity. Benefitting from a long-term spatially explicit dataset, my studies on three demographics of individual level extend findings from previous community and landscape studies on forest dynamics and diversity under climate change (McDowell et al., 2020, Zhang et al., 2015, Astigarraga et al., 2020). A summary of the key outcomes of each chapter of my dissertation is as follows:

In chapter two, using neighbourhood analysis to examine the individual sapling recruitment probability as a function of neighbourhood crowding index, stand age, neighbourhood diversity from shade tolerance dissimilarity and phylogenetic dissimilarity, and their interactions, I show sapling recruitment probability benefits more from the positive effects of shade tolerance dissimilarity in young stands, while phylogenetic dissimilarity has a positive effect on sapling recruitment only in older stands. Importantly, sapling recruitment

probability is less negatively affected by crowding in neighbourhoods with high shade tolerance and phylogenetic dissimilarities. These results extend previously widely observed neighbourhood effects on tree growth and mortality to rarely investigated sapling recruitment. These findings also provide one of the first pieces of observational evidence that functional and phylogenetic dissimilarities can reduce the negative effects of crowding on sapling recruitment, respectively in young and old boreal forest.

In chapter three, I further examined how climate change, represented as temporal trends, directly and indirectly, affects sapling recruitment. I found that sapling recruitment does not respond to temporal variations in CO_2, temperature, or precipitation. However, increasing mortality and growth of established trees exert indirect negative effects on sapling recruitment. These results suggest that the faster turnover in a tree canopy under current climate change may disrupt the compensating role of sapling recruitment for increased tree mortality, as previously predicted. In contrast, increasing neighbourhood crowding, shade tolerance, and phylogenetic dissimilarities have indirect positive effects, leading to a total negative effect of climate change on sapling recruitment. These results provide the first evidence that sapling recruitment is driven largely by the indirect effects of climate change through altered neighbourhood conditions among established trees. These findings highlight that even so-called favourable climate change in the central boreal forest of North America could pose a threat to long-term ecosystem functionality.

Further, in chapter four, taking advantage of the long-term, spatially mapped tree demographic data over a wide range of stand ages, I examined how CNDD influences tree recruitment, survival, and growth simultaneously and how it may regulate tree species diversity dynamics during stand development. CNDD effects decreased significantly with stand age,

with more pronounced changes in the CNDD effects on recruitment and survival than on growth. The strong CNDD effects in young stands could contribute to initial increases in tree species richness. However, the low or lack of CNDD effects in older stands led to reduced species richness, resulting in a hump-shaped species richness pattern with stand age. Although other factors in driving diversity change may not be ruled out, these results represent a step in understanding CNDD-determined diversity in the community using robust estimates of CNDD effects on three demographics. Unlike the previously well-accepted idea that natural enemies drive diversity dynamics, my findings highlight that the influence of CNDD on competition could be the primary mechanism driving diversity dynamics with stand development in the boreal forest.

Although there was a tremendous initial investment by the Manitoba government, which spatially mapped and measured individual trees in 173 permanent sample plots (PSPs) over a span of 25 years, there were some weaknesses in the dataset used in this dissertation. First, the PSPs were established by the government to monitor forest growth and yield, such that there is a lack of information on the initial stages of regeneration, specifically regarding the large seedling pool recruits reaching the height criterion to be recorded. Second, although the PSPs were set up to encompass various age classes, densities, and initial spacing, and each plot appeared visually homogeneous in terms of soil, topography, and composition, the absence of data on canopy, soil and a detailed disturbance history may weaken the conclusions drawn from linking specific mechanisms to the observed results. Overall, the fine-scale and spatially dependent approach of this dissertation demonstrates the effect of spatial and temporal heterogeneity and informs broader-scale pragmatic vegetation models. The pattern-based approach of this dissertation shows phenomenological patterns observed in natural

forests, which necessitates experimental testing of multiple mechanistic predictions that

underlie these patterns.

REFERENCES

Adler, P. B., Fajardo, A., Kleinhesselink, A. R. & Kraft, N. J. (2013) Trait-based tests of coexistence mechanisms. *Ecology Letters,* **16,** 1294-306.10.1111/ele.12157

Adler, P. B., Smull, D., Beard, K. H., Choi, R. T., Furniss, T., Kulmatiski, A., Meiners, J. M., Tredennick, A. T. & Veblen, K. E. (2018) Competition and coexistence in plant communities: intraspecific competition is stronger than interspecific competition. *Ecology Letters,* **21,** 1319-1329.10.1111/ele.13098

Aguirre-Gutierrez, J., Malhi, Y., Lewis, S. L., Fauset, S., Adu-Bredu, S., Affum-Baffoe, K., Baker, T. R., Gvozdevaite, A., Hubau, W., Moore, S., Peprah, T., Zieminska, K., Phillips, O. L. & Oliveras, I. (2020) Long-term droughts may drive drier tropical forests towards increased functional, taxonomic and phylogenetic homogeneity. *Nature Communications,* **11,** 3346.10.1038/s41467-020-16973-4

Anderegg, W. R., Schwalm, C., Biondi, F., Camarero, J. J., Koch, G., Litvak, M., Ogle, K., Shaw, J. D., Shevliakova, E., Williams, A. P., Wolf, A., Ziaco, E. & Pacala, S. (2015) Pervasive drought legacies in forest ecosystems and their implications for carbon cycle models. *Science,* **349,** 528-32.10.1126/science.aab1833

Astigarraga, J., Andivia, E., Zavala, M. A., Gazol, A., Cruz-Alonso, V., Vicente-Serrano, S. M. & Ruiz-Benito, P. (2020) Evidence of non-stationary relationships between climate and forest responses: Increased sensitivity to climate change in Iberian forests. *Glob Chang Biol,* **26,** 5063-5076.10.1111/gcb.15198

Barr, D. J., Levy, R., Scheepers, C. & Tily, H. J. (2013) Random effects structure for confirmatory hypothesis testing: Keep it maximal. *J Mem Lang,* **68**.10.1016/j.jml.2012.11.001

Barry, K. E., Mommer, L., van Ruijven, J., Wirth, C., Wright, A. J., Bai, Y., Connolly, J., De Deyn, G. B., de Kroon, H., Isbell, F., Milcu, A., Roscher, C., Scherer-Lorenzen, M., Schmid, B. & Weigelt, A. (2019) The future of complementarity: Disentangling causes from consequences. *Trends in Ecology Evolution,* **34,** 167-180.10.1016/j.tree.2018.10.013

Barry, K. E. & Schnitzer, S. A. (2021) Are we missing the forest for the trees? Conspecific negative density dependence in a temperate deciduous forest. *PLoS One,* **16,** e0245639.10.1371/journal.pone.0245639

Barton, K., MuMIn: Multi-Model Inference. https://cran.R-project.org/package=MuMIn (2020).

Bates, D., Bolker, B., Walker, S., Christensen, R. H. B., Singmann, H., Dai, B. & Grothendieck, G., lme4: Linear mixed-effects models using Eigen and S4. https://cran.r-project.org/web/packages/lme4/index.html (2019).

Bates, D., Machler, M., Bolker, B. M. & Walker, S. C. (2015) Fitting Linear Mixed-Effects Models Using lme4. *Journal of Statistical Software,* **67,** 1-48.DOI 10.18637/jss.v067.i01

Beguería, S. & Vicente-Serrano, S. M. (2017) SPEI: Calculation of the standardised precipitation-evapotranspiration index. https://cran.r-project.org/web/packages/SPEI/index.html.

Berner, L. T. & Goetz, S. J. (2022) Satellite observations document trends consistent with a boreal forest biome shift. *Global Change Biology,* **28,** 3275-3292.10.1111/gcb.16121

Birch, J. D., Lutz, J. A., Simard, S. W., Pelletier, R., LaRoi, G. H. & Karst, J. (2019) Density-dependent processes fluctuate over 50 years in an ecotone forest. *Oecologia,* **191,** 909-918.10.1007/s00442-019-04534-6

Boisvert‑Marsh, L., Périé, C., de Blois, S. & Bellingham, P. (2019) Divergent responses to climate change and disturbance drive recruitment patterns underlying latitudinal shifts of tree species. *Journal of Ecology,* **107,** 1956-1969.10.1111/1365-2745.13149

Borcard, D. & Legendre, P. (2012) Is the Mantel correlogram powerful enough to be useful in ecological analysis? A simulation study. *Ecology,* **93,** 1473-81.10.1890/11-1737.1

Boucher, D., Gauthier, S., Thiffault, N., Marchand, W., Girardin, M. & Urli, M. (2019) How climate change might affect tree regeneration following fire at northern latitudes: a review. *New Forests,* **51,** 543-571.10.1007/s11056-019-09745-6

Brassard, B. W., Chen, H. Y. H., Cavard, X., Laganière, J., Reich, P. B., Bergeron, Y., Paré, D., Yuan, Z. & Chen, H. (2013) Tree species diversity increases fine root productivity through increased soil volume filling. *Journal of Ecology,* **101,** 210-219.10.1111/1365-2745.12023

Brienen, R. J., Phillips, O. L., Feldpausch, T. R., Gloor, E., Baker, T. R., Lloyd, J., Lopez-Gonzalez, G., Monteagudo-Mendoza, A., Malhi, Y., Lewis, S. L., Vasquez Martinez, R., Alexiades, M., Alvarez Davila, E., Alvarez-Loayza, P., Andrade, A., Aragao, L. E., Araujo-Murakami, A., Arets, E. J., Arroyo, L., Aymard, C. G., Banki, O. S., Baraloto, C., Barroso, J., Bonal, D., Boot, R. G., Camargo, J. L., Castilho, C. V., Chama, V., Chao, K. J., Chave, J., Comiskey, J. A., Cornejo Valverde, F., da Costa, L., de Oliveira, E. A., Di Fiore, A., Erwin, T. L., Fauset, S., Forsthofer, M., Galbraith, D. R., Grahame, E. S., Groot, N., Herault, B., Higuchi, N., Honorio Coronado, E. N., Keeling, H., Killeen, T. J., Laurance, W. F., Laurance, S., Licona, J., Magnussen, W. E., Marimon, B. S., Marimon-Junior, B. H., Mendoza, C., Neill, D. A., Nogueira, E. M., Nunez, P., Pallqui Camacho, N. C., Parada, A., Pardo-Molina, G., Peacock, J., Pena-Claros, M., Pickavance, G. C., Pitman, N. C., Poorter, L., Prieto, A., Quesada, C. A., Ramirez, F., Ramirez-Angulo, H., Restrepo, Z., Roopsind, A., Rudas, A., Salomao, R. P., Schwarz, M., Silva, N., Silva-Espejo, J. E., Silveira, M., Stropp, J., Talbot, J., ter Steege, H., Teran-Aguilar, J., Terborgh, J., Thomas-Caesar, R., Toledo, M., Torello-Raventos, M., Umetsu, R. K., van der Heijden, G. M., van der Hout, P., Guimaraes Vieira, I. C., Vieira, S. A., Vilanova, E., Vos, V. A. & Zagt, R. J. (2015) Long-term decline of the Amazon carbon sink. *Nature,* **519,** 344-8.10.1038/nature14283

Canham, C. D., LePage, P. T. & Coates, K. D. (2004) A neighborhood analysis of canopy tree competition: effects of shading versus crowding. *Canadian Journal of Forest Research,* **34,** 778-787.10.1139/X03-232

Castagneyrol, B., Jactel, H., Vacher, C., Brockerhoff, E. G., Koricheva, J. & Cadotte, M. (2014) Effects of plant phylogenetic diversity on herbivory depend on herbivore specialization. *Journal of Applied Ecology,* **51,** 134-141.10.1111/1365-2664.12175

Chang‑Yang, C. H., Needham, J., Lu, C. L., Hsieh, C. F., Sun, I. F. & McMahon, S. M. (2021) Closing the life cycle of forest trees: The difficult dynamics of seedling‑to‑sapling transitions in a subtropical rainforest. *Journal of Ecology,* **109,** 2705-2716.10.1111/1365-2745.13677

Chen, H. Y. & Klinka, K. (1997) Light availability and photosynthesis of *Pseudotsuga menziesii* seedlings grown in the open and in the forest understory. *Tree Physiology,* **17,** 23-9.10.1093/treephys/17.1.23

Chen, H. Y., Luo, Y., Reich, P. B., Searle, E. B. & Biswas, S. R. (2016a) Climate change-associated trends in net biomass change are age dependent in western boreal forests of Canada. *Ecol Lett,* **19,** 1150-8.10.1111/ele.12653

Chen, H. Y. & Popadiouk, R. V. (2002) Dynamics of North American boreal mixedwoods. *Environmental Reviews,* **10,** 137-166.10.1139/a02-007

Chen, H. Y. H. (1997) Interspecific responses of planted seedlings to light availability in interior British Columbia: survival, growth, allometric patterns, and specific leaf area. *Canadian Journal of Forest Research,* **27,** 1383-1393.10.1139/x97-099

Chen, H. Y. H., Klinka, K. & Kayahara, G. J. (1996) Effects of light on growth, crown architecture, and specific leaf area for naturally established Pinus contorta var latifolia and Pseudotsuga menziesii var glauca saplings. *Canadian Journal of Forest Research,* **26,** 1149-1157.10.1139/x26-128

Chen, Y., Uriarte, M., Wright, S. J. & Yu, S. (2019a) Effects of neighborhood trait composition on tree survival differ between drought and postdrought periods. *Ecology,* **100,** e02766.10.1002/ecy.2766

Chen, L., Wang, Y., Mi, X., Liu, X., Ren, H., Chen, J., Ma, K. & Kraft, N. J. B. (2019b) Neighborhood effects explain increasing asynchronous seedling survival in a subtropical forest. *Ecology,* **100,** e02821.10.1002/ecy.2821

Chen, Y., Wright, S. J., Muller-Landau, H. C., Hubbell, S. P., Wang, Y. & Yu, S. (2016b) Positive effects of neighborhood complementarity on tree growth in a Neotropical forest. *Ecology,* **97,** 776-85.10.1890/15-0625.1

Chesson, P. (2000) Mechanisms of maintenance of species diversity. *Annual review of Ecology and Systematics***,** 343-366.10.1146/annurev.ecolsys.31.1.343

Comita, L. S., Muller-Landau, H. C., Aguilar, S. & Hubbell, S. P. (2010) Asymmetric density dependence shapes species abundances in a tropical tree community. *Science,* **329,** 330-2.10.1126/science.1190772

Condit, R., Hubbell, S. P. & Foster, R. B. (1995) Mortality-Rates of 205 Neotropical Tree and Shrub Species and the Impact of a Severe Drought. *Ecological Monographs,* **65,** 419-439.10.2307/2963497

Connell, J. H. (1971) *On the role of natural enemies in preventing competitive exclusion in some marine animals and in rain forest trees* Centre for Agricultural Publishing and Documentation, Wageningen, The Netherlands.

Connell, J. H. (1978) Diversity in tropical rain forests and coral reefs - High diversity of trees and corals is maintained only in a non-equilibrium state. *Science,* **199,** 1302-10.10.1126/science.199.4335.1302

Connell, J. H., Tracey, J. G. & Webb, L. J. (1984) Compensatory recruitment, growth, and mortality as factors maintaining rain forest tree diversity. *Ecological Monographs,* **54,** 141-164.10.2307/1942659

Coomes, D. A., Lines, E. R. & Allen, R. B. (2011) Moving on from Metabolic Scaling Theory: hierarchical models of tree growth and asymmetric competition for light. *Journal of Ecology,* **99,** 748-756.10.1111/j.1365-2745.2011.01811.x

Das, A., Battles, J., van Mantgem, P. J. & Stephenson, N. L. (2008) Spatial elements of mortality risk in old-growth forests. *Ecology,* **89,** 1744-56.10.1890/07-0524.1

Davis, K. T., Dobrowski, S. Z., Higuera, P. E., Holden, Z. A., Veblen, T. T., Rother, M. T., Parks, S. A., Sala, A. & Maneta, M. P. (2019) Wildfires and climate change push low-

elevation forests across a critical climate threshold for tree regeneration. *Proc Natl Acad Sci U S A,* **116,** 6193-6198.10.1073/pnas.1815107116

De Frenne, P., Lenoir, J., Luoto, M., Scheffers, B. R., Zellweger, F., Aalto, J., Ashcroft, M. B., Christiansen, D. M., Decocq, G., De Pauw, K., Govaert, S., Greiser, C., Gril, E., Hampe, A., Jucker, T., Klinges, D. H., Koelemeijer, I. A., Lembrechts, J. J., Marrec, R., Meeussen, C., Ogee, J., Tyystjarvi, V., Vangansbeke, P. & Hylander, K. (2021) Forest microclimates and climate change: Importance, drivers and future research agenda. *Glob Chang Biol,* **27,** 2279-2297.10.1111/gcb.15569

Detto, M., Visser, M. D., Wright, S. J. & Pacala, S. W. (2019) Bias in the detection of negative density dependence in plant communities. *Ecology Letters,* **22,** 1923-1939.10.1111/ele.13372

Dixon, R. K., Solomon, A. M., Brown, S., Houghton, R. A., Trexier, M. C. & Wisniewski, J. (1994) Carbon pools and flux of global forest ecosystems. *Science,* **263,** 185-90.10.1126/science.263.5144.185

Donkor, N. T. & Fryxell, J. M. (2000) Lowland boreal forests characterization in Algonquin Provincial Park relative to beaver (Castor canadensis) foraging and edaphic factors. *Plant Ecology,* **148,** 1-12.10.1023/a:1009860512339

Dray, S., Dufour, A.-B. & Thioulouse, J., ade4: Analysis of ecological data: Exploratory and euclidean methods in environmental sciences. (2022).

Fajardo, A. & McIntire, E. J. B. (2012) Reversal of multicentury tree growth improvements and loss of synchrony at mountain tree lines point to changes in key drivers. *Journal of Ecology,* **100,** 782-794.10.1111/j.1365-2745.2012.01955.x

Forrister, D. L., Endara, M. J., Younkin, G. C., Coley, P. D. & Kursar, T. A. (2019) Herbivores as drivers of negative density dependence in tropical forest saplings. *Science,* **363,** 1213-1216.10.1126/science.aau9460

Fox, J., Weisberg, S. & Price, B., car: Companion to Applied Regression. https://cran.r-project.org/web/packages/car/index.html (2020).

Franklin, J. F., Spies, T. A., Pelt, R. V., Carey, A. B., Thornburgh, D. A., Berg, D. R., Lindenmayer, D. B., Harmon, M. E., Keeton, W. S., Shaw, D. C., Bible, K. & Chen, J. (2002) Disturbances and structural development of natural forest ecosystems with silvicultural implications, using Douglas-fir forests as an example. *Forest Ecology and Management,* **155,** 399-423.10.1016/s0378-1127(01)00575-8

Gao, B., Taylor, A. R., Searle, E. B., Kumar, P., Ma, Z., Hume, A. M. & Chen, H. Y. H. (2017) Carbon Storage Declines in Old Boreal Forests Irrespective of Succession Pathway. *Ecosystems,* **21,** 1168-1182.10.1007/s10021-017-0210-4

Garrido, M., Hansen, S. K., Yaari, R. & Hawlena, H. (2022) A model selection approach to structural equation modelling: A critical evaluation and a road map for ecologists. *Methods in Ecology and Evolution,* **13,** 42-53.10.1111/2041-210x.13742

Germain, S. J. & Lutz, J. A. (2022) Climate warming may weaken stabilizing mechanisms in old forests. *Ecological Monographs,* **92.**10.1002/ecm.1508

Getzin, S., Wiegand, T., Wiegand, K. & He, F. (2008) Heterogeneity influences spatial patterns and demographics in forest stands. *Journal of Ecology,* **96,** 807-820.10.1111/j.1365-2745.2008.01377.x

Grace, J. B. (2006) *Structural equation modeling and natural systems.* Cambridge University Press, Cambridge, UK.

Graham, M. H. (2003) Confronting multicollinearity in ecological multiple regression. *Ecology,* **84,** 2809-2815.10.1890/02-3114

Green, P. T., Harms, K. E. & Connell, J. H. (2014) Nonrandom, diversifying processes are disproportionately strong in the smallest size classes of a tropical forest. *Proceedings of the National Academy of Sciences of the United States of America,* **111,** 18649-54.10.1073/pnas.1321892112

Grime, J. (1979) *Plant strategies and vegetation processes.* John Wiley and Sons, Chichester.

Grömping, U. (2015) Variable importance in regression models. *Wiley Interdisciplinary Reviews: Computational Statistics,* **7,** 137-152.10.1002/wics.1346

Hanbury-Brown, A. R., Powell, T. L., Muller-Landau, H. C., Wright, S. J. & Kueppers, L. M. (2022) Simulating environmentally-sensitive tree recruitment in vegetation demographic models. *New Phytol,* **235,** 78-93.10.1111/nph.18059

Harrison, S., Spasojevic, M. J. & Li, D. (2020) Climate and plant community diversity in space and time. *Proc Natl Acad Sci U S A,* **117,** 4464-4470.10.1073/pnas.1921724117

Hartig, F., DHARMa: residual diagnostics for hierarchical (multi-level/mixed) regression models. https://cran.r-project.org/web/packages/DHARMa/vignettes/DHARMa.html (2022).

Hegyi, F. (1974) A simulation model for managing jack-pine standssimulation. *Royal College of Forestry. Notes,* **30,** 74-90

Hisano, M. & Chen, H. Y. H. (2020) Spatial variation in climate modifies effects of functional diversity on biomass dynamics in natural forests across Canada. *Global Ecology and Biogeography*.10.1111/geb.13060

Hisano, M., Chen, H. Y. H., Searle, E. B. & Reich, P. B. (2019) Species-rich boreal forests grew more and suffered less mortality than species-poor forests under the environmental change of the past half-century. *Ecol Lett,* **22,** 999-1008.10.1111/ele.13259

Hisano, M., Searle, E. B. & Chen, H. Y. H. (2018) Biodiversity as a solution to mitigate climate change impacts on the functioning of forest ecosystems. *Biological reviews of the Cambridge Philosophical Society,* **93,** 439-456.10.1111/brv.12351

Huang, F., Liang, M., Zheng, Y., Liu, X., Chen, Y., Li, W., Luo, S. & Yu, S. (2020) Soil nitrogen availability intensifies negative density-dependent effects in a subtropical forest. *Journal of Plant Ecology,* **13,** 281-287.10.1093/jpe/rtaa012

Hubbell, S. P., Foster, R. B., O'Brien, S. T., Harms, K. E., Condit, R., Wechsler, B., Wright, S. J. & de Lao, S. L. (1999) Light-Gap disturbances, recruitment limitation, and tree diversity in a neotropical forest. *Science,* **283,** 554-7.10.1126/science.283.5401.554

Hülsmann, L., Chisholm, R. A. & Hartig, F. (2021) Is variation in Conspecific Negative Density Dependence driving tree diversity patterns at large scales? *Trends in Ecology & Evolution,* **36,** 151-163.10.1016/j.tree.2020.10.003

IPCC (2014) Climate change 2014: Synthesis report. Contribution of working groups I, II and III to the fifth assessment report of the intergovernmental panel on climate change. Cambridge University Press, UK and New york.

IPCC (2018) Global warming of 1.5°C: an IPCC special report on the impacts of global warming of 1.5 °C above pre-industrial levels and related global greenhouse gas emission pathways, in the context of strengthening the global response to the threat of climate change, sustainable development, and efforts to eradicate poverty. pp. http://www.ipcc.ch/report/sr15/. http://www.ipcc.ch/report/sr15/.

Jactel, H., Moreira, X. & Castagneyrol, B. (2021) Tree Diversity and Forest Resistance to Insect Pests: Patterns, Mechanisms, and Prospects. *Annual Review of Entomology,* **66,** 277-296.10.1146/annurev-ento-041720-075234

Janzen, D. H. (1970) Herbivores and the number of tree species in tropical forests. *The American Naturalist,* **104,** 501-528.10.1086/282687

Jevon, F. V., De La Cruz, D., LaManna, J. A., Lang, A. K., Orwig, D. A., Record, S., Kouba, P. V., Ayres, M. P. & Matthes, J. H. (2022) Experimental and observational evidence of negative conspecific density dependence in temperate ectomycorrhizal trees. *Ecology*, e3808.10.1002/ecy.3808

Johnson, D. J., Beaulieu, W. T., Bever, J. D. & Clay, K. (2012) Conspecific negative density dependence and forest diversity. *Science,* **336,** 904-7.10.1126/science.1220269

Jucker, T., Bouriaud, O., Avacaritei, D., Dănilă, I., Duduman, G., Valladares, F., Coomes, D. A. & Turnbull, M. (2014) Competition for light and water play contrasting roles in driving diversity-productivity relationships in Iberian forests. *Journal of Ecology,* **102,** 1202-1213.10.1111/1365-2745.12276

Jucker, T., Bouriaud, O., Coomes, D. A. & Baltzer, J. (2015) Crown plasticity enables trees to optimize canopy packing in mixed-species forests. *Functional Ecology,* **29,** 1078-1086.10.1111/1365-2435.12428

Kneeshaw, D. D. & Bergeron, Y. (1998) Canopy Gap Characteristics and Tree Replacement in the Southeastern Boreal Forest. *Ecology,* **79**.10.1890/0012-9658(1998)079[0783:Cgcatr]2.0.Co;2

Kneeshaw, D. D. & Bergeron, Y. (1999) Spatial and temporal patterns of seedling and sapling recruitment within canopy gaps caused by spruce budworm. *Écoscience,* **6,** 214-222.Doi 10.1080/11956860.1999.11682522

Kneeshaw, D. D., Kobe, R. K., Coates, K. D. & Messier, C. (2006) Sapling size influences shade tolerance ranking among southern boreal tree species. *Journal of Ecology,* **94,** 471-480.10.1111/j.1365-2745.2005.01070.x

Korner-Nievergelt, F., Roth, T., Felten, v. S. & Guelat, J., blmeco: Data files and functions accompanying the book "Bayesian Data Analysis in Ecology using R, BUGS and Stan". https://cran.r-project.org/web/packages/blmeco/index.html (2019).

Kroiss, S. J. & Hillerslambers, J. (2015) Recruitment limitation of long-lived conifers: implications for climate change responses. *Ecology,* **96,** 1286-97.10.1890/14-0595.1

Kunstler, G., Falster, D., Coomes, D. A., Hui, F., Kooyman, R. M., Laughlin, D. C., Poorter, L., Vanderwel, M., Vieilledent, G., Wright, S. J., Aiba, M., Baraloto, C., Caspersen, J., Cornelissen, J. H., Gourlet-Fleury, S., Hanewinkel, M., Herault, B., Kattge, J., Kurokawa, H., Onoda, Y., Penuelas, J., Poorter, H., Uriarte, M., Richardson, S., Ruiz-Benito, P., Sun, I. F., Stahl, G., Swenson, N. G., Thompson, J., Westerlund, B., Wirth, C., Zavala, M. A., Zeng, H., Zimmerman, J. K., Zimmermann, N. E. & Westoby, M. (2016) Plant functional traits have globally consistent effects on competition. *Nature,* **529,** 204-7.10.1038/nature16476

LaManna, J. A., Belote, R. T., Burkle, L. A., Catano, C. P. & Myers, J. A. (2017a) Negative density dependence mediates biodiversity-productivity relationships across scales. *Nature Ecology and Evolution,* **1,** 1107-1115.10.1038/s41559-017-0225-4

LaManna, J. A., Jones, F. A., Bell, D. M., Pabst, R. J. & Shaw, D. C. (2022) Tree species diversity increases with conspecific negative density dependence across an elevation gradient. *Ecol Lett,* **25,** 1237-1249.10.1111/ele.13996

LaManna, J. A., Mangan, S. A., Alonso, A., Bourg, N. A., Brockelman, W. Y., Bunyavejchewin, S., Chang, L. W., Chiang, J. M., Chuyong, G. B., Clay, K., Condit, R., Cordell, S., Davies, S. J., Furniss, T. J., Giardina, C. P., Gunatilleke, I., Gunatilleke, C. V. S., He, F., Howe, R. W., Hubbell, S. P., Hsieh, C. F., Inman-Narahari, F. M., Janik, D., Johnson, D. J., Kenfack, D., Korte, L., Kral, K., Larson, A. J., Lutz, J. A., McMahon, S. M., McShea, W. J., Memiaghe, H. R., Nathalang, A., Novotny, V., Ong, P. S., Orwig, D. A., Ostertag, R., Parker, G. G., Phillips, R. P., Sack, L., Sun, I. F., Tello, J. S., Thomas, D. W., Turner, B. L., Vela Diaz, D. M., Vrska, T., Weiblen, G. D., Wolf, A., Yap, S. & Myers, J. A. (2017b) Plant diversity increases with the strength of negative density dependence at the global scale. *Science,* **356,** 1389-1392.10.1126/science.aam5678

LaManna, J. A., Mangan, S. A. & Myers, J. A. (2021) Conspecific negative density dependence and why its study should not be abandoned. *Ecosphere,* **12**.10.1002/ecs2.3322

Lebrija-Trejos, E., Hernandez, A. & Wright, S. J. (2023) Effects of moisture and density-dependent interactions on tropical tree diversity. *Nature*.10.1038/s41586-023-05717-1

Lebrija-Trejos, E., Reich, P. B., Hernandez, A. & Wright, S. J. (2016) Species with greater seed mass are more tolerant of conspecific neighbours: a key driver of early survival and future abundances in a tropical forest. *Ecology Letters,* **19,** 1071-80.10.1111/ele.12643

Lefcheck, J. S., piecewiseSEM: Piecewise Structural Equation Modeling in R. (2023).

Lloret, F., Escudero, A., Iriondo, J. M., Martinez-Vilalta, J. & Valladares, F. (2012) Extreme climatic events and vegetation: the role of stabilizing processes. *Global Change Biology,* **18,** 797-805.10.1111/j.1365-2486.2011.02624.x

Long, J. A., jtools: Analysis and presentation of social scientific data. https://cran.r-project.org/web/packages/jtools/jtools.pdf (2021).

Looney, C. E., Previant, W. J., Bradford, J. B. & Nagel, L. M. (2021) Species mixture effects and climate influence growth, recruitment and mortality in Interior West USA Populus tremuloides conifer communities. *Journal of Ecology,* **109,** 2934-2949.10.1111/1365-2745.13709

Lorentzen Kolstad, A., Austrheim, G., Solberg, E. J., De Vriendt, L. & Speed, J. D. M. (2018) Pervasive moose browsing in boreal forests alters successional trajectories by severely suppressing keystone species. *Ecosphere,* **9**.10.1002/ecs2.2458

Luo, Y. & Chen, H. Y. H. (2011) Competition, species interaction and ageing control tree mortality in boreal forests. *Journal of Ecology,* **99,** 1470-1480.10.1111/j.1365-2745.2011.01882.x

Luo, Y. & Chen, H. Y. H. (2015) Climate change-associated tree mortality increases without decreasing water availability. *Ecology Letters,* **18,** 1207-1215.10.1111/ele.12500

Luo, Y., McIntire, E. J. B., Boisvenue, C., Nikiema, P. P., Chen, H. Y. H. & Bellingham, P. (2019) Climatic change only stimulated growth for trees under weak competition in central boreal forests. *Journal of Ecology,* **108,** 36-46.10.1111/1365-2745.13228

Lutz, J. A., Larson, A. J., Furniss, T. J., Donato, D. C., Freund, J. A., Swanson, M. E., Bible, K. J., Chen, J. & Franklin, J. F. (2014) Spatially nonrandom tree mortality and ingrowth maintain equilibrium pattern in an old-growth Pseudotsuga-Tsuga forest. *Ecology,* **95,** 2047-54.10.1890/14-0157.1

Mace, G. M., Norris, K. & Fitter, A. H. (2012) Biodiversity and ecosystem services: a multilayered relationship. *Trends in Ecology & Evolution,* **27,** 19-26.https://doi.org/10.1016/j.tree.2011.08.006

Marquis, B., Bergeron, Y., Simard, M. & Tremblay, F. (2020) Growing-season frost is a better predictor of tree growth than mean annual temperature in boreal mixedwood forest plantations. *Glob Chang Biol,* **26,** 6537-6554.10.1111/gcb.15327

McDowell, N. G., Allen, C. D., Anderson-Teixeira, K., Aukema, B. H., Bond-Lamberty, B., Chini, L., Clark, J. S., Dietze, M., Grossiord, C., Hanbury-Brown, A., Hurtt, G. C., Jackson, R. B., Johnson, D. J., Kueppers, L., Lichstein, J. W., Ogle, K., Poulter, B., Pugh, T. A. M., Seidl, R., Turner, M. G., Uriarte, M., Walker, A. P. & Xu, C. (2020) Pervasive shifts in forest dynamics in a changing world. *Science,* **368,** eaaz9463.10.1126/science.aaz9463

Messier, C., Parent, S. & Bergeron, Y. (1998) Effects of overstory and understory vegetation on the understory light environment in mixed boreal forests. *Journal of Vegetation Science,* **9,** 511-520.10.2307/3237266

Moeur, M. (1993) Characterising Spatial Patterns of Trees Using Stem-mapped Data. *Forest Science* **39,** 756-775.10.1023/A:1021302930424

Morin, X., Fahse, L., Scherer-Lorenzen, M. & Bugmann, H. (2011) Tree species richness promotes productivity in temperate forests through strong complementarity between species. *Ecol Lett,* **14,** 1211-9.10.1111/j.1461-0248.2011.01691.x

Muledi, J., Bauman, D., Jacobs, A., Meerts, P., Shutcha, M. & Drouet, T. (2020) Tree growth, recruitment, and survival in a tropical dry woodland: The importance of soil and functional identity of the neighbourhood. *Forest Ecology and Management,* **460**.10.1016/j.foreco.2020.117894

Niinemets, Ü. & Valladares, F. (2006) Tolerance to shade, drought, and waterlogging of temperate northern hemisphere trees and shrubs. *Ecological Monographs,* **76,** 521-547.10.1890/0012-9615(2006)076[0521:TTSDAW]2.0.CO;2

Parker, I. M., Saunders, M., Bontrager, M., Weitz, A. P., Hendricks, R., Magarey, R., Suiter, K. & Gilbert, G. S. (2015) Phylogenetic structure and host abundance drive disease pressure in communities. *Nature,* **520,** 542-4.10.1038/nature14372

Parker, T. J., Clancy, K. M. & Mathiasen, R. L. (2006) Interactions among fire, insects and pathogens in coniferous forests of the interior western United States and Canada. *Agricultural and Forest Entomology,* **8,** 167-189.10.1111/j.1461-9563.2006.00305.x

Peng, C. H., Ma, Z. H., Lei, X. D., Zhu, Q., Chen, H., Wang, W. F., Liu, S. R., Li, W. Z., Fang, X. Q. & Zhou, X. L. (2011) A drought-induced pervasive increase in tree mortality across Canada's boreal forests. *Nature Climate Change,* **1,** 467-471.10.1038/Nclimate1293

R Development Core Team, R: A language and environment for statistical computing, R Foundation for Statistical Computing. https://www.R-project.org/ (2021).

R Development Core Team, R: A language and environment for statistical computing. (2022).

Reich, P. B., Bermudez, R., Montgomery, R. A., Rich, R. L., Rice, K. E., Hobbie, S. E. & Stefanski, A. (2022) Even modest climate change may lead to major transitions in boreal forests. *Nature,* **608,** 540-545.10.1038/s41586-022-05076-3

Robin, X., Turck, N. & Hainard, A., pROC: Display and Analyze ROC Curves. https://cran.r-project.org/web/packages/pROC/index.html (2020).

Robin, X., Turck, N. & Hainard, A., pROC: Display and Analyze ROC Curves. https://cran.r-project.org/web/packages/pROC/index.html (2021).

Ruess, R. W., Winton, L. M. & Adams, G. C. (2021) Widespread mortality of trembling aspen (Populus tremuloides) throughout interior Alaskan boreal forests resulting from a novel canker disease. *PLoS One,* **16,** e0250078.10.1371/journal.pone.0250078

Searle, E. B. & Chen, H. Y. (2017) Persistent and pervasive compositional shifts of western boreal forest plots in Canada. *Glob Chang Biol,* **23,** 857-866.10.1111/gcb.13420

Searle, E. B. & Chen, H. Y. H. (2018) Temporal declines in tree longevity associated with faster lifetime growth rates in boreal forests. *Environmental Research Letters,* **13,** 125003.10.1088/1748-9326/aaea9e

Searle, E. B. & Chen, H. Y. H. (2020) Complementarity effects are strengthened by competition intensity and global environmental change in the central boreal forests of Canada. *Ecology Letters,* **23,** 79-87.10.1111/ele.13411

Searle, E. B., Chen, H. Y. H. & Paquette, A. (2022) Higher tree diversity is linked to higher tree mortality. *Proc Natl Acad Sci U S A,* **119,** e2013171119.10.1073/pnas.2013171119

Senici, D., Chen, H. Y. H., Bergeron, Y. & Cyr, D. (2010) Spatiotemporal Variations of Fire Frequency in Central Boreal Forest. *Ecosystems,* **13,** 1227-1238.10.1007/s10021-010-9383-9

Sharma, S., Andrus, R., Bergeron, Y., Bogdziewicz, M., Bragg, D. C., Brockway, D., Cleavitt, N. L., Courbaud, B., Das, A. J., Dietze, M., Fahey, T. J., Franklin, J. F., Gilbert, G. S., Greenberg, C. H., Guo, Q., Hille Ris Lambers, J., Ibanez, I., Johnstone, J. F., Kilner, C. L., Knops, J. M. H., Koenig, W. D., Kunstler, G., LaMontagne, J. M., Macias, D., Moran, E., Myers, J. A., Parmenter, R., Pearse, I. S., Poulton-Kamakura, R., Redmond, M. D., Reid, C. D., Rodman, K. C., Scher, C. L., Schlesinger, W. H., Steele, M. A., Stephenson, N. L., Swenson, J. J., Swift, M., Veblen, T. T., Whipple, A. V., Whitham, T. G., Wion, A. P., Woodall, C. W., Zlotin, R. & Clark, J. S. (2022) North American tree migration paced by climate in the West, lagging in the East. *Proc Natl Acad Sci U S A,* **119**.10.1073/pnas.2116691118

Taylor, A. R., Gao, B. & Chen, H. Y. H. (2020) The effect of species diversity on tree growth varies during forest succession in the boreal forest of central Canada. *Forest Ecology and Management,* **455**.10.1016/j.foreco.2019.117641

Tilman, D. (1982) *Resource competition and community structure.* Princeton University Press, Princeton, New Jersey.

Tilman, D., Isbell, F. & Cowles, J. M. (2014) Biodiversity and Ecosystem Functioning. *Annual Review of Ecology, Evolution, and Systematics,* **45,** 471-493.10.1146/annurev-ecolsys-120213-091917

Trugman, A. T., Medvigy, D., Anderegg, W. R. L. & Pacala, S. W. (2018) Differential declines in Alaskan boreal forest vitality related to climate and competition. *Glob Chang Biol,* **24,** 1097-1107.10.1111/gcb.13952

Usinowicz, J., Chang-Yang, C. H., Chen, Y. Y., Clark, J. S., Fletcher, C., Garwood, N. C., Hao, Z., Johnstone, J., Lin, Y., Metz, M. R., Masaki, T., Nakashizuka, T., Sun, I. F., Valencia, R., Wang, Y., Zimmerman, J. K., Ives, A. R. & Wright, S. J. (2017) Temporal coexistence mechanisms contribute to the latitudinal gradient in forest diversity. *Nature,* **550,** 105-108.10.1038/nature24038

van Mantgem, P. J., Stephenson, N. L., Byrne, J. C., Daniels, L. D., Franklin, J. F., Fule, P. Z., Harmon, M. E., Larson, A. J., Smith, J. M., Taylor, A. H. & Veblen, T. T. (2009)

Widespread increase of tree mortality rates in the western United States. *Science,* **323,** 521-4.10.1126/science.1165000

Vicente-Serrano, S. M., Begueria, S. & Lopez-Moreno, J. I. (2010) A Multiscalar drought index sensitive to global warming: The standardized precipitation evapotranspiration index. *Journal of Climate,* **23,** 1696-1718.10.1175/2009jcli2909.1

Wagg, C., Ebeling, A., Roscher, C., Ravenek, J., Bachmann, D., Eisenhauer, N., Mommer, L., Buchmann, N., Hillebrand, H., Schmid, B. & Weisser, W. W. (2017) Functional trait dissimilarity drives both species complementarity and competitive disparity. *Functional Ecology,* **31,** 2320-2329.https://doi.org/10.1111/1365-2435.12945

Weir, J. M. H., Johnson, E. A. & Miyanishi, K. (2000) Fire frequency and the spatial age mosaic of the mixed-wood boreal forest in western Canada. *Ecological Applications,* **10,** 1162-1177.Doi 10.1890/1051-0761(2000)010[1162:Ffatsa]2.0.Co;2

Wiegand, T., Wang, X., Anderson-Teixeira, K. J., Bourg, N. A., Cao, M., Ci, X., Davies, S. J., Hao, Z., Howe, R. W., Kress, W. J., Lian, J., Li, J., Lin, L., Lin, Y., Ma, K., McShea, W., Mi, X., Su, S. H., Sun, I. F., Wolf, A., Ye, W. & Huth, A. (2021) Consequences of spatial patterns for coexistence in species-rich plant communities. *Nature Ecology and Evolution,* **5,** 965-973.10.1038/s41559-021-01440-0

Williams, L. J., Paquette, A., Cavender-Bares, J., Messier, C. & Reich, P. B. (2017) Spatial complementarity in tree crowns explains overyielding in species mixtures. *Nature Ecology and Evolution,* **1,** 63.10.1038/s41559-016-0063

Yang, X., Gomez-Aparicio, L., Lortie, C. J., Verdu, M., Cavieres, L. A., Huang, Z., Gao, R., Liu, R., Zhao, Y. & Cornelissen, J. H. C. (2022) Net plant interactions are highly variable and weakly dependent on climate at the global scale. *Ecol Lett,* **25,** 1580-1593.10.1111/ele.14010

Yao, J., Bachelot, B., Meng, L., Qin, J., Zhao, X., Zhang, C. & Chu, C. (2020) Abiotic niche partitioning and negative density dependence across multiple life stages in a temperate forest in northeastern China. *Journal of Ecology,* **108,** 1299-1310.10.1111/1365-2745.13335

Young, B., Liang, J. & Stuart Chapin, F. (2011) Effects of species and tree size diversity on recruitment in the Alaskan boreal forest: A geospatial approach. *Forest Ecology and Management,* **262,** 1608-1617.10.1016/j.foreco.2011.07.011

Zambrano, J., Beckman, N. G., Marchand, P., Thompson, J., Uriarte, M., Zimmerman, J. K., Umana, M. N. & Swenson, N. G. (2020) The scale dependency of trait-based tree neighborhood models. *Journal of Vegetation Science,* **31,** 581-593.10.1111/jvs.12880

Zellweger, F., De Frenne, P., Lenoir, J., Vangansbeke, P., Verheyen, K., Bernhardt-Romermann, M., Baeten, L., Hedl, R., Berki, I., Brunet, J., Van Calster, H., Chudomelova, M., Decocq, G., Dirnbock, T., Durak, T., Heinken, T., Jaroszewicz, B., Kopecky, M., Malis, F., Macek, M., Malicki, M., Naaf, T., Nagel, T. A., Ortmann-Ajkai, A., Petrik, P., Pielech, R., Reczynska, K., Schmidt, W., Standovar, T., Swierkosz, K., Teleki, B., Vild, O., Wulf, M. & Coomes, D. (2020) Forest microclimate dynamics drive plant responses to warming. *Science,* **368,** 772-775.10.1126/science.aba6880

Zhang, J., Huang, S. & He, F. (2015) Half-century evidence from western Canada shows forest dynamics are primarily driven by competition followed by climate. *Proceedings of the National Academy of Sciences of the United States of America,* **112,** 4009-14.10.1073/pnas.1420844112

Zhang, Y., Chen, H. Y. H. & Reich, P. B. (2012) Forest productivity increases with evenness, species richness and trait variation: a global meta-analysis. *Journal of Ecology,* **100,** 742-749.10.1111/j.1365-2745.2011.01944.x

Zhang, Y., Chen, H. Y. H., Taylor, A. R. & Ostertag, R. (2016) Positive species diversity and above‑ground biomass relationships are ubiquitous across forest strata despite interference from overstorey trees. *Functional Ecology,* **31,** 419-426.10.1111/1365-2435.12699

Zhu, Y., Comita, L. S., Hubbell, S. P., Ma, K. & Shefferson, R. (2015) Conspecific and phylogenetic density-dependent survival differs across life stages in a tropical forest. *Journal of Ecology,* **103,** 957-966.10.1111/1365-2745.12414

Zhu, Y., Queenborough, S. A., Condit, R., Hubbell, S. P., Ma, K. P. & Comita, L. S. (2018) Density-dependent survival varies with species life-history strategy in a tropical forest. *Ecology Letters,* **21,** 506-515.10.1111/ele.12915

Zhu, Y., Searle, E. B. & Chen, H. Y. H. (2022) Functionally and phylogenetically diverse boreal forests promote sapling recruitment. *Forest Ecology and Management,* **524**.10.1016/j.foreco.2022.120522

Zuur, A. F., Ieno, E. N. & Elphick, C. S. (2010) A protocol for data exploration to avoid common statistical problems. *Methods in Ecology and Evolution,* **1,** 3-14.10.1111/j.2041-210X.2009.00001.x

# APPENDIX I: SUPPLEMENTAL INFORMATION FOR CHAPTER 2
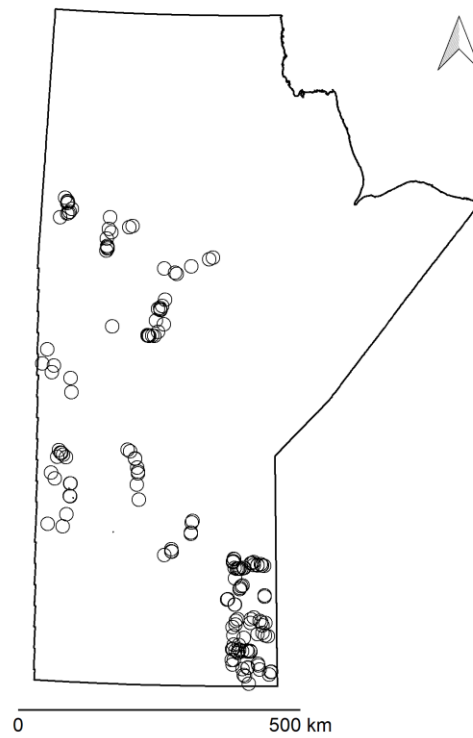
Figure S2-1 Plot locations of 173 permanent sample plots of boreal forest in Manitoba, Canada.
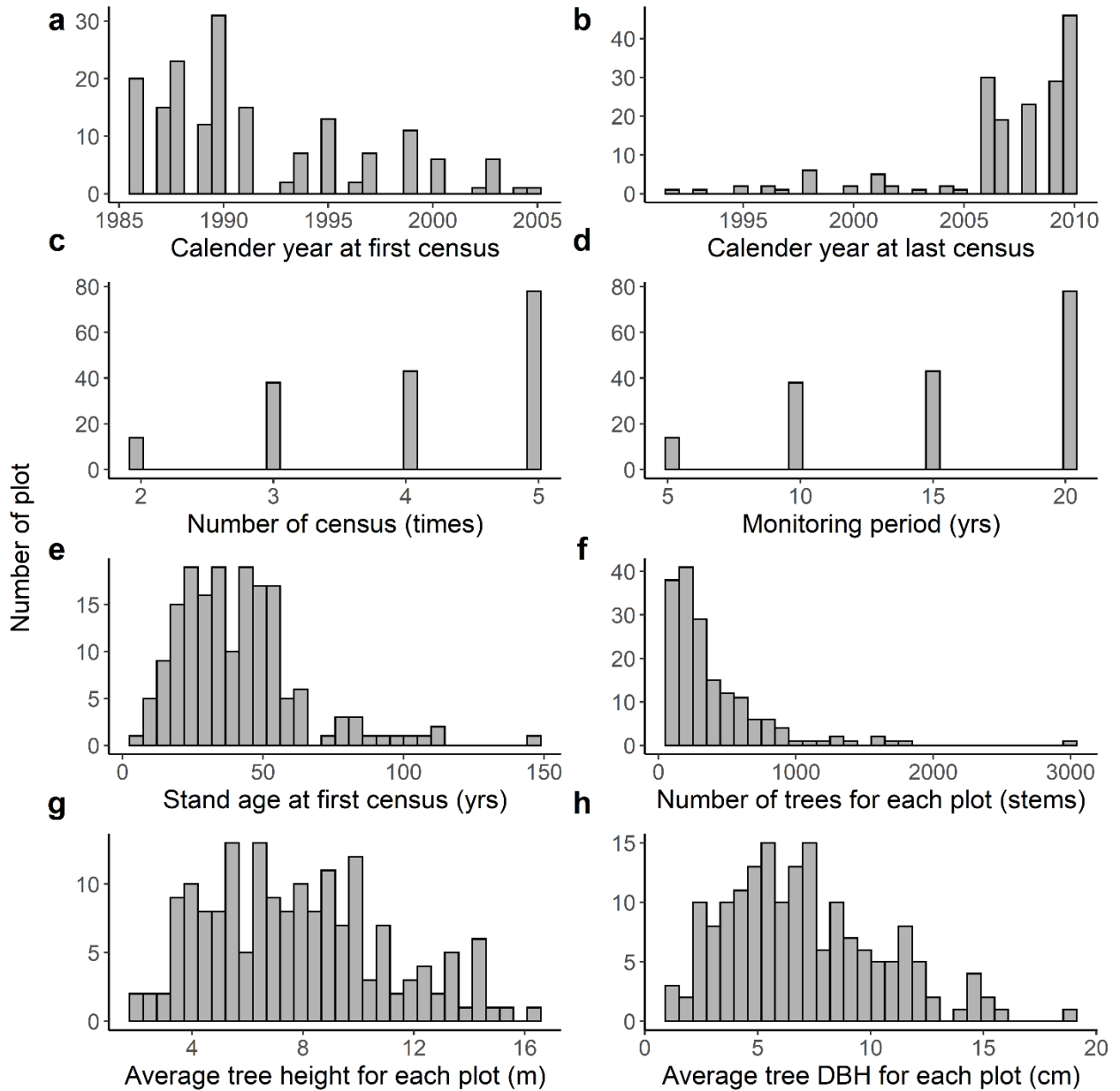
Figure S2-2 Distribution histograms of the selected 173 plots. a calendar year at the first census. b calendar year at the final census. c number of censuses. d length of the monitoring period. e stand age at the first census, f number of trees for each plot, g average tree height for each plot, and h average tree DBH for each plot.
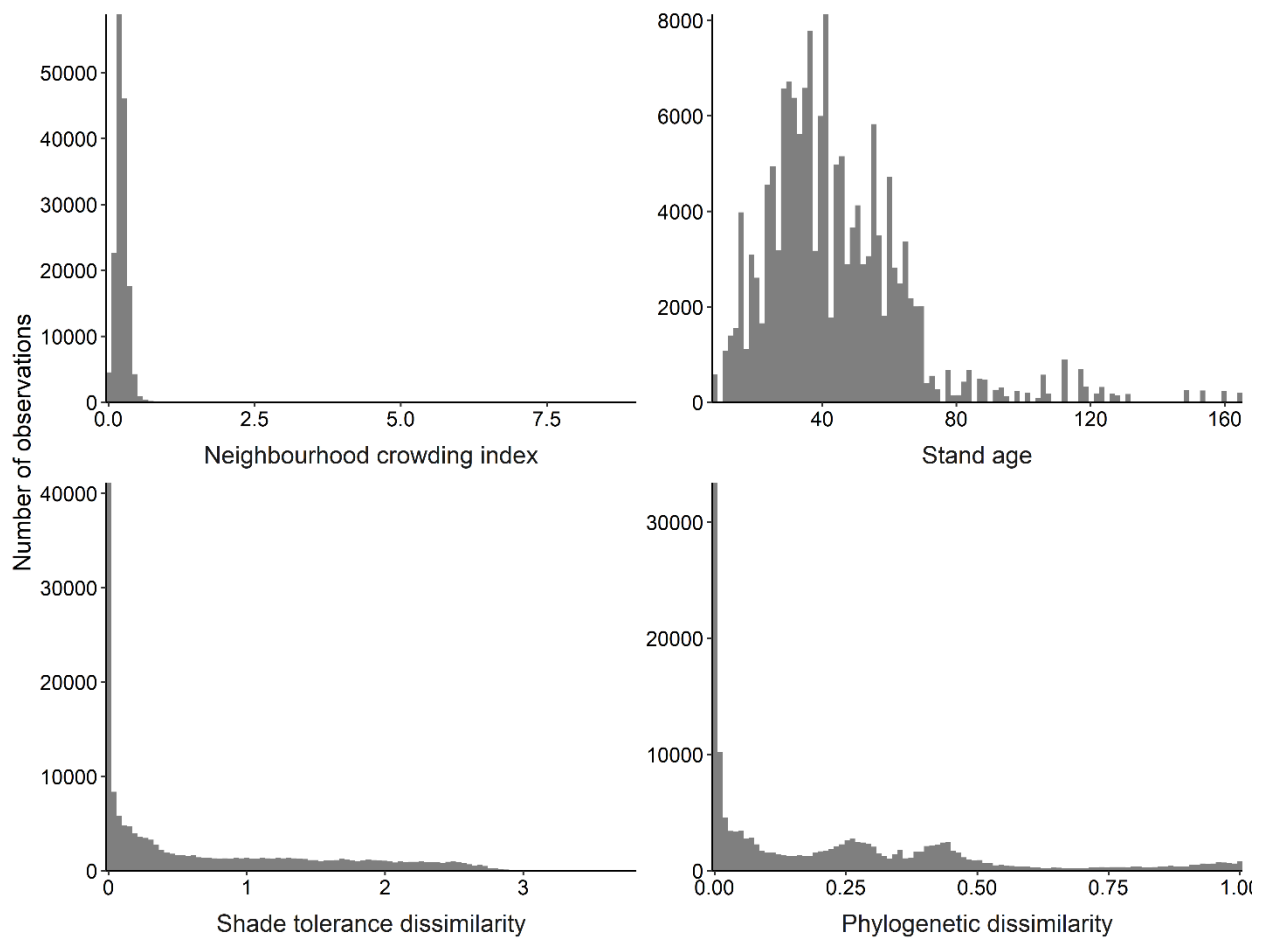
Figure S2-3 Histograms of measured explanatory variables
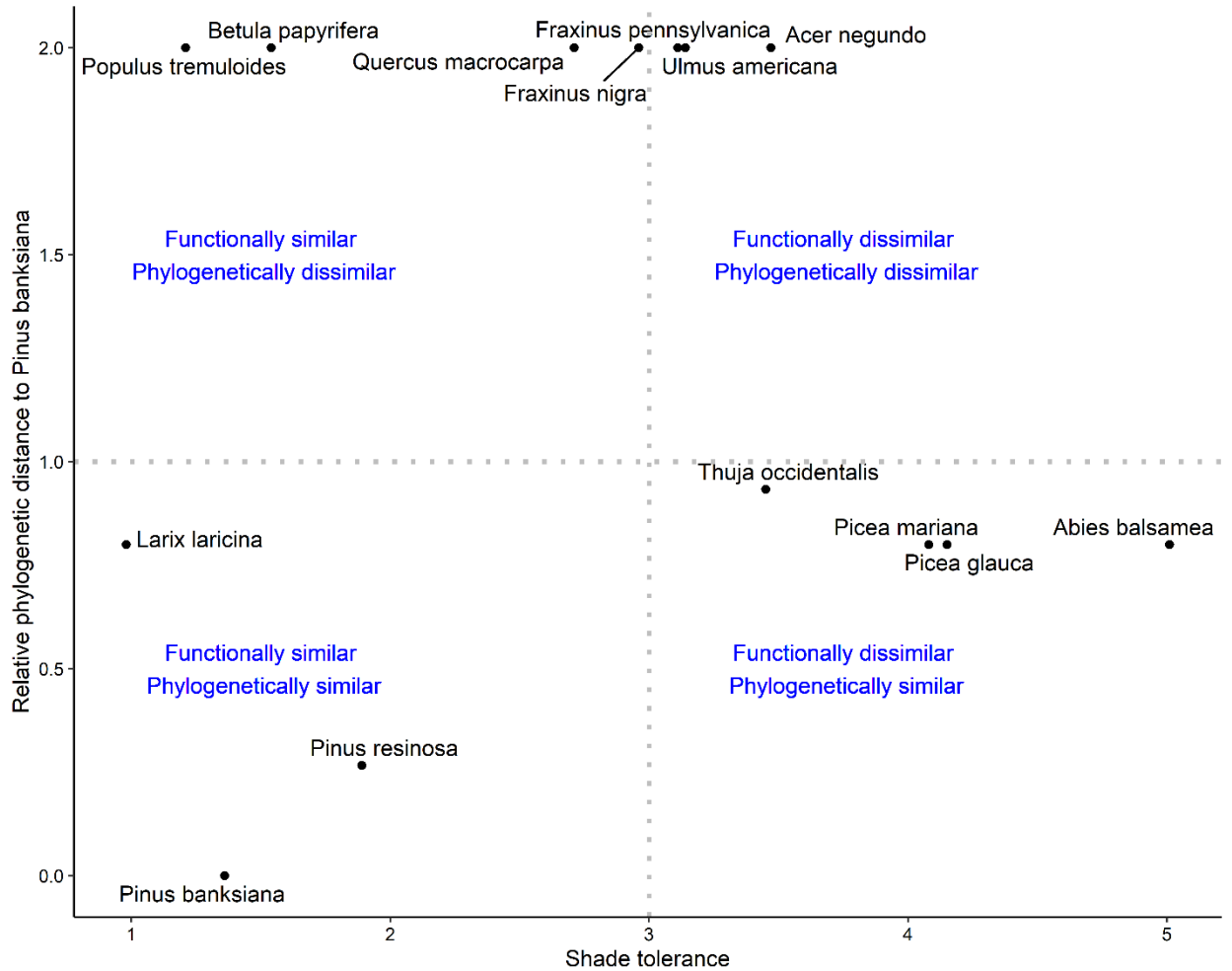
Figure S2-4 Shade tolerance of each species *versus* phylogenetic similarity to *Pinus banksiana*. Species in the bottom left are functionally (i.e., similar shade tolerance values) and phylogenetically similar to *Pinus banksiana*; species in the top left are functionally similar but phylogenetically dissimilar to *Pinus banksiana*; species in the top right are functionally and phylogenetically dissimilar to *Pinus banksiana*; and, species in the bottom right are functionally dissimilar but phylogenetically similar to *Pinus banksiana*. The horizontal dotted line denotes the break between gymnosperms and angiosperms in the phylogeny while the vertical line is approximately the average shade tolerance observed in the dataset.

101
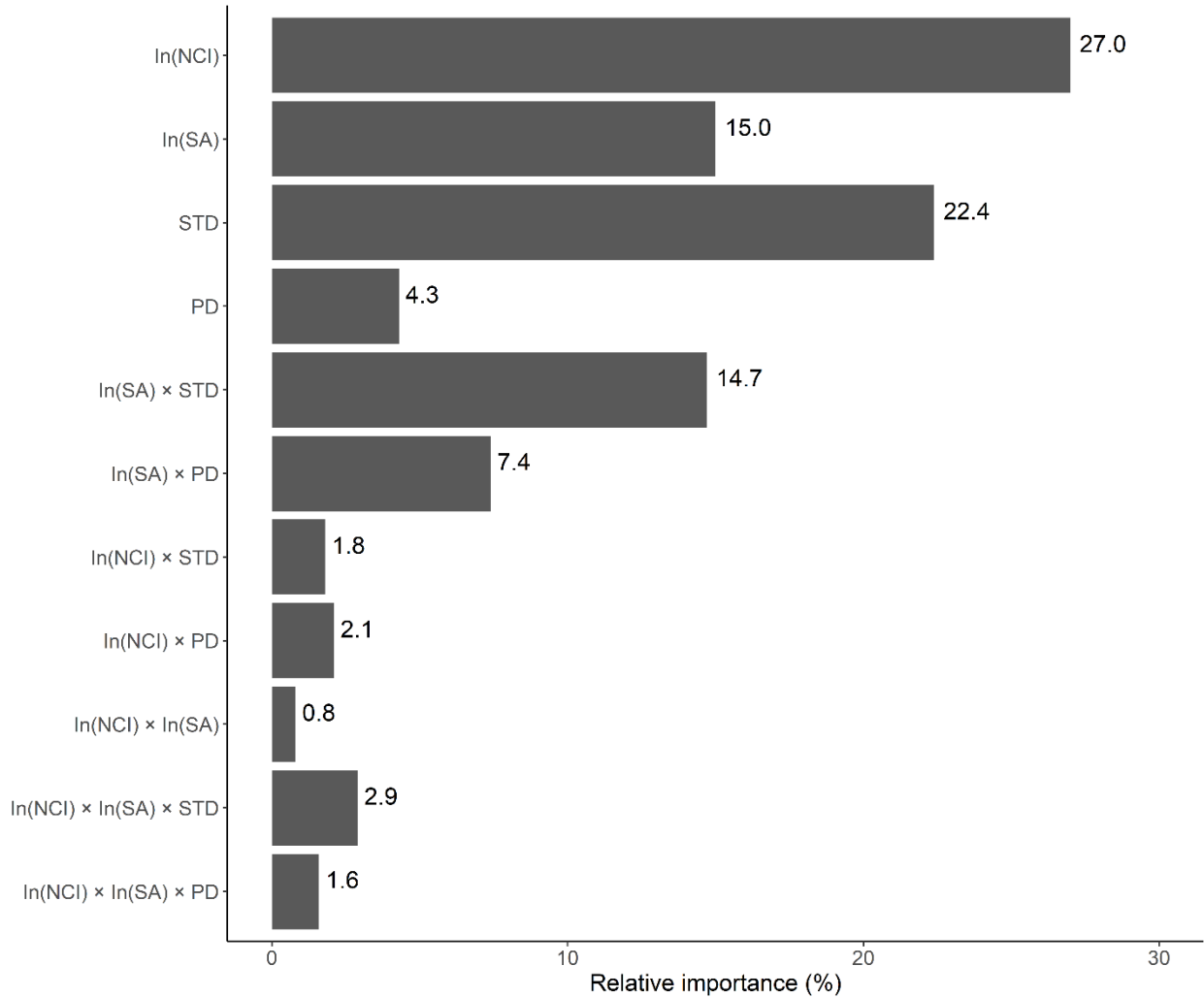
Figure S2-5 The relative importance of neighbourhood crowding index (NCI), stand age (SA), shade tolerance dissimilarity (STD), and phylogenetic dissimilarity (PD) on *sapling* recruitment in boreal forest. The NCI and SA were natural log-transformed. Relative importance was calculated as the proportion of standardized coefficients of the fitted model (Table 2-1).

APPENDIX II: SUPPLEMENTAL INFORMATION FOR CHAPTER 3

Supplement methods

Model 1:

$$logit(p_{ijkl}) = \beta_{0a} + \beta_1 Y_{ij} + \beta_2 logM_{ij} + \beta_3 logG_{ij} + \beta_4 logNCI_{ij} + \beta_5 FD_{ij} +$$

$$\beta_6 PD_{ij} + \alpha_j + \alpha_k + \varepsilon_{ijkl} \tag{1}$$

$$logM_{ijl} = \beta_{0b} + \beta_7 Y_{ij} + \alpha_j + \varepsilon_{ijl} \tag{2}$$

$$logG_{ijl} = \beta_{0c} + \beta_8 Y_{ij} + \alpha_j + \varepsilon_{ijl} \tag{3}$$

$$logNCI_{ijl} = \beta_{0d} + \beta_9 Y_{ij} + \alpha_j + \varepsilon_{ijl} \tag{4}$$

$$FD_{ijl} = \beta_{0e} + \beta_{10} Y_{ij} + \alpha_j + \varepsilon_{ijl} \tag{5}$$

$$PD_{ijl} = \beta_{0f} + \beta_{11} Y_{ij} + \alpha_j + \varepsilon_{ijl} \tag{6}$$

The calculation of direct, indirect, and total impacts of climate change based on the

standardized effects of β_s, as:

Direct effect of Y: β_1
Indirect effect through M: $\beta_2 \times \beta_7$
Indirect effect through G: $\beta_3 \times \beta_8$
Indirect effect through NCI: $\beta_4 \times \beta_9$
Indirect effect through FD: $\beta_5 \times \beta_{10}$
Indirect effect through PD: $\beta_6 \times \beta_{11}$
Total effect through NCI: $\beta_1 + \beta_2 \times \beta_7 + \beta_3 \times \beta_8 + \beta_4 \times \beta_9 + \beta_5 \times \beta_{10} + \beta_6 \times \beta_{11}$

Model 2:

$$logit(p_{ijkl}) = \beta_{0a} + \beta_1 Y_{ij} + \beta_2 logM_{ij} + \beta_3 logG_{ij} + \beta_4 logNCI_{ij} + \beta_5 FD_{ij} +$$

$$\beta_6 PD_{ij} + \alpha_j + \alpha_k + \varepsilon_{ijkl} \tag{1}$$

$$logM_{ijl} = \beta_{0b} + \beta_7 Y_{ij} + \alpha_j + \varepsilon_{ijl} \tag{2}$$

$$logG_{ijl} = \beta_{0c} + \beta_8 Y_{ij} + \alpha_j + \varepsilon_{ijl} \tag{3}$$

$$logNCI_{ijl} = \beta_{0d} + \beta_9 Y_{ij} + \beta_{10} logM_{ij} + \beta_{11} logG_{ij} + \alpha_j + \varepsilon_{ijl} \tag{4}$$

$$FD_{ijl} = \beta_{0e} + \beta_{12} Y_{ij} + \beta_{13} logM_{ij} + \beta_{14} logG_{ij} + \alpha_j + \varepsilon_{ijl} \tag{5}$$

$$PD_{ijl} = \beta_{0f} + \beta_{15} Y_{ij} + \beta_{16} logM_{ij} + \beta_{17} logG_{ij} + \alpha_j + \varepsilon_{ijl} \tag{6}$$

Model 3:

$$logit(p_{ijkl}) = \beta_{0a} + \beta_1 Y_{ij} + \beta_2 logM_{ij} + \beta_3 logG_{ij} + \beta_4 logNCI_{ij} + \beta_5 FD_{ij} +$$

$$\beta_6 PD_{ij} + \alpha_j + \alpha_k + \varepsilon_{ijkl} \tag{1}$$

$$logM_{ijl} = \beta_{0b} + \beta_7 Y_{ij} + \beta_8 logNCI_{ij} + \beta_9 FD_{ij} + \beta_{10} PD_{ij} + \alpha_j + \varepsilon_{ijl} \tag{2}$$

$$logG_{ijl} = \beta_{0c} + \beta_{11} Y_{ij} + \beta_{12} logNCI_{ij} + \beta_{13} FD_{ij} + \beta_{14} PD_{ij} + \alpha_j + \varepsilon_{ijl} \tag{3}$$

$$logNCI_{ijl} = \beta_{0d} + \beta_{15}Y_{ij} + \alpha_j + \varepsilon_{ijl} \tag{4}$$
$$FD_{ijl} = \beta_{0e} + \beta_{16}Y_{ij} + \alpha_j + \varepsilon_{ijl} \tag{5}$$
$$PD_{ijl} = \beta_{0f} + \beta_{17}Y_{ij} + \alpha_j + \varepsilon_{ijl} \tag{6}$$

Model 4:

$$logit(p_{ijkl}) = \beta_{0a} + \beta_1 Y_{ij} + \beta_2 logSA_{ij} + \beta_3 logM_{ij} + \beta_4 logG_{ij} + \beta_5 logNCI_{ij} +$$
$$\beta_6 FD_{ij} + \beta_7 PD_{ij} + \alpha_j + \alpha_k + \varepsilon_{ijkl} \tag{1}$$
$$logM_{ijl} = \beta_{0b} + \beta_8 Y_{ij} + \beta_9 logSA_{ij} + \alpha_j + \varepsilon_{ijl} \tag{2}$$
$$logG_{ijl} = \beta_{0c} + \beta_{10}Y_{ij} + \beta_{11} logSA_{ij} + \alpha_j + \varepsilon_{ijl} \tag{3}$$
$$logNCI_{ijl} = \beta_{0d} + \beta_{12}Y_{ij} + \beta_{13} logSA_{ij} + \alpha_j + \varepsilon_{ijl} \tag{4}$$
$$FD_{ijl} = \beta_{0f} + \beta_{14}Y_{ij} + \beta_{15} logSA_{ij} + \alpha_j + \varepsilon_{ijl} \tag{5}$$
$$PD_{ijl} = \beta_{0g} + \beta_{15}Y_{ij} + \beta_{16} logSA_{ij} + \alpha_j + \varepsilon_{ijl} \tag{6}$$

Model 5:

$$logit(p_{ijkl}) = \beta_{0a} + \beta_1 PC1_{ij} + \beta_2 logM_{ij} + \beta_3 logG_{ij} + \beta_4 logNCI_{ij} + \beta_5 FD_{ij} +$$
$$\beta_6 PD_{ij} + \alpha_j + \alpha_k + \varepsilon_{ijkl} \tag{1}$$
$$logM_{ijl} = \beta_{0b} + \beta_7 PC1_{ij} + \alpha_j + \varepsilon_{ijl} \tag{2}$$
$$logG_{ijl} = \beta_{0c} + \beta_8 PC1_{ij} + \alpha_j + \varepsilon_{ijl} \tag{3}$$
$$logNCI_{ijl} = \beta_{0d} + \beta_9 PC1_{ij} + \alpha_j + \varepsilon_{ijl} \tag{4}$$
$$FD_{ijl} = \beta_{0e} + \beta_{10} PC1_{ij} + \alpha_j + \varepsilon_{ijl} \tag{5}$$
$$PD_{ijl} = \beta_{0f} + \beta_{11} PC1_{ij} + \alpha_j + \varepsilon_{ijl} \tag{6}$$

where: p is sapling recruitment probability per 5-year interval, βs are coefficients to be estimated, i indicates the ith census of a plot, j indicates the jth plot, k indicates the kth species, and l indicates the lth stem within the jth plot. Y, SA stand for middle age of calendar year and stand age between two consecutive censuses. M, G stand for basal area loss from dead trees and net basal is increment from living trees in neighbourhood between two consecutive censuses, NCI, FD, PD stand for neighbourhood crowding index, functional dissimilarity, and phylogenetic dissimilarity between two consecutive censuses. $PC1$ stands for the first principal component of the three climate change drivers (CO_2, ATA and SPEI).

Table S3-1. The number of plots, stems of total and each demography for all and abundant tree species in studied boreal forest. Demographic rates (mean with 95% confidence interval in bracket) were calculated as the percentage of sapling recruit/dead tree from the total number of stems or the average net basal mass increment per species per plot per 5-year census.

Species	No.of plots	No. of stems				Demographic rate		
		Total	Recruitment	Dead	Growth	Recruitment %	Mortality %	Growth cm^2
All tree species	173	69470	10893	21754	65728	5.5 (5.1 - 5.9)	14.0 (13.5 – 14.5)	12.38 (11.78 - 12.98)
Picea mariana	114	24431	6990	3537	23122	4.8 (4.0 - 5.6)	11.3 (10.2 - 12.4)	7.88 (7.02 - 8.74)
Populus tremuloides	111	15395	1139	7575	14579	6.0 (4.8 - 7.2)	16.5 (15.1 - 17.9)	14.14 (12.72 - 15.56)
Pinus banksiana	97	18762	1349	6124	17878	5.1 (4.1 - 6.1)	12 (10.9 - 13.1)	13.31 (12.04 - 14.58)
Betula papyrifera	85	2202	452	933	1997	6.3 (4.8 - 7.8)	14.4 (13 - 15.8)	8.52 (7.43 - 9.61)
Picea glauca	56	1299	104	256	1250	4.7 (3.3 - 6.1)	14.5 (12.4 - 16.6)	18.21 (15.26 - 21.16)
Fraxinus nigra	44	1964	263	1103	1764	6.7 (4.7 - 8.7)	15.6 (13.8 - 17.4)	11.00 (8.89 - 13.11)
Abies balsamea	42	3603	381	1852	3415	5.8 (3.7 - 7.9)	17.9 (14.7 - 21.1)	11.79 (9.55 - 14.03)
Larix laricina	36	1038	29	267	1019	3.9 (2.5 - 5.3)	9.6 (7.7 - 11.5)	21.64 (18.41 - 24.87)
Thuja occidentalis	6	694	123	87	671	4.7 (2.2 - 7.2)	10.7 (6.9 - 14.5)	9.24 (5.15 - 13.33)

Table S3-2. The number of dead trees and the mortality rate of established trees per size class. Mortality rate (mean with 95% confidence interval in bracket) was calculated as the percentage of dead trees from total stems per size class per plot per 5-year census.

Class	No. of dead tree	Mortality rate %
$0.1 \leq DBH < 5$	44248	14.0 (13.0 - 15.0)
$5 \leq DBH < 10$	20543	14.0 (13.0 - 15.0)
$10 \leq DBH < 15$	8427	14.1 (13.1 -15.1)
$15 \leq DBH < 50$	3536	14.6 (13.4 - 15.8)

Table S3-3. Summary statistics (Mean ± sd and range in brackets) of explanatory variables.

Explanatory variable	Summary statistics
Atmospheric CO_2 (ppm)	365.8 ± 10.88 ($347.4 \sim 384.7$)
Annual temperature anomaly (ATA, ºC)	0.10 ± 0.68 ($-2.50 \sim 2.26$)
Standardized precipitation evapotranspiration index (SPEI)	0.00 ± 0.49 ($-2.31 \sim 1.65$)
Calendar year (Y)	1999 ± 5.74 ($1988 \sim 2008$)
Mortality of established trees (M)	112.6 ± 261.2 ($0 \sim 21905$)
Growth of established trees (G)	320.3 ± 301.8 ($0 \sim 12586$)
Neighbourhood crowding index (NCI)	2273 ± 1310 ($10 \sim 89908$)
Shade tolerance dissimilarity (STD)	0.70 ± 0.82 ($0.00 \sim 3.80$)
Phylogenetic dissimilarity (PD)	0.24 ± 0.27 ($0.00 \sim 1.00$)
Stand age (SA, yrs)	43.71 ± 21.49 ($7.47 \sim 164.1$)
The first principal component of the three climate change drivers (PC1) (see *Methods*)	0.00 ± 1.36 ($-2.39 \sim 2.90$)

Table S3-4. Fitting statistics of alternative structural equation models (SEMs) for sapling recruitment (R). All abbreviations are described in Table S3-3. The single-direction arrow represents the path, and the double-direction arrow represents the relationship between each pair of predictors. n indicates the number of censuses of plots for the model is fitted to. Fisher's C, attendant degree of freedom (DF), and *P* value indicate whether candidate models are a good fit for the data (e.g., whether omitted pathways are non-informative). A *P* value greater than 0.05 indicates that the model is a good fit (e.g., all informative pathways are included). Akaike information criterion (AIC) is used to compare candidate models. See *Methods* for model selection.

SEM	Description	n	Fisher's C	DF	*P* value	AIC
1	Y → (NCI/STD/PD ↔ M/G) → R	532	1.307	4	0.86	59.3
2	Y → M/G → NCI/STD/PD → R	532	0.227	2	0.89	72.2
3	Y → NCI/STD/PD → M/G → R	532	1.307	4	0.86	71.3
4	Y/SA → (NCI/STD/PD ↔ M/G) → R	532	1.306	4	0.86	71.3
5	PCA1 → (NCI/STD/PD ↔ M/G) → R	532	1.808	4	0.77	59.7

Table S3-5. Spatial dependency for plots on means 5-year sapling recruitment rate and residuals of all submodels in Fig. 3-3. The observed correlation in Mantel statistic, r value, ranges between -1 to 1. An r value of -1 suggests a strong negative correlation, 0 suggests no relationship at all and 1 suggests a strong positive relationship. The *P* value > 0.05 indicates no spatial autocorrelations.

Model	r value	*P* value
Mean 5-year sapling recruitment rate	-0.026	0.821
Sapling recruitment submodel	-0.005	0.621
Mortality submodel	-0.048	0.951
Growth submodel	0.032	0.165
Neighbourhood crowding index submodel	0.022	0.227
Shade tolerance dissimilarity submodel	-0.072	0.998
Phylogenetic dissimilarity submodel	-0.034	0.873

Table S3-6. Standardized coefficient estimates for the structural equation models with the middle value of calendar year representing climate change as a whole (Y) and the first principal component of the three climate change drivers (PC1). Numbers represent mean estimates, and colours identify the blocks in Fig. 3-2. Standardized estimates are presented to allow for the comparison of effect size. Estimates represent the standard coefficient with 95% Wald confidence intervals for paths and correlation coefficient for correlations. The single-direction arrow represents the path, and the wavy line represents the relationship between each pair of predictors. n indicates the number of censuses of each plot that for both models are fitted to. NCI, STD, PD represent neighbourhood crowding index, shade tolerance dissimilarity and phylogenetic dissimilarity.

Pathway	Y		PC1		n
	Estimate	*P* value	Estimate	*P* value	
Climate change block					
Y or PC1 → Recruitment	0.027 ± 0.032	0.096	0.053 ± 0.031	6.0×10^{-4}	532
Y or PC1 → Mortality	0.421 ± 0.005	$<1.0 \times 10^{-300}$	0.389 ± 0.005	$<1.0 \times 10^{-300}$	532
Y or PC1 → Growth	0.063 ± 0.003	$<1.0 \times 10^{-300}$	0.049 ± 0.003	$<1.0 \times 10^{-300}$	532
Y or PC1 → NCI	0.153 ± 0.002	$<1.0 \times 10^{-300}$	0.147 ± 0.002	$<1.0 \times 10^{-300}$	532
Y or PC1 →STD	0.014 ± 0.003	9.1×10^{-17}	0.013 ± 0.003	$<9.1 \times 10^{-17}$	532
Y or PC1 → PD	0.007 ± 0.001	8.2×10^{-34}	0.006 ± 0.001	$<8.2 \times 10^{-34}$	532
Demography block					
Mortality → Recruitment	-0.053 ± 0.051	0.038	-0.060 ± 0.050	0.019	532
Grow → Recruitment	-0.122 ± 0.047	2.6×10^{-7}	-0.117 ± 0.047	8.7×10^{-7}	532
Mortality ~ Growth	0.074	5.0×10^{-7}	0.085	$<1.0 \times 10^{-50}$	532

Neighbourhood interactions block					
NCI → Recruitment	-1.041 ± 0.057	2.5×10^{-283}	-0.106 ± 0.057	3.9×10^{-291}	532
STD → Recruitment	0.652 ± 0.052	3.8×10^{-135}	0.665 ± 0.052	3.8×10^{-140}	532
PD → Recruitment	0.077 ± 0.046	0.001	0.073 ± 0.047	0.002	532
STD ~ PD	0.489	$<1.0 \times 10^{-50}$	0.489	$<1.0 \times 10^{-50}$	532
Correlation between blocks					
Mortality ~ NCI	0.203	$<1.0 \times 10^{-50}$	0.223	$<1.0 \times 10^{-50}$	532
Mortality ~ STD	0.012	6.9×10^{-7}	0.014	4.4×10^{-8}	532
Mortality ~ PD	0.011	3.3×10^{-6}	0.014	1.1×10^{-8}	532
Growth ~ NCI	0.397	$<1.0 \times 10^{-50}$	0.405	$<1.0 \times 10^{-50}$	532
Growth ~ STD	-0.007	0.010	-0.005	0.019	532
Growth ~ PD	0.028	$<1.0 \times 10^{-50}$	0.029	$<1.0 \times 10^{-50}$	532

Table S3-7. Path estimates for the model in Figure 3-3. Estimates represent the standard coefficient with 95% Wald confidence intervals for submodels. DF represents the degree of freedom in the denominator while the degree of freedom for the nominator is 1 for all continuous predictors in structural equation models. The z value was fitted for the recruitment model with a binomial distribution, and the t value was fitted for other submodels with Gaussian distributions and the critical (c) value was fitted for correlations. Other abbreviations are described in Table S3-3.

Source	Estimate	DF	z/t/c value	*P* value
Recruitment submodel				
Intercept	-3.111 ± 0.904		-6.746	1.5×10^{-11}
Year	0.027 ± 0.032		1.666	0.096
Mortality	-0.053 ± 0.051		-2.070	0.038
Growth	-0.122 ± 0.047		-5.154	2.6×10^{-7}
NCI	-1.041 ± 0.057		-35.97	2.5×10^{-283}
STD	0.652 ± 0.052		24.74	3.8×10^{-135}
PD	0.077 ± 0.046		3.243	0.001
Mortality submodel				
Intercept	4.372 ± 0.005	172	45.85	2.2×10^{-98}
Year	0.421 ± 0.005	155950	173.0	$<1.0 \times 10^{-300}$
Growth submodel				
Intercept	5.757 ± 0.076	172	149.0	1.2×10^{-183}
Year	0.063 ± 0.003	156023	40.18	$<1.0 \times 10^{-300}$
NCI submodel				
Intercept	7.660 ± 0.071	172	214.2	8.0×10^{-211}
Year	0.153 ± 0.002	155934	191.7	$<1.0 \times 10^{-300}$
STD submodel				
Intercept	0.574 ± 0.089	172	12.74	1.3×10^{-26}
Year	0.014 ± 0.003	156009	8.317	9.1×10^{-17}
PD submodel				
Intercept	0.209 ± 0.028	172	14.70	3.4×10^{-32}
Year	0.007 ± 0.001	156019	12.12	8.2×10^{-34}
Correlations				
Mortality ~ Growth	0.074	156048	29.29	$<1.0 \times 10^{-50}$
STD ~ PD	0.489	156048	221.5	$<1.0 \times 10^{-50}$

Mortality ~ NCI	0.203	156048	82.02	$<1.0 \times 10^{-50}$
Mortality ~ STD	0.012	156048	4.828	6.9×10^{-7}
Mortality ~ PD	0.011	156048	4.506	3.3×10^{-6}
Growth ~ NCI	0.397	156048	171.1	$<1.0 \times 10^{-50}$
Growth ~ STD	-0.006	156048	-2.327	0.010
Growth ~ PD	0.027	156048	10.86	$<1.0 \times 10^{-50}$
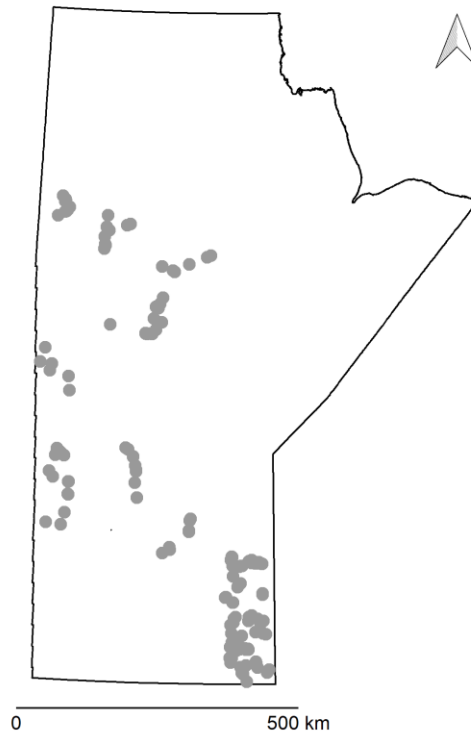
Figure S3-1 Plot locations of 173 permanent sample plots of boreal forest in Manitoba, Canada. The plots were in the boreal forest regions of Manitoba, while the top regions are boreal taiga transition to tundra. The left bottom regions are prairies.
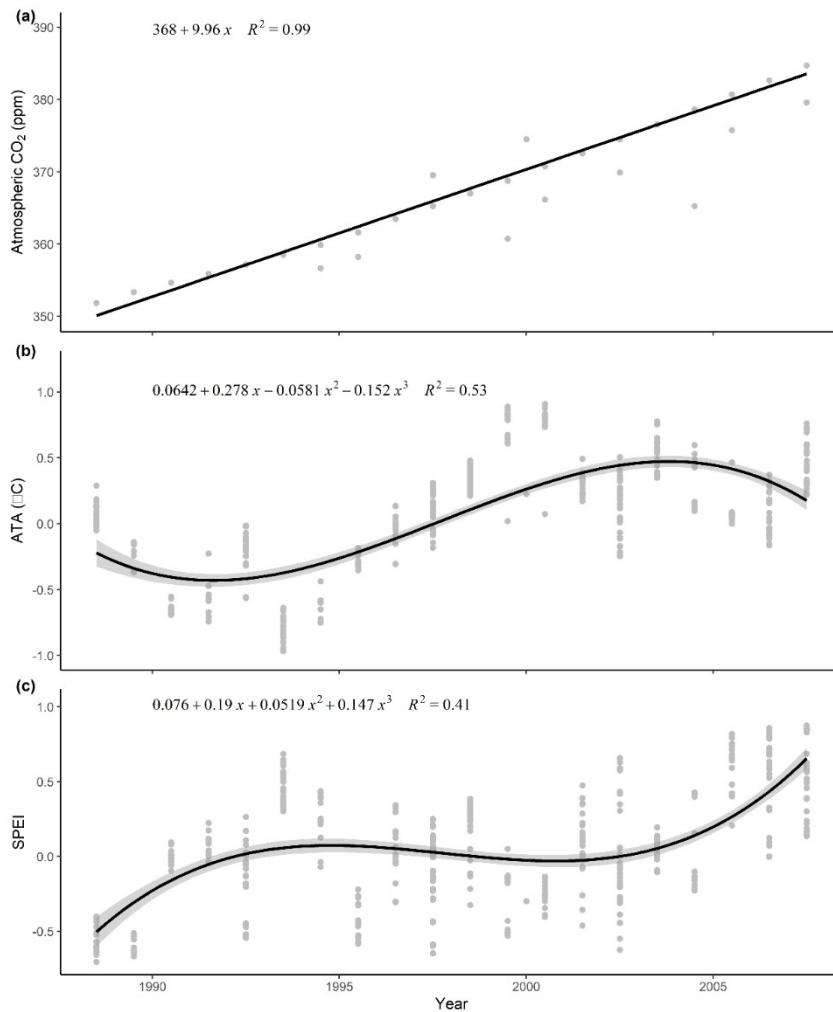
Figure S3-2 Temporal trends in climate drivers. Points are values at the individual tree level, while black lines represent Loess smoothing for the atmospheric CO_2 concentration (CO_2), annual temperature anomaly (ATA), and annual standardized precipitation–evapotranspiration index (SPEI), respectively. The graphical assessment indicated a linear between CO_2 but multiphasic relationships between ATA and SPEI and calendar year.
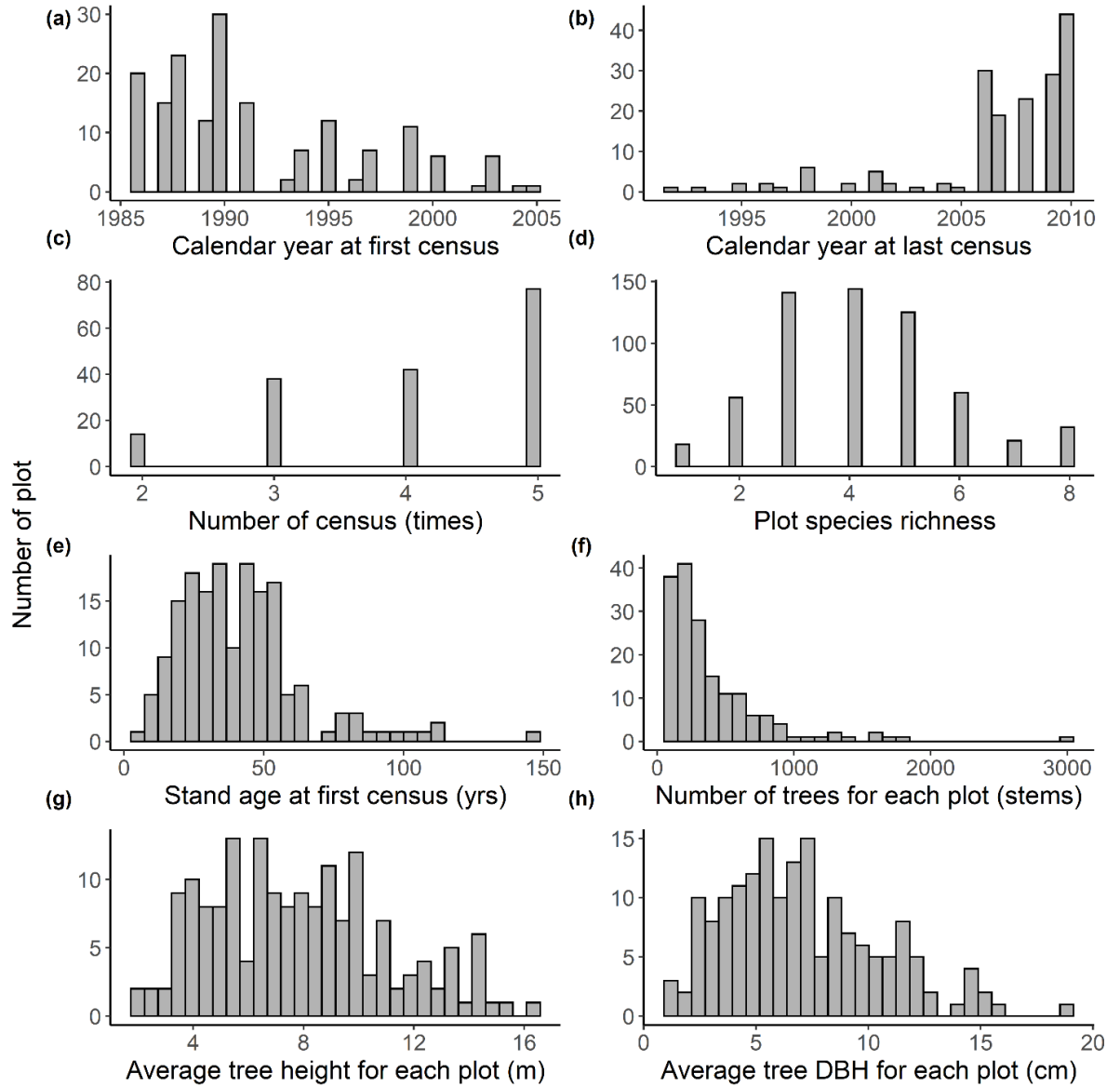
Figure S3-3 Distribution histograms of the selected 173 plots. (a) calendar year at the first census, (b) calendar year at the last census, (c) number of censuses, (d) plot species richness, (e) stand age at the first census, (f) the number of trees for each plot, (g) average tree height for each plot, and (h) average tree DBH for each plot.
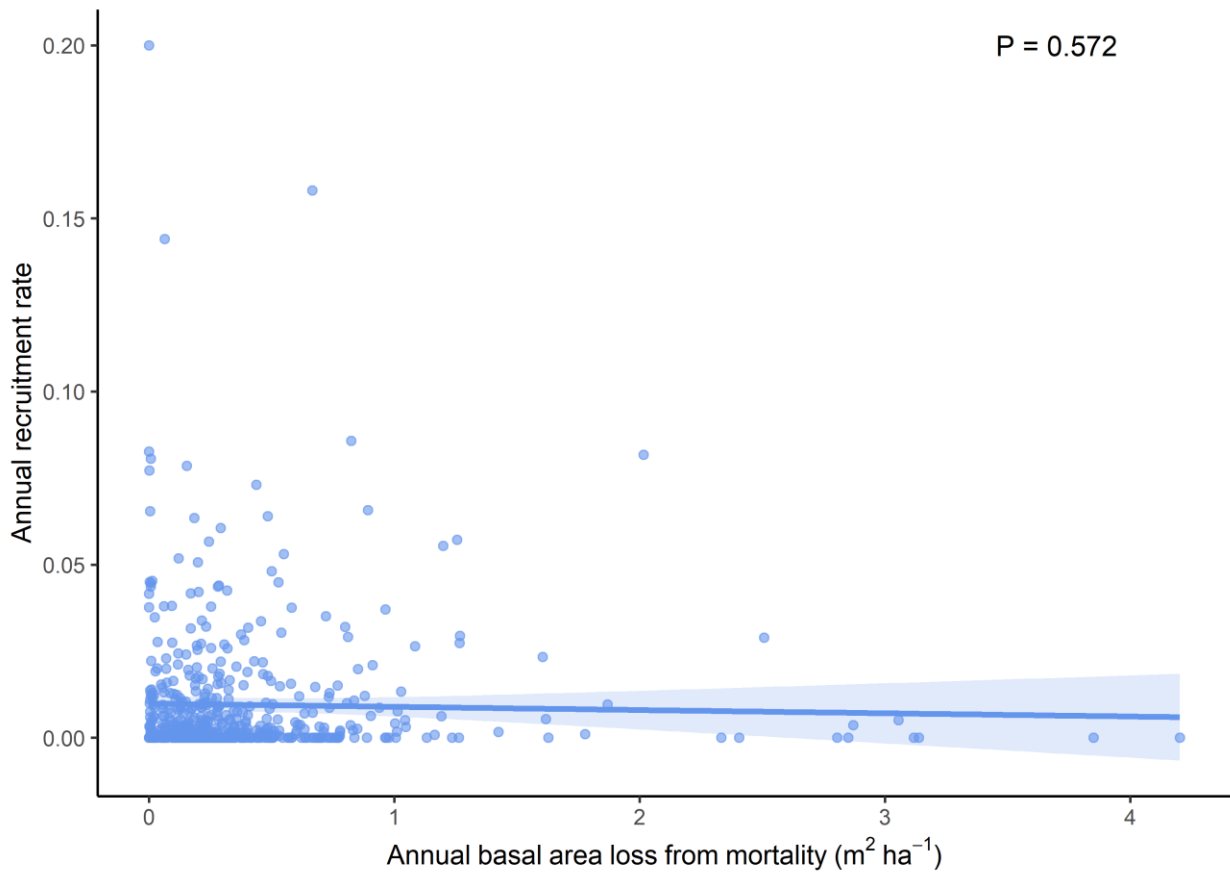
Figure S3-4 The recruitment rate response to basal area loss from mortality at the plot level. Annual mortality rates were derived from basal area loss during two consecutive censuses divided by 5-year interval. Annual recruitment rates were the occurrence of recruit numbers per total stems at the current census compared with the previous census per plot, then divided by 5-year interval. The line and shades are the mean and 95% confidence intervals of the slope fitted by linear mixed-effect models with the plot as a random effect; the dots represent each observation per plot per census.
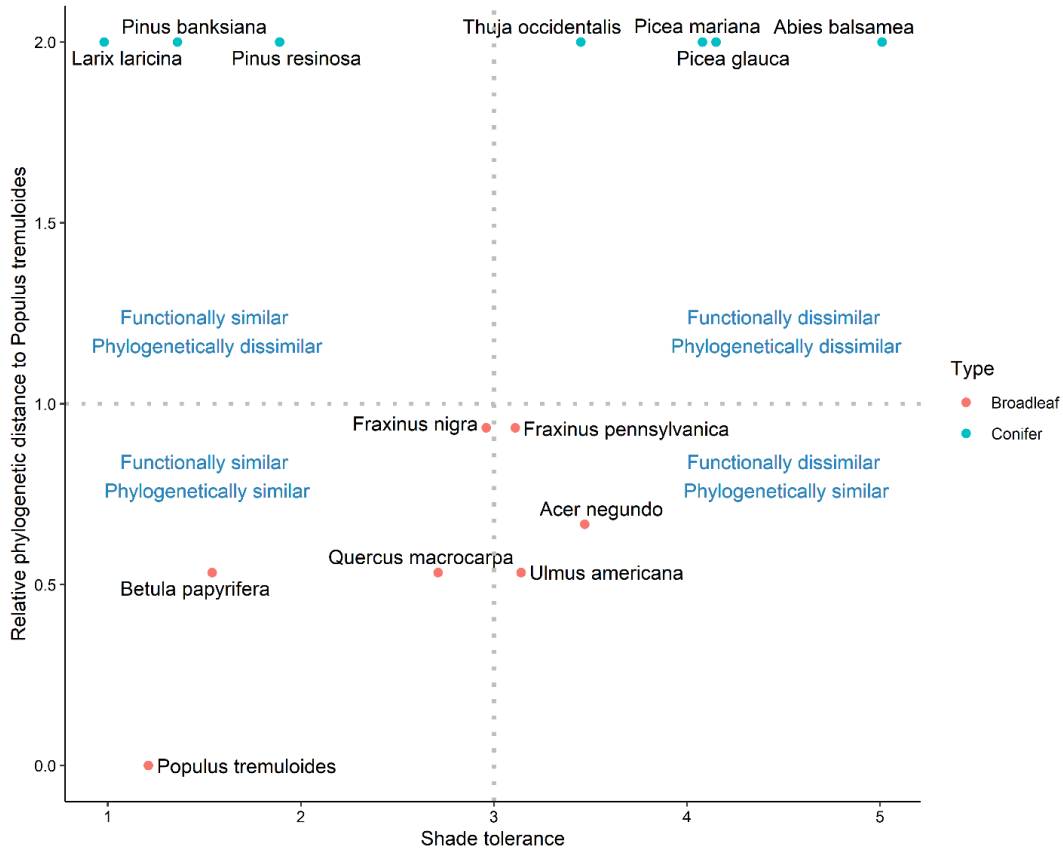
Figure S3-5 Shade tolerance of each species *versus* phylogenetic similarity to postfire pioneer species *Populus tremuloides*. The horizontal dotted line denotes the break between conifer and broadleaf in the phylogeny, while the vertical line is approximately the average shade tolerance observed in the dataset. The left bottom represents the early successional species, and the right top represents the late-successional species in mixedwood boreal forest following a stand-replacing fire.
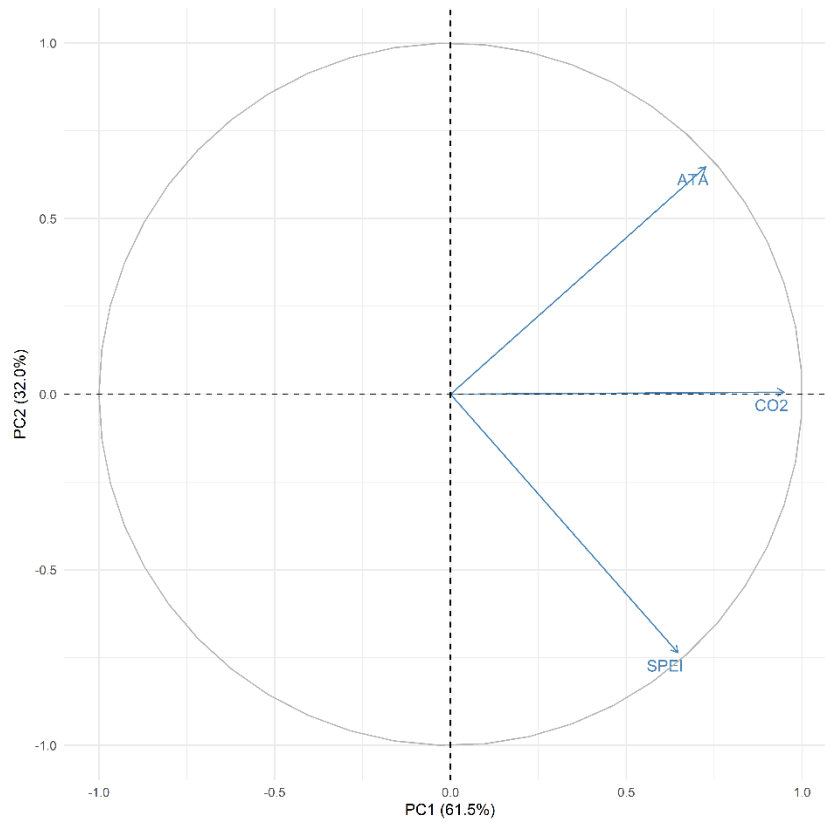
Figure S3-6 Results of principal component analysis calibrated on three climate variables. PC1 (the first axis of principal component analysis) and PC2 (the second axis of principal component analysis) represent the first two principal components, explaining 93.5% of the total variability. CO_2, ATA, and SPEI represent the atmospheric CO_2, annual temperature anomaly and annual standardized precipitation–evapotranspiration index, respectively.
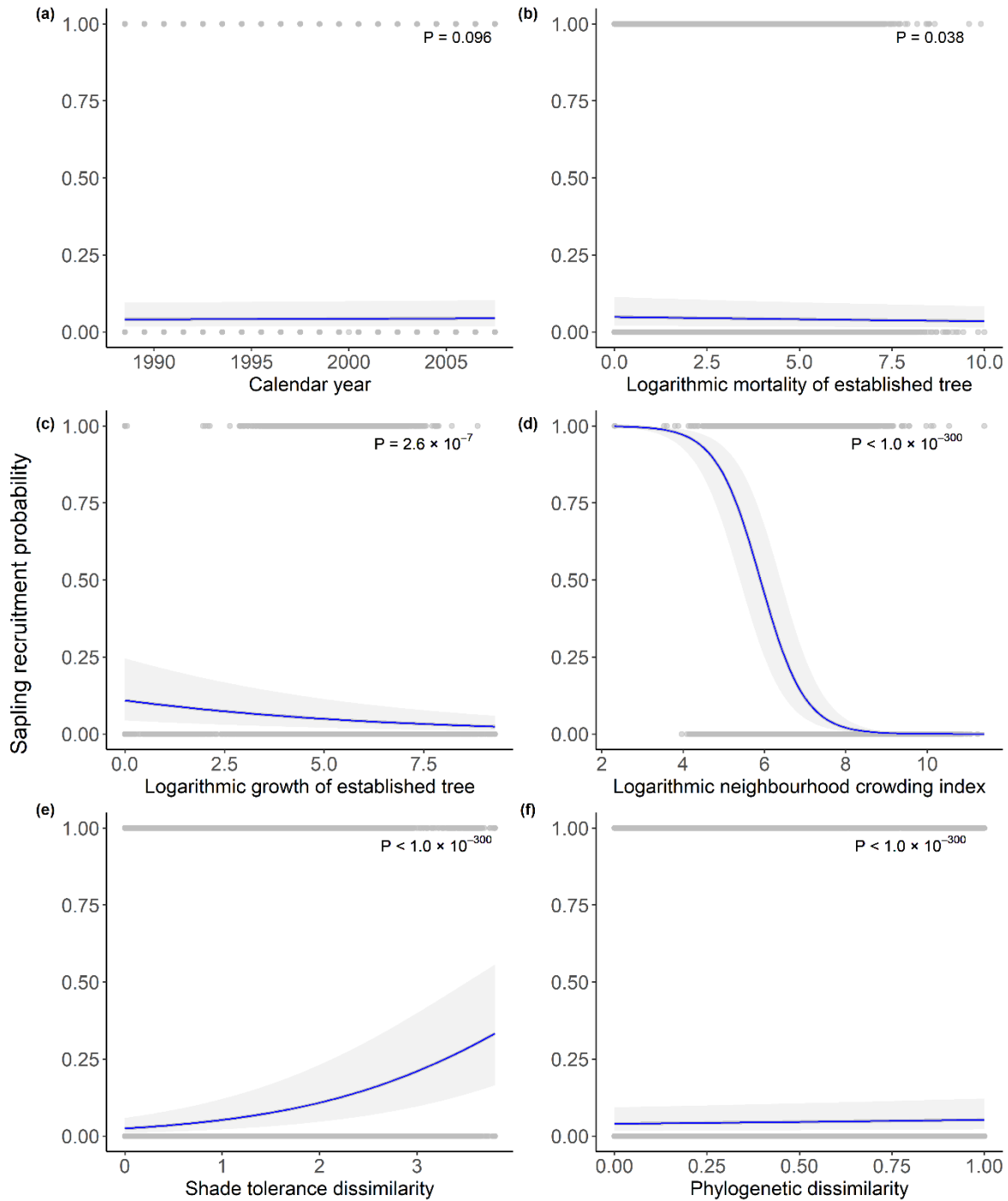
Figure S3-7 Partial regression plots of sapling recruitment probability. Points are the observed values of sapling recruitment probability with the effects of all other predictors removed. Black lines represent simple linear fits, while grey bands indicate 95% confidence intervals. Coefficients are presented in Table S3-7.
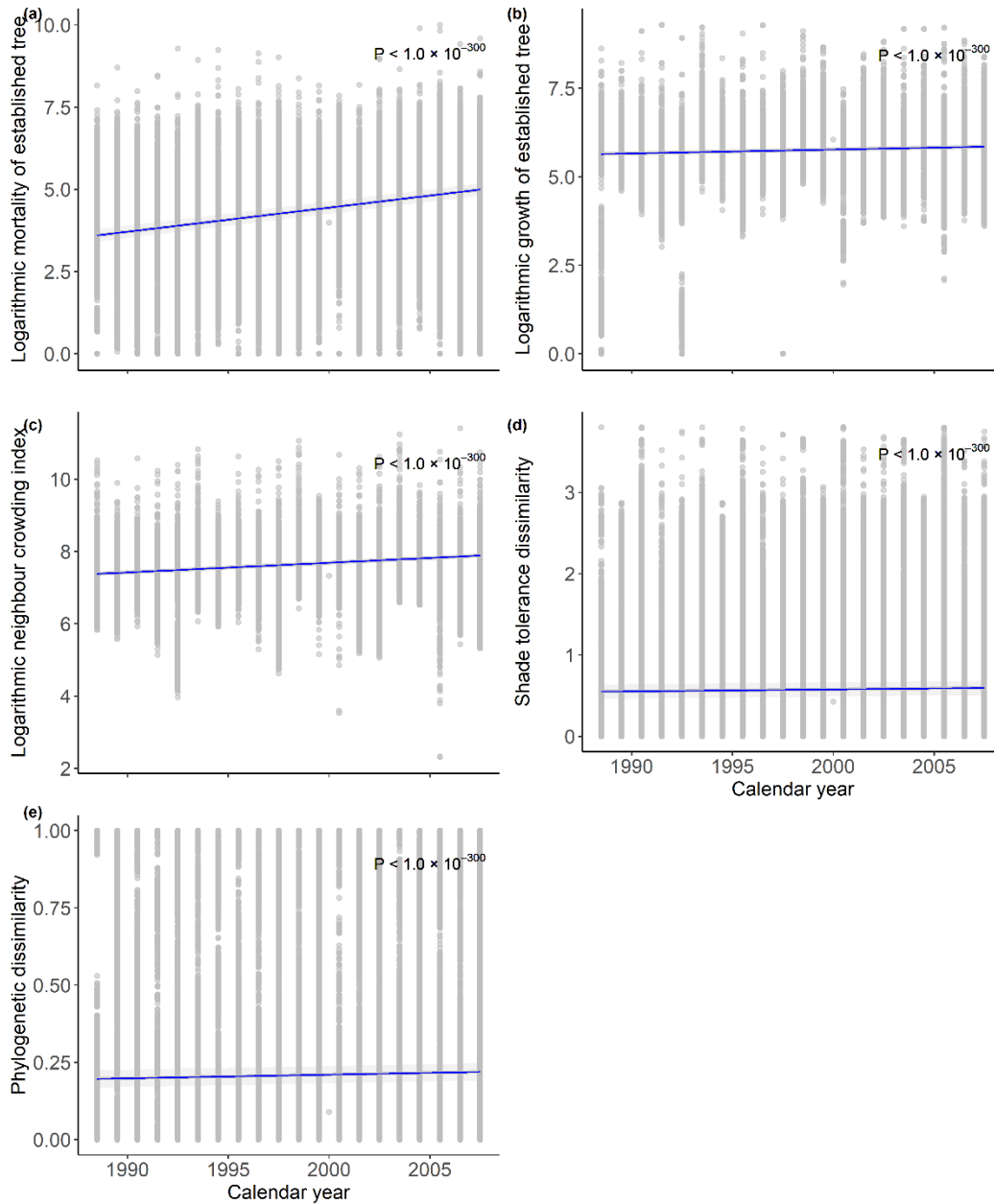
Figure S3-8 Bivariate relationships between the calendar year and mortality and growth of established trees, neighbourhood crowding index, shade tolerance dissimilarity and phylogenetic dissimilarity. Points are the observed values of sapling recruitment probability with the effects of all other predictors removed. Black lines represent simple linear fits, while grey bands indicate 95% confidence intervals. Coefficients are presented in Table S3-7.

APPENDIX III: SUPPLEMENTAL INFORMATION FOR CHAPTER 4

Table S4-1. Numbers (No.) of plots, trees, and observations for all tree species. Relative abundance (RA) was calculated by a percentage of total recruit/living tree counts. Species in grey were minor species (<0.1% in total).

Species	No. of plot	No. of tree			No. of observation	RA of recruit (%)	RA of tree (%)
		Recruit	Dead	Living			
All	153	10,433	19,380	63,548	215,612	100	100
Picea mariana	109	6,858	3,292	23,426	86,170	65.7	36.9
Pinus banksiana	86	1,157	5,316	16,105	51,764	11.1	25.3
Populus tremuloides	105	1,018	6,597	13,570	43,217	9.8	21.4
Abies balsamea	42	378	1,852	3,601	12,218	3.6	5.7
Betula papyrifera	83	443	592	1,797	5,512	4.3	2.8
Picea glauca	55	104	255	1,292	3,757	2.5	3.1
Fraxinus nigra	43	260	1,102	1,944	6,184	1.0	2.0
Larix laricina	36	29	267	1,038	3,903	0.3	1.6
Thuja occidentalis	6	123	87	694	2,719	1.2	1.1
Ulmus americana	4	26	3	35	64	0.3	0.1
Quercus macrocarpa	6	13	2	19	45	0.1	0.0
Acer negundo	2	12	3	14	31	0.1	0.0
Fraxinus pennsylvanica	1	12	12	12	24	0.1	0.0
Pinus resinosa	1	0	0	1	4	0.0	0.0

Table S4-2. Summary statistics (Mean ± 1 SD and range in brackets) of explanatory variables for the three demographic datasets. The conspecific/heterospecific density was based on the neighbourhood crowding index (NCI) for recruitment and the Hegyi index (H) for the survival and growth.

Explanatory variable	Recruitment	Survival	Growth
Conspecific density (CD)	1421 ± 1310 (0 ~ 58021)	566.4 ± 2667 (0 ~ 293560)	425 ± 2243 (0 ~ 292208)
Heterospecific density (HD)	795 ± 999 (0 ~ 90241)	558.1 ± 2884 (0 ~ 320240)	531 ± 2244 (0 ~ 227096)
Stand age (SA, yrs)	44.0 ± 20.9 (10.5 ~ 164.1)	44.2 ± 20.9 (10.5 ~ 164.1)	43.9 ± 20.8 (10.5 ~ 164.1)

Table S4-3. Spatial and temporal dependency of residuals for all demographic models. P-values < 0.05 indicate the existence of spatial or temporal autocorrelation. Mantel r values (rM) can range between -1 to 1. An r value of -1 suggests a strong negative correlation, 0 suggests no relationship, and 1 suggests a strong positive relationship. Durbin Watson (DW) statistic can range between 0 and 4. A DW value of 2.0 indicates no autocorrelation, values from 0 to less than 2 mean positive autocorrelation and values from 2 to 4 mean negative autocorrelation.

	Recruitment probability per 5-year interval	Survival probability per 5-year interval	Annual growth rate
P value	0.788	0.955	0.409
r_M	-0.015	-0.045	0.005
P value	0.260	0.685	0.455
DW	2.110	2.040	2.073
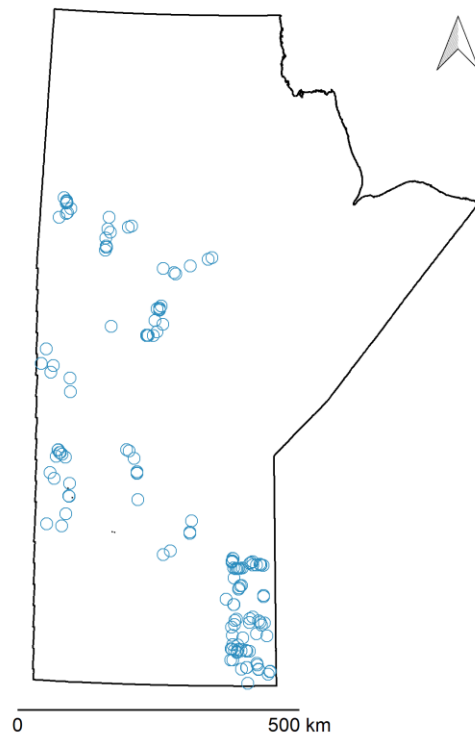
Figure S4-1 Plot locations of the 153 permanent sample plots of boreal forest in Manitoba, Canada.
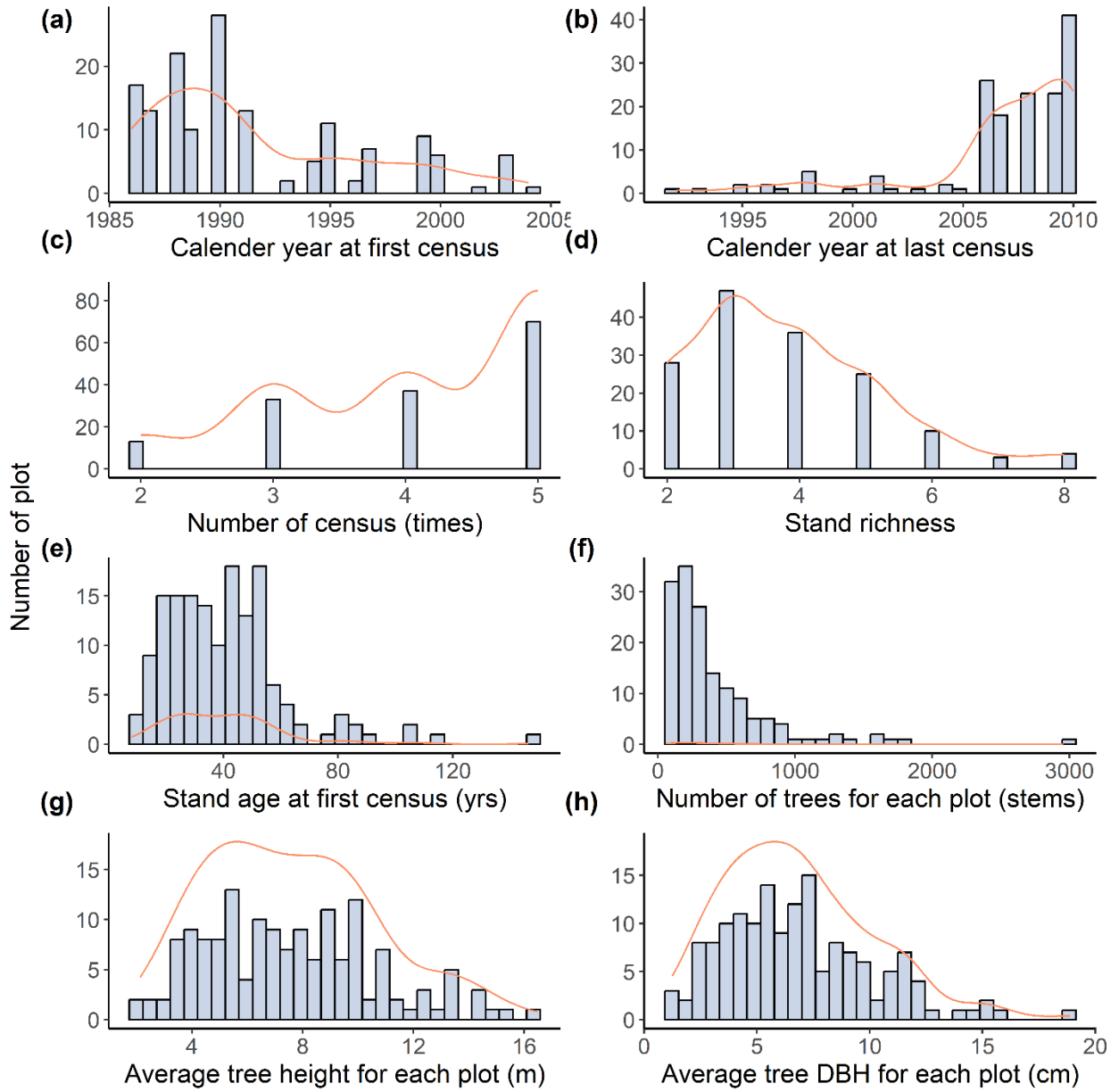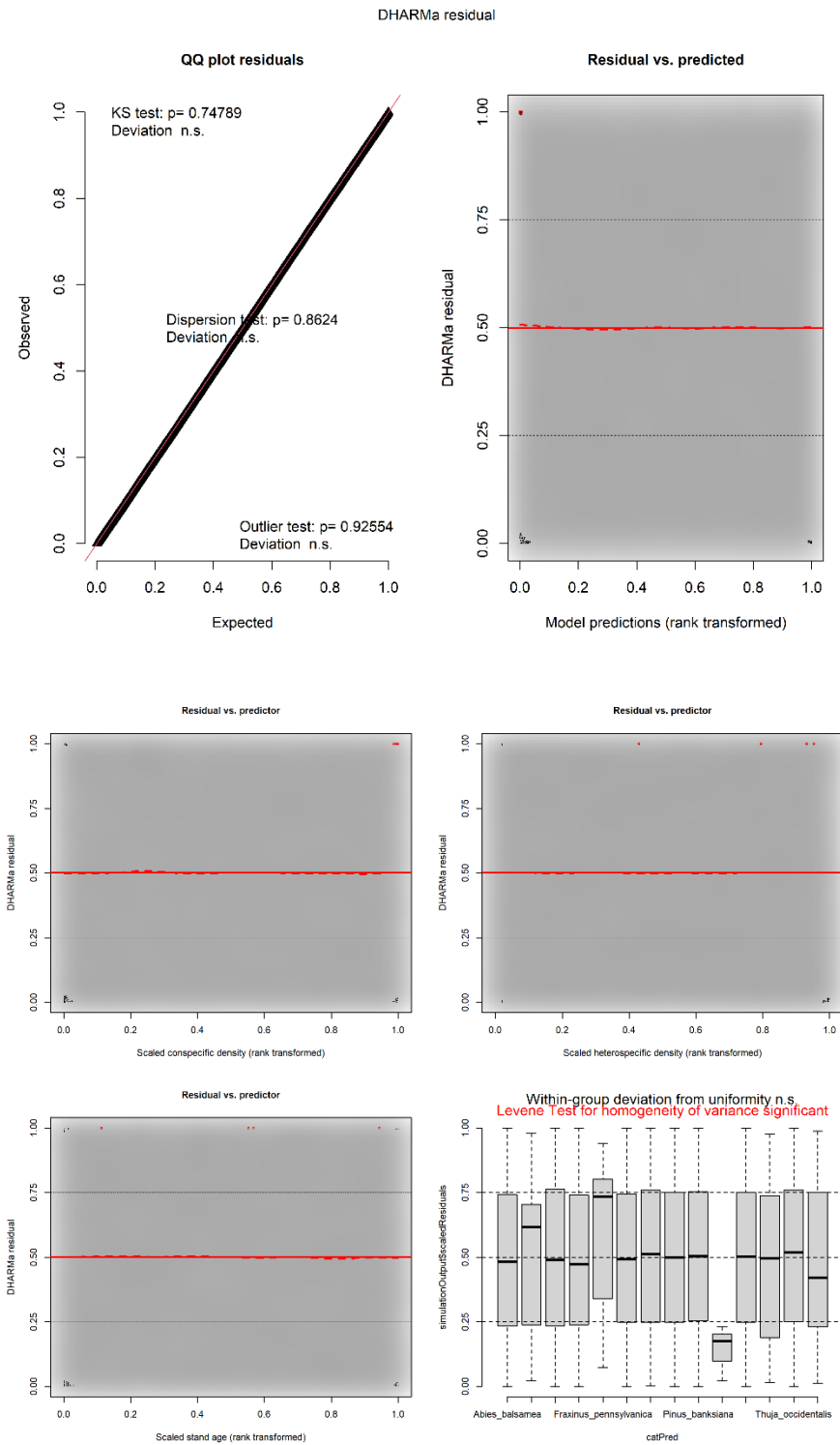
Figure S4-2 Distribution histograms and density of the selected 153 plots.
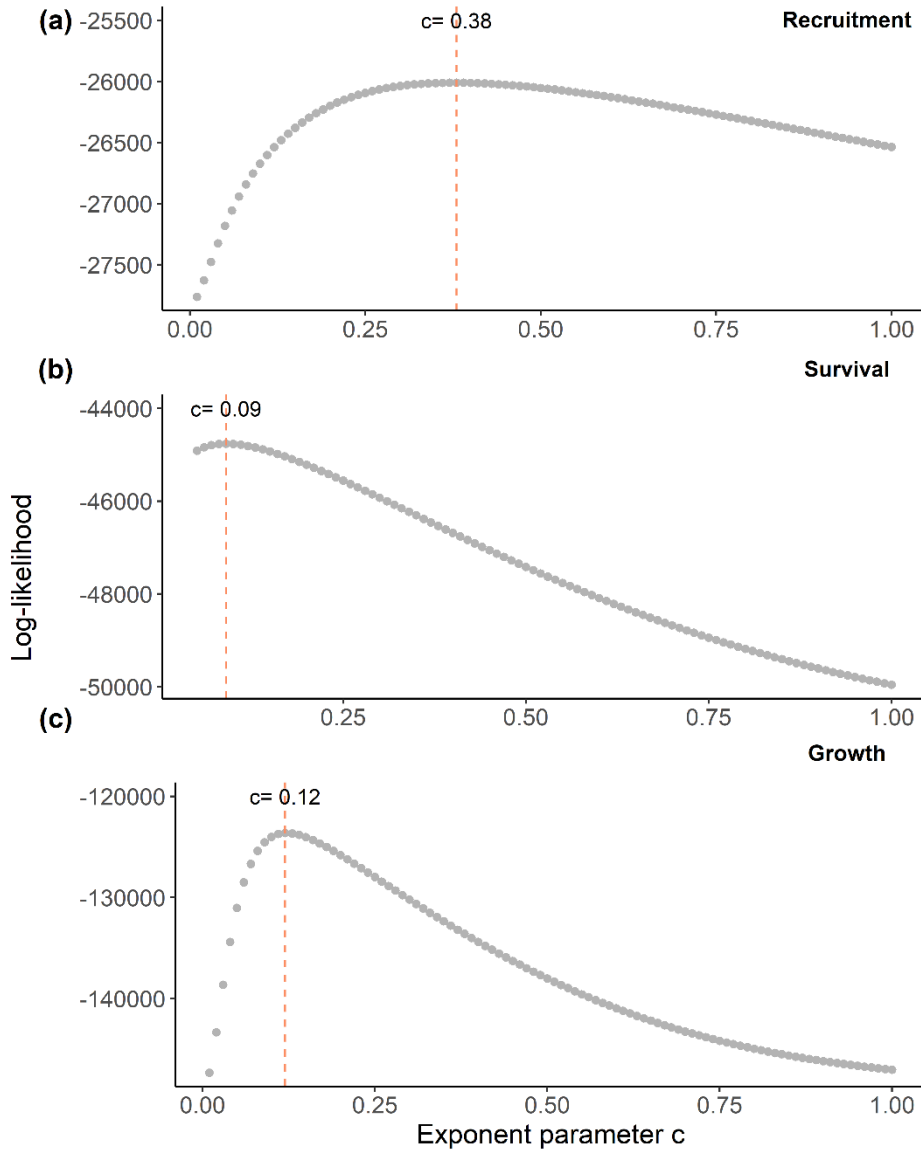
Figure S4-3 Values of maximum log-likelihood and selected exponent parameter c of conspecific density and heterospecific density for three demographic models of Eqn. 3, 4.
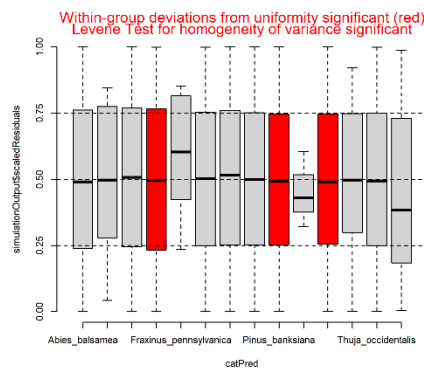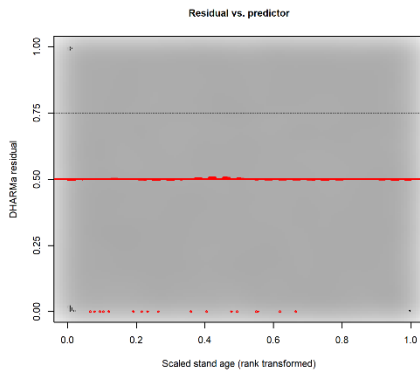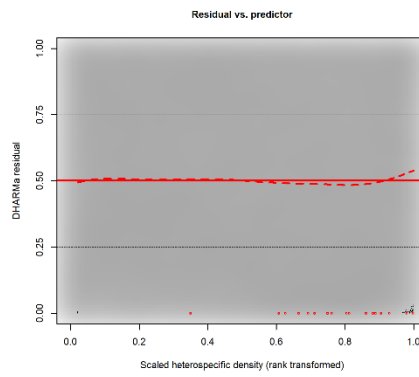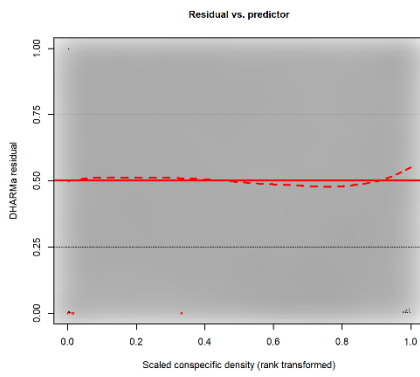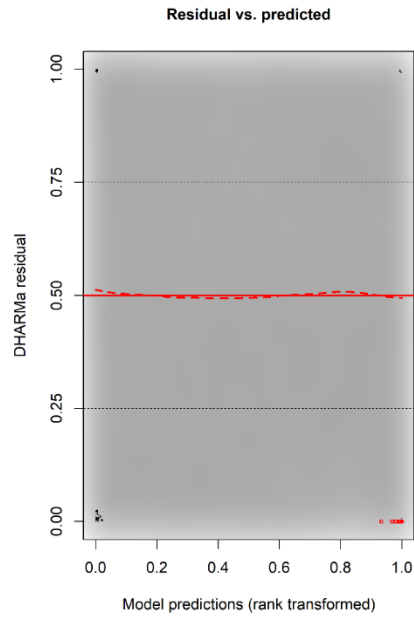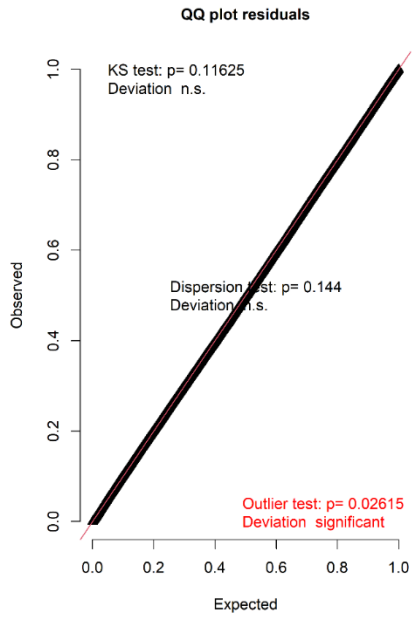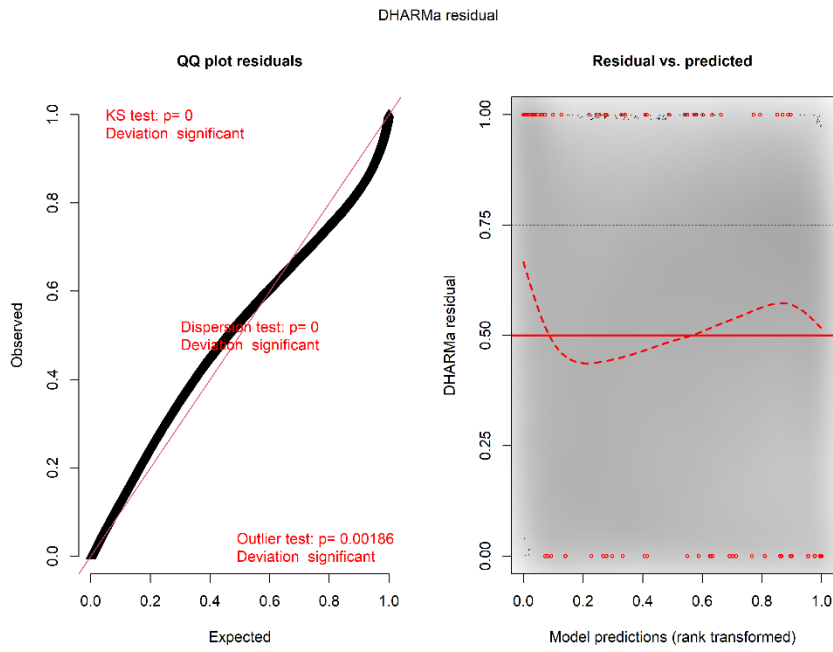
(A) Recruitment

Figure S4-4 Simulated residual plots for models of three demographics. Plots of residuals against fitted model values and predictor variables are shown for (A) recruitment, (B) survival, (C) growth. Residuals were simulated n = 2,500 using the 'DHARMa' R package.

(B) Survival

(c) Growth

DHARMa residual

APPENDIX V: SUPPLEMENTAL INFORMATION FOR R-CODE FOR

MAIN MODELS

Chapter 2:

mrec<-glmer(ING~scale(log(NCI))*(scale(FD)+scale(PD))*scale(log(SA))+ (1|PLOT_ID),
data=MB, family=binomial(link = "logit"), verbose=TRUE, nAGQ=0,
control=glmerControl(optimizer='bobyqa'), na.action = na.fail)

Note: ING recorded as 1 for recruit, 0 for living tree. The initiation of predictors can be found in main text.

Chapter 3:

```
Model1:
SEM_Y<-psem(
        glmer(ING~Y+log(M)+log(G)+log(NCI)+FD+PD+(1|PLOT_ID)+(1|SPECIES),
data=MB, family= binomial(link = "logit"), verbose=TRUE, nAGQ=0,
glmerControl(optim='Nelder_Mead')),
        lme(log(M)~Y, random = ~1|PLOT_ID, data=MB,control = lmeControl(opt = 'optim')),
        lme(log(G)~ Y, random = ~1|PLOT_ID, data=MB,control = lmeControl(opt = 'optim')),
        lme(log(NCI)~Y,random = ~1|PLOT_ID, data=MB,control = lmeControl(opt =
'optim')),
        lme(FD~Y, random = ~1|PLOT_ID, data=MB,control = lmeControl(opt = 'optim')),
        lme(PD~Y, random = ~1|PLOT_ID, data=MB,control = lmeControl(opt = 'optim')),
        log(NCI)%~~% log(M),
        log(NCI)%~~% log(G),
        FD%~~% log(M),
        FD%~~% log(G),
        PD%~~% log(M),
        PD%~~% log(G),
        FD%~~% PD,
        log(M) %~~% log(G)
        )


Model2:

SEM_MG<- psem(
        glmer(ING~Y+log(M)+log(G)+log(NCI)+FD+PD+(1|PLOT_ID)+(1|SPECIES),
data=MB, family= binomial(link = "logit"), verbose=TRUE, nAGQ=0,
glmerControl(optim='Nelder_Mead')),
        lme(log(M)~Y, random = ~1|PLOT_ID, data=MB,control = lmeControl(opt = 'optim')),
```

```
        lme(log(G)~Y, random = ~1|PLOT_ID, data=MB,control = lmeControl(opt = 'optim')),
        lme(log(NCI)~ Y+log(M)+log(G), random = ~1|PLOT_ID, data=MB,control =
lmeControl(opt = 'optim')),
        lme(FD~Y+log(M)+log(G), random = ~1|PLOT_ID, data=MB,control =
lmeControl(opt = 'optim')),
        lme(PD~Y+log(M)+log(G), random = ~1|PLOT_ID, data=MB,control=lmeControl(opt
        = 'optim')),
        FD%~~% PD,
        log(M) %~~% lme(log(G)
        )
```
Note: ING recorded as 1 for recruit, 0 for living tree. The initiation of predictors can be found in main text.

Model3:

```
SEM_NFD<- psem(
        glmer(ING~Y+log(M)+log(G)+log(NCI)+FD+PD+(1|PLOT_ID)+(1|SPECIES),
data=MB, family="binomial(link = "logit"), verbose=TRUE, nAGQ=0,
glmerControl(optim='Nelder_Mead')),
        lme(log(M)~Y)+log(NCI)+FD+PD, random = ~1|PLOT_ID, data=MB,control =
lmeControl(opt = 'optim')),
        lme(log(G)~Y+log(NCI)+FD+PD, random = ~1|PLOT_ID, data=MB,control =
lmeControl(opt = 'optim')),
        lme(log(NCI)~ Y,random = ~1|PLOT_ID, data=MB,control = lmeControl(opt =
'optim')),
        lme(FD~Y, random = ~1|PLOT_ID, data=MB,control = lmeControl(opt = 'optim')),
        lme(PD~Y, random = ~1|PLOT_ID, data=MB,control=lmeControl(opt = 'optim')),
        FD%~~% PD,
        log(M) %~~% lme(log(G)
        )
```

Model4:

```
SEM_SA<-psem(
        glmer(ING~Y+log(SA)+log(M)+log(G)+log(NCI)+FD+PD+(1|PLOT_ID)+(1|SPECIE
S), data=MB, family="binomial(link = "logit"), verbose=TRUE, nAGQ=0,
glmerControl(optim='Nelder_Mead')),
        lme(log(M)~Y+log(SA), random = ~1|PLOT_ID, data=MB,control = lmeControl(opt =
'optim')),
        lme(log(G)~ Y+log(SA), random = ~1|PLOT_ID, data=MB,control = lmeControl(opt =
'optim')),
```

```
        lme(log(NCI)~Y+log(SA),random = ~1|PLOT_ID, data=MB,control = lmeControl(opt
= 'optim')),
        lme(FD~Y+log(SA), random = ~1|PLOT_ID, data=MB,control = lmeControl(opt =
'optim')),
        lme(PD~Y+log(SA), random = ~1|PLOT_ID, data=MB,control = lmeControl(opt =
'optim')),
      log(NCI)%~~% log(M),
      log(NCI)%~~% log(G),
      FD%~~% log(M),
      FD%~~% log(G),
      PD%~~% log(M),
      PD%~~% log(G),
      FD%~~% PD,
      log(M)%~~%log(G),
      Y%~~% log(SA)
      )

Model5:

#calculate PCA composite first
CLMT<-MB[,c("ATA","CO2","SPEI")]
PCA <- prcomp(CLMT,scale=TRUE)
summary(PCA)#PC1 explains 61; PC2 explains 32; totally 94%
PC1<-as.data.frame(PCA$x[,1])#use first axis
MB<-merge(MB, PC1,by="UID")
#replace Y in model1
SEM_PCA<-psem(
        glmer(ING~ PC1+log(M)+log(G)+log(NCI)+FD+PD+(1|PLOT_ID)+(1|SPECIES),
data=MB, family="binomial(link = "logit"), verbose=TRUE, nAGQ=0,
glmerControl(optim='Nelder_Mead')),
        lme(log(M)~ PC1, random = ~1|PLOT_ID, data=MB,control = lmeControl(opt =
'optim')),
        lme(log(G)~ PC1, random = ~1|PLOT_ID, data=MB,control = lmeControl(opt =
'optim')),
        lme(log(NCI)~ PC1,random = ~1|PLOT_ID, data=MB,control = lmeControl(opt =
'optim')),
        lme(FD~ PC1, random = ~1|PLOT_ID, data=MB,control = lmeControl(opt = 'optim')),
        lme(PD~ PC1, random = ~1|PLOT_ID, data=MB,control = lmeControl(opt = 'optim')),
        log(NCI)%~~% log(M),
        log(NCI)%~~% log(G),
        FD%~~% log(M),
```

```
FD%~~% log(G),
PD%~~% log(M),
PD%~~% log(G),
FD%~~% PD,
log(M) %~~% log(G)
)
```

Chapter 4:

Recruitment:
```
M1<- glmer(ING~ (scale(CD^0.38)+ scale(HD^0.38))*scale(log(SA))+(1|SPECIES)
+(1|PLOT_ID), MB_rec, family=binomial(link = "logit"), verbose=TRUE, nAGQ=0,
      control=glmerControl(optimizer='bobyqa',optCtrl=list(maxfun=2e6)))
```
Survival:
```
M3<- glmer(SUR~ (scale(CD^0.09)+scale(HD^0.09))*scale(log(SA))+ (1|SPECIES)
+(1|PLOT_ID), MB_surv, family=binomial(link = "logit"), verbose=TRUE, nAGQ=0,
      control=glmerControl(optimizer='bobyqa',optCtrl=list(maxfun=2e6)))
```
Growth:
```
M2<- lmer(Iog(G)~ (scale(CD^0.12)+scale(HD^0.12))*scale(log(SA))+(1| SPECIES)
+(1|PLOT_ID/ T_N),   MB_grow,
control=lmerControl(optimizer='bobyqa',optCtrl=list(maxfun=2e6)))
```

Note: ING recorded as 1 for recruit, 0 for living tree. SUR recored as 1 for living tree, 0 for dead tree. G recorded as net basal area increment of individual live tree during two censuses. The initiation of predictors can be found in main text.